TRANSPORTATION RESEARCH
RECORD

No. 1418

Soils, Geology, and Foundations;
Materials and Construction

Performance-Related Testing and Evaluation of Characteristics of Aggregates and New Geomaterials

A peer-reviewed publication of the Transportation Research Board

TRANSPORTATION RESEARCH BOARD
NATIONAL RESEARCH COUNCIL

NATIONAL ACADEMY PRESS
WASHINGTON, D.C. 1993

Transportation Research Record 1418
ISSN 0361-1981
ISBN 0-309-05566-0
Price: $24.00

Subscriber Categories
IIIA soils, geology, and foundations
IIIB materials and construction

TRB Publications Staff
Director of Reports and Editorial Services: Nancy A. Ackerman
Associate Editor/Supervisor: Luanne Crayton
Associate Editors: Naomi Kassabian, Alison G. Tobias
Assistant Editors: Susan E. G. Brown, Norman Solomon
Office Manager: Phyllis D. Barber
Senior Production Assistant: Betty L. Hawkins

Printed in the United States of America

Transportation Research Record 1418

Contents

Foreword

Aggregate characteristics have a significant, and possibly in many cases the major, effect on the performance and longevity of pavement structures. The nine papers in this Record provide information on performance-related testing and evaluation of characteristics of aggregates and geomaterials.

Barksdale et al. describe the use of a loaded wheel for laboratory testing of resistance to rutting of asphalt concrete mixtures. The rut depth in the test asphalt concrete beam after 8,000 applications of a deadweight loaded wheel is a measure of that asphalt mixture's resistance to rutting, according to the researchers.

Lane reports on the suitability of the ASTM P214 test for determining the potential of Virginia aggregates to alkali-silica deterioration when used in portland cement concrete. On the basis of field observations and laboratory test results it was concluded that the current ASTM P214 test criteria are not suitable for evaluating aggregates in Virginia.

Kandhal et al. evaluated the frictional properties of limestone aggregate in asphalt concrete wearing surfaces after 9 hr of accelerated polishing, using a British pendulum tester. The frictional properties exhibited a general relationship to the insoluble residue content of the limestone aggregate.

Skerritt relates friction numbers determined using an ASTM E274 trailer with the coarse aggregate rock used in asphalt concrete pavement in New York State. A semilog plot of friction number versus lane average daily traffic for each rock type showed traffic conditions under which the aggregate would perform adequately.

Garrick and Chan evaluated waste incinerator bottom ash for use in asphalt concrete. They conclude that a significant quantity of undesirable material must be removed from the bottom ash to provide an aggregate of acceptable quality.

Abdul-Malak et al. compared aggregate mineralogy with the friction number when it is used as a cover aggregate in a bituminous seal coat. They found that the aggregate particle application rate has an influence on the friction number.

Negussey and Jahanandish, on the basis of their investigation of expanded polystyrene (EPS), present a comparison of strength and deformation behavior of soils and EPS. They indicate that engineering properties of EPS can be quantified in a manner similar to those of earth materials.

Lee and Fishman report on the results of a study on the resilient modulus and plastic deformation of fly ash produced from coal combustion, a by-product of aggregate processing, and a mixture of the two materials. The mixture showed greater improvement in resilient and plastic behavior than either of its constituents considered alone.

Crockford et al. describe results of laboratory and field studies on the effects of mixing fibrillated fibers on physical behavior of sand or clay soils. They found that the tested fibers could enhance the performance of chemically stabilized materials.

Test Device for Evaluating Rutting of Asphalt Concrete Mixes

RICHARD D. BARKSDALE, TIMOTHY J. MIROCHA, AND JON SHENG

A loaded wheel test apparatus for direct laboratory comparison of the rutting susceptibility of asphalt concrete mixes is described. The test consists of applying a loaded, rubber-tired wheel to a small rectangular beam specimen. For the mechanical apparatus described, the wheel, which is loaded by deadweight, remains stationary while the beam moves back and forth. The stress state applied by this system is similar to that which occurs in the field, including the application of stress reversals. About 50 two-directional loads are applied to a specimen each minute with the total number of repetitions being 8,000. A test can be performed in about 3 hr. The testing concept is straightforward, and the loading system is entirely mechanical. Hence, the test can be conducted and the tester can be maintained at a minimum of cost by a laboratory technician having a very modest level of technical and mechanical ability. Also, complicated electronic instrumentation is not required to obtain good results, which significantly reduces the equipment cost and makes setting up and performing the rutting test simple.

Field studies reported in 1967 indicated that rutting in flexible pavements at that time was generally not a problem within the United States (*1*). However, during the 25 years following that study, rutting has become an important factor in pavement design. For example, excessive rutting has been reported in asphalt concrete pavements in Florida, Georgia, Illinois, Pennsylvania, Tennessee, and Virginia (*2*). A number of factors help to account for the observed increase in the rutting problem associated with asphalt concrete pavements, including increase in overall vehicle traffic volume, increase in the percentage of truck traffic, increase in tire pressures, increase in axle loadings, and the occurrence of several years of higher than average summer temperatures in at least some areas of the United States.

A Federal Highway Administration study has shown that a 20 percent increase in total interstate traffic occurred from 1970 to 1984 (*3*). Accompanying this increase in traffic was a 49 percent increase in the number of trucks and a 126 percent increase in the number of 80-kN (18-kip) equivalent single-axle loads applied to the pavements. Also, with the advent of steel-belted radial tires, truck tire pressures have increased from about 586 kN/m^2 (85 psi) to 758 to 861 kN/m^2 (110 to 125 psi).

To design asphalt concrete mixes with good resistance to rutting, a simple but reliable test is needed. This paper describes the construction and operation of a small loaded wheel tester suitable for routine laboratory use and also gives a suggested test procedure. The proposed test is suitable for comparing one asphalt concrete mix directly with another, is simple to perform, and does not require complicated instrumentation and test equipment.

R. D. Barksdale, School of Civil Engineering, Georgia Institute of Technology, Atlanta, Ga. 30332. T. J. Mirocha, Atlanta Testing and Engineering, 11420 Johns Creek Parkway, Duluth, Ga. 30136. J. Sheng, R & D Drilling and Testing, 2739 Waters Road Southwest, Atlanta, Ga. 30354.

METHODS FOR EVALUATING RUTTING OF ASPHALT CONCRETE

Sousa et al. (*4*), as a part of the SHRP program, have given a good summary and general review of available methods for measuring the susceptibility of asphalt concrete mixes to rutting. For evaluating rutting in asphalt concrete, the repeated load simple shear test was given the best overall ranking by Sousa et al., and the repeated load, triaxial shear test was given the next-to-highest ranking. The loaded wheel test, which was not given a good ranking in the SHRP report, offers a practical alternative to the simple shear and triaxial tests rated so highly by Sousa et al.

The repeated simple shear test appears to have been ranked the highest by Sousa et al. for the following reasons:

1. The simple shear test applies a pure state of shear to a specimen. Sousa et al. point out that permanent deformation in asphalt concrete is primarily caused by a change in shape due to the application of shear stress rather than a change in volume associated with a mean normal stress. The change in shape of the asphalt concrete through plastic shear flow is evidenced in the field, for example, by shoving of asphalt concrete to the sides of the loaded area (*5,6*). Deformation is also caused by densification of the asphalt concrete.
2. The direction of the applied shear stress reverses as a wheel moves toward and then away from a given small element of material beneath the pavement. This reversal of shear stress can be readily applied in the simple shear laboratory test.

An important concept in materials testing, emphasized in the SHRP report and by many other researchers, is that the stress state applied during testing should duplicate, as closely as practical, the stress state caused in the field by the applied loading. The repeated, simple shear test offers a practical trade-off for applying a realistic stress state compared with more sophisticated tests such as the complicated hollow cylinder test. The test, however, is more suited for research than routine laboratory testing.

LOADED WHEEL TESTER

The loaded wheel test consists of placing a loaded wheel on the surface of an asphalt concrete specimen and moving the

wheel in a line back and forth across the surface of the specimen. The loaded wheel tester (LWT) applies a stress state similar to that within the asphalt concrete when subjected to a wheel loading moving in a straight line. Stresses due to a wheel turning and breaking are not applied in this type of test.

An element of material within the pavement near the surface is subjected to both reversal of shear stress and rotation of principal planes. The LWT reproduces these general stress conditions except that the scale is changed. In contrast, the simple shear test can apply shear stress reversals but does not reproduce the complete stress state or rotation of principal stress planes that occurs in the field.

The LWT offers an excellent device for quantitatively comparing the relative rut susceptibility of one asphalt concrete mix with another. The testing concept is straightforward and the loading system is entirely mechanical. Hence, the tester can be maintained at a minimum of cost by a laboratory technician having a very modest level of mechanical ability. Also, electronic instrumentation is not required to obtain good results. Because of these features, the loaded wheel test offers an excellent alternative to other laboratory testing techniques when the performance of one mix is to be compared with that of another.

This does not necessarily imply that the LWT is a better test than the simple shear test. Considerably more testing and field validation is necessary before a conclusion can be reached. An important advantage of the simple shear test over the LWT is that the resilient shear modulus, G_r, can be directly obtained from the simple shear test. The well-known resilient modulus of elasticity, M_r, is related to the resilient shear modulus, G_r, for a linearly elastic, isotropic material by the following expression:

$$M_r = 2(1 + \nu)\, G_r \quad (1)$$

where ν is Poisson's ratio.

Thus, M_r can be estimated from simple shear test results if a value of Poisson's ratio is measured or assumed. M_r is required for use in mechanistic-based pavement design procedures and for selecting structural coefficients from the 1986 AASHTO *Design Guide*.

Neither the resilient modulus nor the structural coefficients can be obtained from the loaded wheel test at this time. This is because a relationship has not been found between rutting, which is a permanent deformation mechanism, and the resilient modulus, which is associated with recoverable deformation. Following the 1986 AASHTO *Design Guide*, structural coefficients are determined using resilient moduli values.

LOADED WHEEL TEST APPARATUS

The LWT described in this paper was developed to carry out an investigation for the Georgia Department of Transportation (Georgia DOT) to study the influence of aggregate properties on rutting in asphalt concrete mixes (*7*). Georgia DOT has for a number of years used an LWT to investigate the susceptibility of asphalt concrete mixes to rutting. In the Georgia DOT LWT apparatus, the loaded wheel is pulled back and forth by a large vertically oriented cam and arm system; the specimen remains fixed in position during the test.

The primary advantages of the Georgia Tech testing system over the Georgia DOT's system include (*a*) a much smoother and more consistent operation, (*b*) the ability to easily change the loaded length of specimen, and (*c*) the ability to change the speed of the wheel loading. Figures 1 through 4 show general views of the Georgia Tech LWT. The LWT applies a constant load, through a wheel, to the surface of a rectangular asphalt concrete beam specimen. The asphalt concrete beam, which is placed in an adjustable steel box for alignment and to provide a small degree of confinement, rests on a rectangular steel plate. The steel plate, which rolls on precision bearing wheels, is pulled back and forth by a mechanical system driven by a motor. The general concept for the Georgia Tech LWT was obtained from the one developed at the University of Nottingham, England.

Wheel Loading

Load is applied to the rectangular asphalt concrete beam specimen by a wheel 28.6 mm (1.125 in.) wide and having a diameter of 203 mm (8 in.). In the future, a wheel 32 to 38 mm (1.25 to 1.5 in.) wide will be used for most tests to give a better ratio of wheel width to maximum aggregate size. The wheel used to date has a hard rubber cover and must be periodically replaced because of wear. During operation of the system, the wheel remains at one location but rotates through a little less than one-half revolution as the beam moves back and forth. A constant dead load weight is applied to the wheel through a lever arm arrangement consisting of a load hanger, lever arm, and pivot as shown in Figures 1, 2, and 4. The lever arm supporting the dead load hanger is attached to a test frame 1.52 m (5 ft) long by 0.61 m (2 ft) wide by 0.9 m (3 ft) high. The load lever arm and test frame are constructed of 51- by 51-mm (2- by 2-in.) steel box sections 6.4 mm (0.25 in.) in thickness.

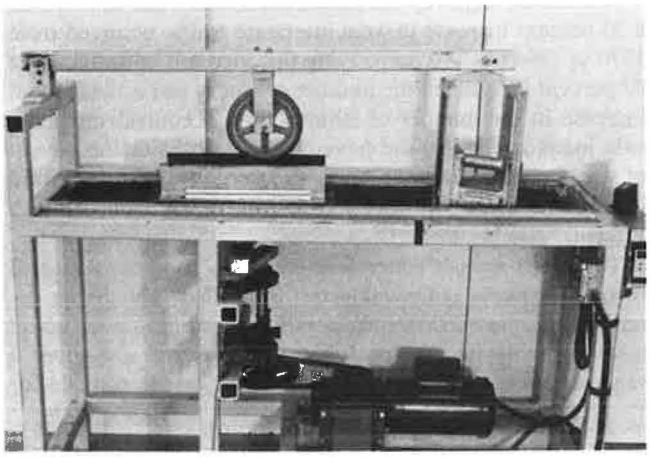

FIGURE 1 Photograph of LWT.

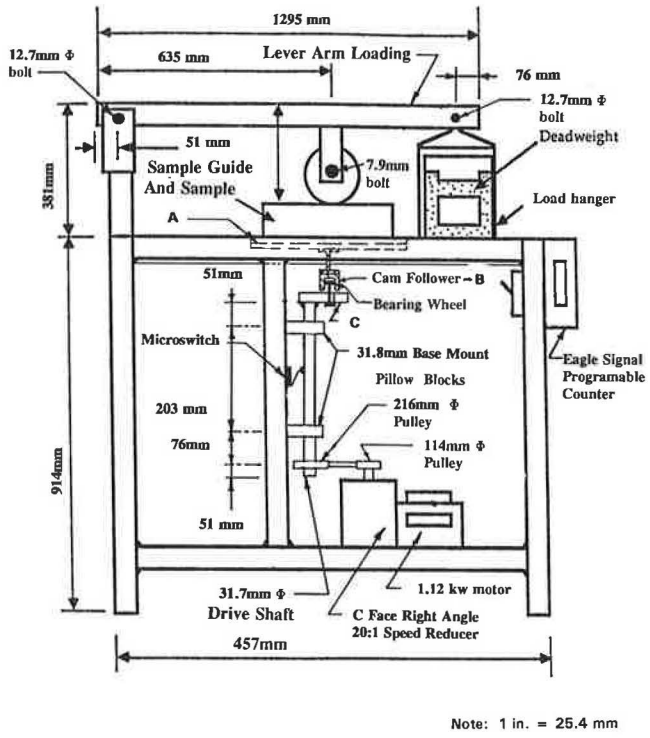

Note: 1 in. = 25.4 mm

FIGURE 2 LWT—elevation view.

Mechanical Movement of Beam Specimen

The flat steel plate (labeled A in Figure 2), and hence the asphalt concrete specimen, is pulled back and forth through a travel path 292 mm (11.5 in.) long by a 1.12-kW (1.5-hp) motor operating at a speed of 1,725 rpm. Fifty load repetitions per minute are applied to the asphalt concrete beam using the following mechanical system shown in Figures 2 and 3:

1. The 1,725-rpm motion of the motor is reduced to 86 rpm by using a 20 to 1 (nominal) gear reduction box attached to the end of the motor.
2. The 86-rpm motion coming out of the gear reduction box is further reduced by going from a pulley 114 mm ($4\frac{1}{2}$ in.) in diameter attached to the drive shaft leaving the gear reduction box to a pulley 216 mm ($8\frac{1}{2}$ in.) in diameter. The two pulleys lie in the same horizontal plane. The axes of the two pulleys are 254 mm (10 in.) apart and connected by a flexible drive belt.
3. The larger pulley turns a vertical drive shaft 31.8 mm (1.25 in.) in diameter attached by two pillow blocks to a vertical member of the test frame.
4. The drive shaft, in turn, has a cam lever arm system attached to it that drives the horizontal beam support plate back and forth (A, Figure 2).

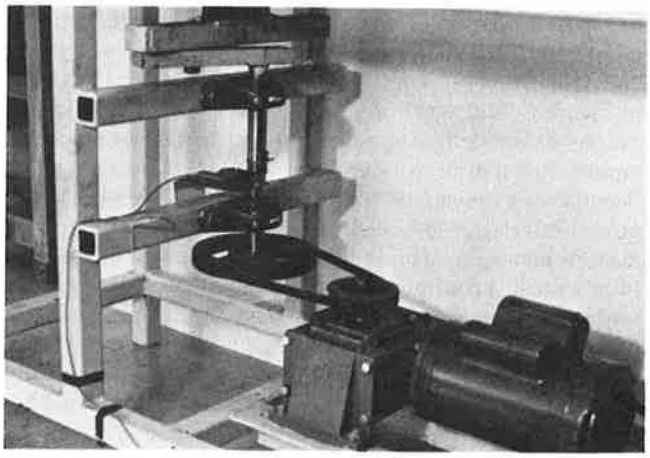

FIGURE 3 Mechanical system used to achieve linear motion.

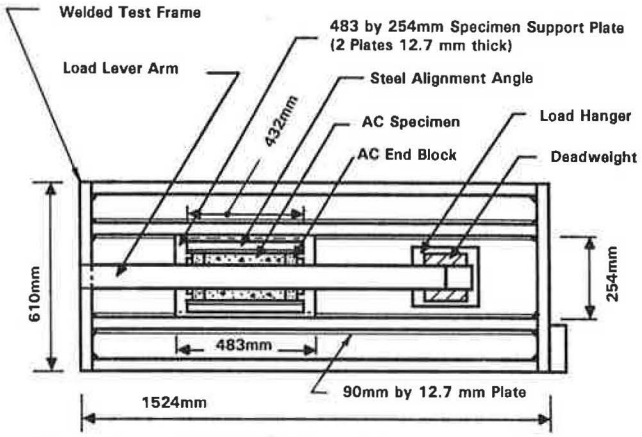

Note: Test Frame is Welded 51 by 51 mm Steel Box Section 6.4 mm Thick.

1 In. = 25.4 mm

FIGURE 4 Plan view drawing of LWT.

The articulated arm system consists of a cam and cam follower. The cam follower segment, labeled B in Figure 2, is rigidly attached by means of a 152-mm (6-in.) length of steel channel to the specimen support plate (A). This segment of the articulated lever arm system consists of a steel channel 51 mm (2 in.) wide and 445 mm (17.5 in.) long. The inside of the channel is machined to form a slot so that a precision bearing 41.3 mm ($1\frac{5}{8}$ in.) in diameter can roll back and forth inside it.

The cam segment of the articulated system (C in Figure 2) consists of a flat steel plate 267 mm ($10\frac{1}{2}$ in.) long by 51 mm (2 in.) wide by 25 mm (1 in.) thick. A hole drilled through one end of this plate allows it to be welded to the vertical drive shaft. Nine additional holes 16 mm ($\frac{5}{8}$ in.) in diameter are drilled in this plate, which allows quick adjustment of the length of travel of the wheel across the specimen. To achieve the desired 292-mm (11.5-in.) length of travel, the pivot point of the cam-follower system is located 63.5 mm ($2\frac{1}{2}$ in.) from the drive shaft.

To change the circular motion of the drive shaft to linear motion of the specimen support plate, the cam, which is connected to the drive shaft, is also connected using a precision bearing to the channel. The channel in turn is rigidly attached to the specimen support plate. A steel bolt extends vertically through the cam plate and has a horizontally oriented precision bearing fitted to the bolt above the plate. This bearing rolls back and forth in the machined slot of the channel that comprises the cam follower. Thus, as the vertical drive shaft rotates, the cam lever arm also rotates. The cam, in turn,

pulls the support plate back and forth as the bearing rolls along the slot in the channel that is rigidly attached to the specimen support plate.

The flat support plate (A) is guided along the test frame by means of eight precision steel bearings, with two of these bearings located at each corner of the plate. One bearing is oriented vertically and rides along a flat steel plate welded to the bottom of the two center members of the test frame (Figure 4). The other bearing is oriented horizontally and rides along the side of the steel box section.

Specimen Alignment and Confinement

The specimen is placed in a rectangular box to provide alignment and a small degree of confinement. The box consists of four independent lengths of steel angle. Each steel angle has either two or three slots machined in it. The slots allow adjustment of the angles snugly against the specimen. In practice, the angles on two adjacent orthogonal sides are tightly fastened after being properly aligned to the horizontal plate that supports the specimen. The remaining two angles are tightened down after the asphalt concrete specimen is positioned in the apparatus.

Rut Depth Measurement Template

The maximum rut depth resulting from wheel loading is measured at a different number of load repetitions at several locations along the beam. To reestablish the exact position of these measurements each time, a template was developed that can be repositioned on an asphalt concrete beam specimen at exactly the same location each time. To accomplish this, a horizontally oriented rectangular template is placed on top of two parallel sides of the steel angle box that holds the specimen in place. The template, which is machined from aluminum, has 13 rectangular slots oriented perpendicular to the direction of the wheel movement and spaced 25.4 mm (1 in.) apart. The slots are 38 mm (1.5 in.) long and 9.5 mm ($\frac{3}{8}$ in.) wide. To measure rut depth, a 0.025-mm (0.001-in.) dial indicator is placed successively in each desired slot and slowly moved across the transverse rut profile. The largest observed dial reading is recorded as the maximum rut depth. The transverse rut profile at some locations has been observed to be nonuniform. The nonuniformity is usually caused by the presence of aggregate particles near the surface (see Figure 5). Measuring the maximum rut depth in the manner described tends to produce less scatter in test results than taking a reading at a fixed location.

To accurately reposition the template over the specimen after each series of load repetitions, one corner of the template and one corner of one of the steel angles that hold the asphalt concrete specimen in position have a notch machined in them so that the template fits into the notched angle exactly the same way each time.

The method described for measuring rut depth worked satisfactorily. However, readings must be taken manually at the desired number of load repetitions. A potential improvement to this testing system would be to rigidly mount a single spring-loaded LVDT to measure the rut depth as the beam moves back and forth. The LVDT would have a roller mounted at its tip. Rut depths would then be measured over the center 50 to 75 mm (2 to 3 in.) of the beam at the desired number of load repetitions. Measurements could be performed automatically and stored digitally using a data acquisition system. The average value of rutting would then be calculated using the stored data. The data acquisition could be triggered externally with the data then being collected at a specified rate and for a specified time. A microswitch could be used to trigger the data acquisition system when the beam reaches a position near its midpoint of travel.

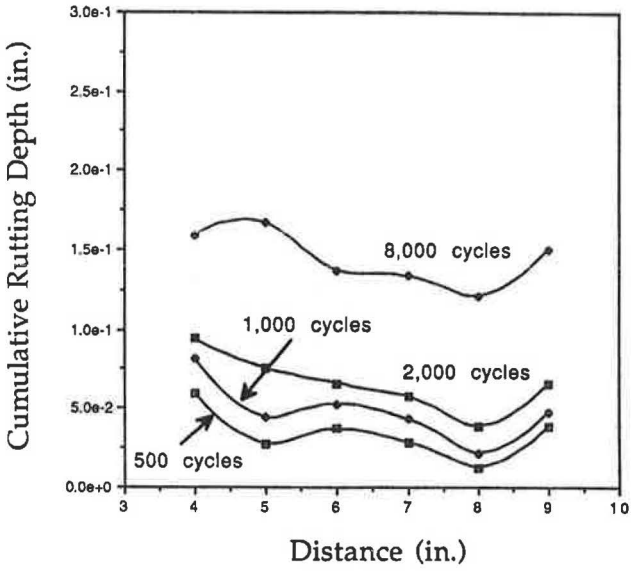

FIGURE 5 Transverse rut profile obtained using LWT.

RUT TEST PROCEDURE

Load Repetitions

A total of 8,000 wheel passes are applied to an asphalt concrete specimen. When the wheel moves in either direction over a particular point, one wheel loading is considered to have been applied. The maximum transverse rut depth is usually measured before the beginning of the test and at the end of 500, 1,000, 2,000, and 8,000 load repetitions as shown in Figure 6. Rut depth is measured at the middle three locations of the deflection template, which correspond to the middle 50.8 mm (2 in.) of a specimen. Measurement of deflection over the middle 50.8 mm (2 in.) was found, because of end effects, to give slightly better results than if the rut measurements are averaged over a longer length of beam. A programmable controller is used to automatically stop the test at the end of each load sequence. Use of the programmable controller greatly minimizes the time required to monitor the test. A counter was also used to measure the total cumulative number of load repetitions applied. The counter was used as a check to verify the total number of repetitions applied since the programmable counter must be set back to zero after each load increment.

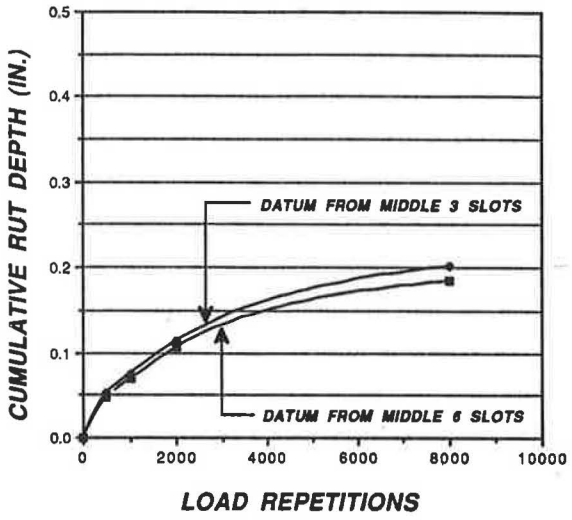

FIGURE 6 Typical variation of observed maximum rut depth with load repetitions.

Wheel Loading

The asphalt concrete beams are subjected to a 903-kN/m^2 (131-psi) average tire pressure through a solid rubber tire. A solid rubber tire has been used in the United Kingdom for a number of years. This type of wheel is considered acceptable by the authors for general comparisons of rut resistance between different mixes. The rubber tire is dead loaded by means of 223 N (50 lb) of lead weight suspended from the loaded hanger. The weight of the wheel and support frame, load hanger, and lever arm supporting the load hanger is also included in determining the total weight applied to the specimen. The load applied by the lever arm load system to a specimen should be accurately measured by temporarily replacing the wheel with a calibrated proving ring. The total applied load is then equal to this value plus the weight of the wheel and its support frame.

Use of a pneumatic rubber tire would be most desirable. A rather extensive search, however, has not identified a suitable source of tire. An alternative approach, developed by Lai (*8*), is to use a heavy hose with plugs inserted in the ends of the hose and clamped. The hose is inflated to the desired air pressure and then stretched out along the wheelpath on the surface of the asphalt concrete beam. A solid metal wheel specially machined to fit the top half of the rubber hose is run back and forth over the hose. The use of a long rubber hose, however, does not give the same loading as a circular pneumatic tire.

For comparisons involving the effect of different tire pressures, a pneumatic tire system should certainly be used. For other types of direct comparisons between mixes, it is the belief of the authors that a solid rubber tire is satisfactory. The LWT test involves a significant reduction in scale of the load and size of the loaded area from the field. This effect is considered a more important possible limitation of the test than whether a solid or pneumatic tire is used. When a suitable source of a pneumatic tire is located, it will be incorporated into the test.

Test Temperature

Rutting in asphalt concrete is very sensitive to test temperature (*5*). Therefore, the loaded wheel test must be conducted at a realistic temperature that is constant to within about ± 0.6°C (± 1°F). The testing temperature used for conditions in Georgia is 104°F, which is about 10°F higher than the average pavement temperature at which rutting occurs in Georgia (*5*).

The loaded wheel tests are performed in a large constant temperature room. After a slight modification of the control system, a temperature controller and a 1350-W heater were used to maintain the temperature within a ± 0.2°F temperature control. The thermostat in the heater was removed with the heater being controlled only by the controller. An electrical relay was placed between the temperature controller and the heater. Good air circulation must also be maintained to achieve a high level of temperature control.

Use of a large temperature-controlled room 4 m by 4 m (13 by 13 ft) in plan and 2.3 m (7.5 ft) high permits storage of specimens at the desired testing temperature and gives free access to a specimen being tested without causing a measurable reduction in temperature of the specimen. Because of the large volume of air in the temperature-controlled room and its large mass of material, rapidly opening and closing the door has no noticeable effect on temperature of the specimen. A thermometer is embedded in a dummy block of asphalt concrete located by the beam to be tested to measure changes in temperature. The asphalt concrete temperature is recorded three times during the test.

Asphalt Concrete Specimens

To date, asphalt concrete beams 127 mm (5 in.) wide and either 76 mm (3 in.) or 90 mm (3.5 in.) thick have been tested in the LWT device described in this paper. The beams 76 mm (3 in.) thick were used to model surface mixes that are usually placed at this thickness in the field. When beams 76 mm (3 in.) thick are used, a steel plate 12.7 mm (0.5 in.) thick is placed in the bottom of the mold. Binder and base mixes tested have been 90 mm (3.5 in.) thick.

The test system is presently set up to take an asphalt concrete beam up to 457 mm (18 in.) long. However, to reduce the required materials used and specimen preparation time, to date only beams that are 254 mm (10 in.) long have been prepared and tested. To account for the shorter length of beam, asphalt concrete filler blocks 76 mm (3 in.) long, which are frequently replaced, are positioned at the ends of the beam to permit using a 292-mm (11.5-in.) length of wheel travel. Use of this length of wheel travel reduces the effects of the wheel stopping and reversing direction that would have occurred for a shorter travel length associated with using just a 254-mm (10-in.) beam length without the extra blocks. Use of 254-mm (10-in.) beams with filler blocks has worked well while reducing the required volume of the asphalt concrete mix by 33 percent.

DISCUSSION AND TEST RESULTS

More than 300 tests have been performed on asphalt concrete surface, binder, and base mixes using the LWT described in

this paper. The only problem encountered has been that one precision bearing required replacement. The system requires periodic maintenance such as the greasing of moving parts. The LWT apparatus can be readily fabricated in a machine shop using about $2,500 in materials and equipment. A list of mechanical and electrical parts used in the apparatus is available from the senior author.

The present Georgia Tech LWT system (as well as the Georgia DOT's system) applies a two-directional loading to the beam. That is, the loaded wheel causes rutting in each direction as the beam (or load) moves back and forth. In contrast, the loading on a pavement is in only one direction. The LWT system described in this paper could easily be changed to one-directional loading by using a pneumatic cylinder to apply the downward force through the wheel while the beam is moving in one direction. While the beam is returning, the pressure on the pneumatic cylinder would be released and then reapplied as the next cycle begins. Also, the Georgia Tech system is designed so that two beams can be tested simultaneously, although this has not yet been done.

The reproducibility of the rut depths determined from the loaded wheel test results, including the effects of sample preparation, is an important consideration. On the basis of 93 tests, the average standard deviation of the test between similar specimens (which should exhibit the same rut depth) is about 14 percent of the average measured rut depth. The standard deviation increases from 11.5 percent for surface mixes to 13 percent for binders and 16 percent for base mixes. The maximum aggregate sizes for the surface, binder, and base mixes are 13 to 19 mm (0.5 to 0.75 in.), 19 to 25 mm (0.75 to 1.0 in.), and 25 to 38 mm (1.0 to 1.5 in.), respectively. The top sizes given correspond to the size for which 100 percent of the particles pass. A study has not been carried out to determine the effect of the 127-mm (5-in.) specimen width on specimen performance. A limited study carried out using a wider wheel [about 37 mm (1.5 in.)] indicated that similar comparisons were obtained between the 28.6-mm (1.125-in.) and 37-mm (1.5-in.) wheels.

These results include the effects of a limited number of different personnel preparing and testing specimens. Perhaps some effects of aggregate properties changing with time are included, since aggregates were obtained from several of the sources at two different times.

Samples were prepared in a steel mold preheated to 177°C (350°F) using a static compaction procedure. The preheated materials were mixed by hand. The aggregate was preheated to 177°C (350°F) and the asphalt cement to 171°C (340°F) following the recommendations of the Asphalt Institute. The specimens were compacted by placing the heated mold containing the loose mixture in a testing machine and compressing the material to the desired thickness using a heavy steel plate the size of the mold. Lai (*9*) reports that this compaction procedure gives results similar to those of the kneading compactor. Details of the procedure used are given elsewhere (*7*).

To illustrate how the LWT can be used, some typical rut depth measurement results are given in Table 1. These results are for (*a*) a standard Georgia DOT mix design and (*b*) a coarser mix, having a slightly larger top size, which was designed to reduce rutting. Mixes from a large number of quarries (up to 21) were included in this study. Although the standard (and also the coarse-graded) mixes are similar for all quarries, some slight variations in grading are present. The results developed using the LWT, for example, indicate that the proposed coarser base mix exhibits an average of 16 percent reduction in rutting compared with the standard Georgia DOT base mix presently used. These results were statistically significant at the 95 percent level. Much larger reductions in rutting are, of course, possible by using the coarser mix for only selected quarries.

The reasonably large variation in rutting for a particular type mix (surface, binder or base) suggests the importance that aggregate properties play in rutting of asphalt concrete mixes. The importance of aggregate properties on rutting has been shown on the basis of results obtained from the LWT (*7*). The Georgia DOT is presently conducting a study to determine whether rut depths observed in the laboratory using the loaded wheel test correlate with observed rutting in the field.

CONCLUSIONS

The LWT offers an excellent device for quantitatively comparing the relative rut susceptibility of one asphalt concrete mix with another. The LWT has several advantages. The stress state applied to the asphalt concrete is similar to that occurring in the field. The testing concept is straightforward, and the loading system is entirely mechanical. Hence, the test can be performed and the tester can be maintained at a minimum of cost by a laboratory technician having a very modest level of technical and mechanical ability. Also, expensive and hard-to-use electronic instrumentation is not required to obtain good results. The loaded wheel test offers an excellent alternative to other laboratory testing techniques when the rutting performance of one mix is to be compared with that of another.

A possible disadvantage of the LWT is that the 1986 AASHTO structural coefficients cannot be evaluated using this procedure since the resilient modulus is not obtained from the test.

TABLE 1 Summary of Measured Rut Depths for Georgia Asphalt Concrete Mixes and Quarries

MIX TYPE	AVERAGE (in.)	RANGE (in.)	STANDARD DEVIATION
1. Base Mix Comparisons			
Standard DOT (39 samples)	0.21	0.09-0.34	0.07
Coarse (32 samples)	0.16	0.07-0.28	0.06
2. Binder Mix Comparisons			
Standard DOT (35 samples)	0.24	0.09-0.40	0.09
Coarse (39 samples)	0.21	0.09-0.34	0.07
3. Surface Mix Comparisons			
Standard DOT (15 samples)	0.30	0.13-0.44	0.11
Coarse (14 samples)	0.25	0.11-0.33	0.07

ACKNOWLEDGMENT

The authors are grateful to the Georgia DOT for sponsoring the study involving the influence of aggregate properties on rutting in asphalt concrete. Special appreciation is expressed to Ronald Collins and Lamar Caylor, who coordinated the project, for their assistance.

REFERENCES

1. *NCHRP Report 39: Factors Involved in the Design of Asphaltic Pavement Surface*. HRB, National Research Council, Washington, D.C., 1967.
2. Kandhal, P. S., S. A. Cross, and E. R. Brown. *Evaluation of Bituminous Pavements for High Pressure Truck Tires*. Report 90-2. National Center for Asphalt Technology, Auburn University, Auburn, Ala., 1990.
3. Godfrey, D. A. Truck Weight Enforcement of a WIM. *Civil Engineering*, American Society of Civil Engineers, Nov. 1986.
4. Sousa, J. B., J. Craus, and C. L. Monismith. *Summary Report on Permanent Deformation in Asphalt Concrete*. SHRP-A/IR-91-104. Strategic Highway Research Program, National Research Council, Washington, D.C., 1991.
5. Barksdale, R. D., and H. A. Todres. *A Study of Factors Affecting Crushed Stone Base Performance*. Report SCEGIT-82-109. School of Civil Engineering, Georgia Institute of Technology, Atlanta, Ga., 1983.
6. Barksdale, R. D., and J. H. Miller. *Developing of Equipment and Techniques for Evaluating Fatigue and Rutting Characteristics of Asphalt Concrete Mixes*. Report SCEGIT-77-147. School of Civil Engineering, Georgia Institute of Technology, Atlanta, Ga., 1977.
7. Barksdale, R. D., C. O. Pollard, T. Siegel, and S. Moeller. *Evaluation of the Effects of Aggregate on Rutting and Fatigue of Asphalt*. Project E20-835. School of Civil Engineering, Georgia Institute of Technology, Atlanta, 1992.
8. Lai, J. S. *Development of a Simplified Test Method to Predict Rutting Characteristics of Asphalt Mixes*. Georgia DOT Research Project 8502. Final report. Georgia Department of Transportation, 1986.
9. Lai, J. S. *Development of a Laboratory Rutting Resistance Testing Method for Asphalt Mixes*. Georgia DOT Research Project 8717. Final report. Georgia Department of Transportation, 1989.

Publication of this paper sponsored by Committee on Mineral Aggregates.

Experience with ASTM P214 in Testing Virginia Aggregates for Alkali-Silica Reactivity

D. S. LANE

Recently identified occurrences of concrete deterioration resulting from alkali-silica reactivity (ASR) have prompted an effort to evaluate Virginia aggregates for their susceptibility to this reaction. The aggregates thus far associated with ASR have been metamorphic rocks of varied composition and quartzose sands and gravels in which the reactive constituents are believed to be microcrystalline or strained quartz. These forms of quartz are present in many aggregates from Virginia. A review of the literature suggests that although the traditional tests (ASTM C227 and C289) for identifying aggregates susceptible to ASR are not effective with aggregates containing microcrystalline or strained quartz, ASTM P214, which is a new method, is promising. To evaluate P214's effectiveness, tests have been conducted on aggregates from Virginia, and the results are being compared with field performance and other relevant information. The results thus far indicate that expansions in P214 may be caused by both ASR and alkali-carbonate reactivity and that current P214 criteria are not suitable for aggregates in Virginia. Further experience with the method is necessary to determine whether suitable criteria can be established to discriminate between nonreactive aggregates and reactive aggregates containing microcrystalline or strained quartz.

Virginia was one of the 19 states in a Strategic Highway Research Program (SHRP) survey (*1*) indicating that it had experienced expansion and cracking of concrete as a result of alkali-silica reactivity (ASR). Although occurrences of ASR in Virginia had been reported in 1941 at a hydroelectric plant (*2*), in 1968 in a pavement (*3*), and in 1972 in a bridge deck (*4*), it was not considered to be of major concern for highway construction. Alkali-carbonate reactivity (ACR), which also causes expansion and cracking of concrete, has received considerable attention in Virginia (*5,6*). The expansion caused by ASR is the result of the swelling of a gel upon the absorption of water. The gel is produced by the dissolution of silica in the aggregate. The expansion caused by ACR is related to the dedolomitization of certain argillaceous, dolomitic limestones.

In 1979, significant longitudinal cracking was observed in a continuously reinforced concrete pavement (CRCP) that had been constructed near Charlottesville in 1970. The cause of this distress was identified as ASR involving the metabasalt (greenstone) coarse aggregate. In 1986, continuing and mounting maintenance problems with this pavement resulted in the decision to remove and replace approximately 6 mi of it.

Virginia Transportation Research Council, Box 3817 University Station, Charlottesville, Va. 22903-0817.

The types of distress associated with ASR are well illustrated in the SHRP handbook by Stark (*7*). These patterns of distress have been observed in CRCP, jointed pavements, bridge decks, substructures, parapets, retaining walls, and median barriers in Virginia. Aggregates associated with alkali-silica gel in such concretes have included metabasalt, granite gneiss, metarhyolite, calc schist, and quartzose natural sands and gravels. These aggregates contain varying amounts of quartz, which occurs in a variety of forms including strained quartz and microcrystalline quartz. Strained quartz has a distorted crystal lattice resulting from postcrystallization deformation evidenced by undulating extinction when viewed with crossed polarized light. Although quartz is apparently less reactive than other forms of silica more traditionally associated with ASR, such as opal, chalcedony, and volcanic glasses, it is sufficiently reactive to cause deterioration (*8*).

The traditional tests for identifying alkali-silica reactive aggregates [ASTM C289 (Quick Chemical Method) and ASTM C227 (Mortar Bar Method)] have been reported to be unreliable in predicting the reactivity of aggregates containing microcrystalline or strained quartz as the reactive constituent (*9–13*). In C227 tests of several Virginia aggregates, expansions have not exceeded the traditional 3-month limit of 0.05 percent, much less the 6-month limit of 0.10 percent, even with tests extended for 27 months. Because quartz appears to be the reactive constituent in the Virginia aggregates, a method that can predict its reactivity is needed if the traditional approach of screening aggregates for ASR potential is to be followed. Hooton and Rogers (*14*) have reported good results using a rapid mortar bar method proposed by Oberholster and Davies (*15*). For the purpose of evaluation, an adaptation of this test was adopted by ASTM as "P214 Proposed Test Method for Accelerated Detection of Potentially Deleterious Expansion of Mortar Bars Due to Alkali-Silica Reaction" (*16*).

PURPOSE AND SCOPE

As part of a project investigating the occurrence of alkali-silica reactivity in Virginia, a number of aggregates were tested using P214. The results were compared with other available information pertaining to the potential ASR of the aggregates to evaluate the effectiveness of method P214 for screening or specification purposes.

METHODOLOGY

Samples of aggregates known or suspected to be susceptible to ASR as well as several aggregates believed to be nonreactive were obtained. The aggregates were tested according to method P214. In this method, aggregates are crushed (if necessary) to fine aggregate size (<4.75 mm, < No. 4), washed, and screened to a fixed gradation:

Sieve Size	*Mass (%)*
4.75–2.36 mm (No. 4–No. 8)	10
2.36–1.18 mm (No. 8–No. 16)	25
1.18 mm–600 μm (No. 16–No. 30)	25
600–300 μm (No. 30–No. 50)	25
300–150 μm (No. 50–No. 100)	15

Mortars are mixed using portland cement and a water-cement ratio of 0.44 if the aggregate is a natural sand or 0.50 if crushed. After mixing, 25- by 25- by 275-mm (1- by 1- by 11-in.) bars are fabricated and stored moist for 24 hr.

When the bars are 1 day old, they are stripped from the molds, measured for length, immersed in room temperature water, and placed in an environment at 80°C. When the bars are 2 days old, they are measured for length (zero reading) and then placed in 1 N sodium hydroxide (NaOH) solution at 80°C. Bars are stored in the NaOH solution at 80°C for 14 days or longer and are periodically measured for changes in length. A large increase in length may be indicative of the potential for ASR.

A low-alkali Type II portland cement from one plant was used in mixing all of the batches. According to P214, expansions in the test are not significantly affected by the alkali content of the cement used. The chemical composition of the cement was as follows:

Component	*Percentage*
SiO_2	21.1
Al_2O_3	3.6
Fe_2O_3	2.3
CaO	62.7
MgO	3.8
SO_3	2.5
$Na_2O + 0.658 \times K_2O$	0.43

Duplicate batches for aggregates were mixed on separate days. Three bars from each batch were soaked in the NaOH solution. In most cases, the bars were soaked for at least 28 days.

RESULTS

The results of the P214 tests are given in Table 1. The expansion listed for each batch is the average expansion of three bars. Aggregates classified as alkali-silica reactive in Table 1 have been associated with alkali-silica gel in concretes exhibiting typical ASR crack patterns. The granite gneiss from Shelton, which is classified as suspected ASR, was used in concrete exhibiting typical ASR crack patterns, but field concrete has not yet been examined for the presence of ASR gel. A classification of undetermined indicates that the field performance of the aggregate has not yet been characterized.

The dolomite from Harrisonburg was a sample of the highly expansive alkali-carbonate reactive aggregate "1–8" discussed by Newlon and Sherwood (*5*). Some particles of the Augusta limestone exhibit the characteristic texture associated with alkali-carbonate rocks of dolomite rhombs in a matrix of fine-grained calcite and finely disseminated clay.

Collections of alkali-silica gel were visible in polished slabs of tested bars made with all of the aggregates except the Augusta, Harrisonburg, and Blacksburg carbonates. When broken, the surface of an Augusta limestone bar was examined using the UV-gel fluorescence test (*7*), and gel was indicated on the surfaces of some aggregate particles. The presence of gel was not indicated in the specimens made with the Harrisonburg and Blacksburg aggregates when examined with this method. In a rough, qualitative sense, the amount of gel produced appeared to be related to the amount of expansion for most aggregates. The notable exceptions were the Augusta and Harrisonburg aggregates.

DISCUSSION OF RESULTS

The criteria used in ASTM P214 (*14*) for evaluating test results are as follows:

- Mean expansion of test specimens exceeding 0.20 percent after 14 days of exposure to NaOH solution is indicative of potentially deleterious expansion with respect to ASR.
- Mean expansion of test specimens of less than 0.10 percent after 14 days is indicative of innocuous behavior with respect to ASR.
- Mean expansion of test specimens of 0.10 to 0.20 percent after 14 days is not yet conclusive with respect to ASR.

The preceding criteria were used to classify the susceptibility of the tested aggregates to ASR (see Table 1).

Of the aggregates classified as potentially reactive, the Richmond gravel and Rockville metarhyolite have been associated with ASR in the field. The Sylvatus quartzite has only recently been used as a concrete aggregate, and a service history is not available. Given its petrographic character, it should be classified as potentially reactive.

The Augusta limestone, although expanding considerably in the test, did not produce large amounts of gel, which would be expected if the expansion were resulting from ASR. Some particles exhibit the petrographic characteristics of ACR rocks. The Harrisonburg dolomite, which is a known ACR rock, expanded in the test about the same amount. This suggests that the expansion of the Augusta limestone in P214 may be the result of combined ASR and ACR effects or the ACR effects alone. The expansion of the Harrisonburg dolomite indicates that the P214 test may be effective in detecting aggregates susceptible to ACR. It is interesting that the ACR aggregate reduced to the size of sand expands considerably in this test since size reduction is the general explanation given for the ineffectiveness of the ASTM C227 mortar bar test to detect ACR aggregates.

The inconclusive group includes two aggregates associated with ASR in the field (Richmond sand and Mt. Athos calc schist) and a third (Shelton granite gneiss), which is suspected of field reactivity. All three give expansions in excess of 0.15 percent (but less than 0.20 percent) after 14 days in NaOH.

The Warrenton diabase and the Fredericksburg gravel both yield expansions between 0.10 and 0.15 percent. Although

TABLE 1 Aggregate Source, Type, Performance, and P214 Results

Aggregate Source	Rock Type	Field Performance	C 227 Expansion	P214 Expansion (%) Batch	14 d	28 d	P 214 Classification
Augusta	Dolomitic Limestone	Undetermined	—	1	0.24	—	
				2	0.22	—	
				Avg	0.23		Reactive
Harrisonburg	Argillaceous Calcitic Dolomite	Alkali-carbonate reactive	—	1	0.24	—	
				2	0.22	—	
				Avg	0.23		Reactive
Blacksburg	Argillaceous Dolomite	Good	—	1	0.09	—	
				2	0.08	—	
				Avg	0.09	—	Innocuous
Warrenton	Diabase	Good	—	1	0.15	0.36	
				2	0.11	—	
				Avg	0.13	0.36	Inconclusive
Fredericksburg	Quartzose Sand	Undetermined	—	1	0.10	0.19	
				2	0.08	0.21	
				Avg	0.09	0.20	Innocuous
Fredericksburg	Quartzose Gravel	Undetermined	—	1	0.13	0.28	
				2	0.10	0.28	
				Avg	0.12	0.28	Inconclusive
Richmond	Quartzose Sand	Alkali-silica reactive	0.045% (1) @ 27 months	1	0.18	0.38	
				2	0.19	0.36	
				Avg	0.19	0.37	Inconclusive
Richmond	Quartzose Gravel	Alkali-silica reactive	0.016% (2) @ 6 months	1	0.31	0.50	
				2	0.32	0.48	
				Avg	0.32	0.49	Reactive
Rockville	Metarhyolite	Alkali-silica reactive	0.014% (2) @ 6 months	1	0.40	0.59	
				2	0.38	—	
				Avg	0.39	0.59	Reactive
Sylvatus	Quartzite	Undetermined	0.021% (2) @ 6 months	1	0.27	0.42	
				2	0.30	0.43	
				Avg	0.29	0.43	Reactive
Mt. Athos	Calc schist	Alkali-silica reactive	0.012% (2) @ 6 months	1	0.18	0.32	
				2	0.16	0.28	
				Avg	0.17	0.30	Inconclusive
Shelton	Granite gneiss	Suspected alkali-silica reactive	—	1	0.18	0.30	
				2	0.16	0.26	
				Avg	0.17	0.28	Inconclusive
Red Hill	Granite gneiss	Alkali-silica reactive	0.049% (1) @ 27 months	1	0.07	0.14	
				2	0.06	—	
				Avg	0.07	0.14	Innocuous
Shadwell	Metabasalt	Alkali-silica reactive	0.038% (1) @ 27 months	1	0.08	0.14	
				2	0.09	0.16	
				Avg	0.09	0.15	Innocuous

(1) Personal communication, D. Stark. Tests conducted by CTL, Inc. under SHRP contract using cement with 1% Na_2O equivalent.
(2) Tests conducted by Virginia Transportation Research Council using cement with 1% Na_2O equivalent.

the field performance of the Warrenton aggregate is reported to be good, that of the Fredericksburg gravel has yet to be determined. However, gravel from Fredericksburg was used by Buck and Mather (*10*) in their work on the reactivity of quartz because its composition was similar to that of sands and gravels associated with ASR in Charleston, South Carolina. The Fredericksburg gravels are composed primarily of quartz and quartzite and differ from those of the Richmond area in being relatively chert-free. The relative abundance of chert composed of microcrystalline quartz is at least a partial explanation of the higher expansions of the Richmond gravels and sands. Although Buck and Mather (*10*) conclude that the reactive constituent in these aggregates is strained quartz, Grattan-Bellew (*17*) suggests that strained quartz per se is not reactive; rather, microcrystalline quartz associated with the strained quartz in such aggregates is the reactive element.

In any case, it appears that the Fredericksburg gravel, the Richmond sand, the Mt. Athos calc schist, and Shelton granite gneiss should be considered potentially reactive. The results with the Warrenton diabase, which would seem an unlikely candidate for ASR, are still unclear. Because of the expansions and the gel produced, a closer look at field structures, particularly older ones, should be taken.

The Blacksburg dolomite, the Fredericksburg sand, the Red Hill granite gneiss, and the Shadwell metabasalt were classified as innocuous with respect to ASR. The Blacksburg dolomite showed no evidence of reactivity in the tested mortar bars; undoubtedly, it is innocuous with respect to ASR. However, both the Red Hill granite gneiss and Shadwell metabasalt have been associated with field occurrences of ASR. The low expansions of these aggregates in the P214 test present a drawback to its widespread use until the relationship between deleterious reactivity in the field and expansion in the test is more clearly understood. The Fredericksburg sand (like the Fredericksburg gravel discussed above) is compositionally similar to aggregates in a reported case of ASR.

The Red Hill granite gneiss, Shadwell metabasalt, and probably the Fredericksburg sand should be considered potentially reactive.

CONCLUSIONS

The P214 method for testing an aggregate's potential for deleterious ASR appears to be capable of causing both the alkali-silica reaction and the alkali-carbonate reaction to occur in mortar bars in approximately 2 weeks. In this respect, it is a significant improvement over the C227 method.

However, the criteria listed in P214 for evaluating expansion results do not appear to be reliable in classifying the ASR potential of all the aggregates tested. Lowering the expansion limit for potentially deleterious reactivity to 0.10 percent would improve the situation but would not totally solve the problem because there are at least two reactive aggregates with expansions less than 0.10 percent. One of these, the Red Hill granite gneiss, has many petrographically similar counterparts in the Piedmont of Virginia, and establishing a limit that excludes it may result in the misclassification of other reactive aggregates. Clearly, more experience with the test is needed to develop a better understanding of the relationship between an aggregate's expansion in the test and its reactivity in the field.

Although P214 is capable of identifying many reactive aggregates not so identified by C289 or C227, the results reported here are supportive of Hooton's suggestion (*18*) that because some reactive gneisses and quartzites from the eastern seaboard of the United States do not expand in the method, it may not be suitable for evaluating those aggregates.

To establish appropriate criteria, a wide range of aggregates with known performance histories should be tested to determine whether expansions in P214 can be used to discriminate between deleteriously and nondeleteriously reactive aggregates. At the present time, appropriate limits cannot be established that would allow the use of P214 as a specification tool for Virginia aggregates.

REFERENCES

1. *SHRP Focus*. Strategic Highway Research Program, April 1989.
2. Kammer, H. A., and R. W. Carlson. Investigation of Causes of Delayed Expansion of Concrete in Buck Hydroelectric Plant. *Journal of the American Concrete Institute*, Vol. 37, June 1941, pp. 665–671.
3. Walker, H. N. *Deterioration of the Pentagon Network of Roads—Concrete Durability Studies*. Virginia Transportation Research Council, Charlottesville, 1969.
4. Whitlow, B. S. Investigation of Deterioration in Concrete Roadway Slab of the Robert E. Lee Bridge, Richmond, Virginia. *23rd Annual Highway Geology Symposium*, Virginia Transportation Research Council, Charlottesville, 1972, pp. 91–108.
5. Newlon, H. H., Jr., and W. C. Sherwood. Methods for Reducing Expansion of Concrete by Alkali-Carbonate Rock Reactions. In *Highway Research Record 45*, HRB, National Research Council, Washington, D.C., 1964, pp. 134–150.
6. Sherwood, W. C., and H. H. Newlon, Jr. A Survey for Reactive Carbonate Aggregates in Virginia. In *Highway Research Record 45*, HRB, National Research Council, Washington, D.C., 1964, pp. 222–234.
7. Stark, D. *Handbook for the Identification of Alkali-Silica Reactivity in Highway Structures*. SHRP-C/FR-91-101. Strategic Highway Research Program, 1991.
8. Ozol, M. A., and D. O. Dusenberry. Deterioration of Precast Concrete Panels with Crushed Quartz Coarse Aggregate Due to Alkali-Silica Reaction. *Durability of Concrete, G. M. Idorn International Symposium* (J. Holm and M. Geiker, eds.). ACI SP-131. American Concrete Institute, Detroit, Mich., 1992, pp. 407–415.
9. Grattan-Bellew, P. E. Study of the Expansivity of a Suite of Quartzwackes, Argillites, and Quartz Arenites. *Proc., Fourth International Conference on the Effects of Alkalies in Cement and Concrete*, Publication CE-MAT-1-78, Purdue University, West Lafayette, Ind., 1978, pp. 113–140.
10. Buck, A. D., and K. Mather. *Reactivity of Quartz at Normal Temperatures*. Technical Report SL-84-12. U.S. Army Corps of Engineers Waterways Experiment Station, Vicksburg, Miss., 1984.
11. Berra, M., and G. Baronio. The Potential Alkali-Aggregate Reactivity in Italy: Comparison of Some Methods to Test Aggregates and Different Cement-Aggregate Combinations. *Concrete Alkali-Aggregate Reactions* (P. E. Grattan-Bellew, ed.), Noyes Publications, Park Ridge, N.J., 1986, pp. 231–236.
12. Oberholster, R. E., M. A. Brandt, and A. C. Weston. The Evaluation of Graywacke, Hornfels, and Granite Aggregates for Potential Alkali Reactivity. *Proc., Fourth International Conference on the Effects of Alkalies in Cement and Concrete*, Publication CE-MAT-1-78, Purdue University, West Lafayette, Ind., 1978, pp. 141–162.
13. Oberholster, R. E. Results of an International Inter-Laboratory Test Program To Determine the Potential Alkali Reactivity of Aggregates by the ASTM C227 Mortar Prism Method. *Concrete Alkali-Aggregate Reactions* (P. E. Grattan-Bellew, ed.), Noyes Publications, Park Ridge, N.J., 1986, pp. 368–374.
14. Hooton, R. D., and C. A. Rogers. Evaluation of Rapid Methods for Detecting Alkali-Reactive Aggregates. Alkali-Aggregate Reaction (K. Okada, S. Nishibayashi, and M. Kawamura, eds.), Elsevier Applied Science, New York, 1989. pp. 439–444.
15. Oberholster, R. E., and G. Davies. An Accelerated Method for Testing the Potential Alkali Reactivity of Siliceous Aggregates. *Cement and Concrete Research*, Vol. 16, No. 2, 1986, pp. 181–189.
16. P214 Proposed Test Method for Accelerated Detection of Potentially Deleterious Expansion of Mortar Bars Due to Alkali-Silica Reaction. *Annual Book of ASTM Standards, Vol. 04.02 Concrete and Aggregates*, ASTM, Philadelphia, Pa., 1990, pp. 739–742.
17. Grattan-Bellew, P. E. Is High Undulatory Extinction in Quartz Indicative of Alkali-Expansivity of Granitic Aggregates? *Concrete Alkali-Aggregate Reactions* (P. E. Grattan-Bellew, ed.), Noyes Publications, Park Ridge, N.J., 1986, pp. 434–438.
18. Hooton, R. D. *New Aggregate Alkali-Reactivity Test Methods*. MAT-91-14. Ontario Ministry of Transportation, Toronto, Ontario, Canada, 1991.

The opinions, findings, and conclusions expressed in this paper are those of the author and not necessarily those of the sponsoring agencies.

Publication of this paper sponsored by Committee on Mineral Aggregates.

Evaluation of Alabama Limestone Aggregates for Asphalt Wearing Courses

PRITHVI S. KANDHAL, FRAZIER PARKER, JR., AND EMAD A. BISHARA

The Alabama Highway Department does not permit the use of limestone coarse aggregate in asphalt wearing courses because of potential long-term skid resistance problems. A laboratory study was undertaken to evaluate 32 sources of limestone aggregates in Alabama for possible use in the wearing courses. Twelve approved sources of gravel aggregate were also evaluated for comparison. The frictional properties of all aggregates were determined using the British pendulum tester (ASTM E303) after 9 hr of accelerated polishing on the British wheel (ASTM D3319). Aggregates were also subjected to petrographic analysis. The percentage of noncarbonate material in limestone aggregates was determined by two methods: percent insoluble residue (ASTM D3042) and percent loss on ignition (Tennessee DOT method). The British pendulum number (BPN) values were found to follow a hyperbolic relationship with polishing time. This relationship can possibly be used to predict the limiting BPN value after infinite polish time. There was a general trend that the value of BPN9 (BPN value after 9 hr of polishing) increased as the percentage of insoluble residue increased or the percentage loss by ignition decreased. On the basis of BPN9 values, limestone aggregates were divided into three categories: potentially low, medium, and high skid-resistance levels. If BPN9 is used as an acceptance criterion, the limestone aggregates of the medium and high categories have the potential to provide skid resistance levels comparable with gravel aggregates used at the present time.

The highway pavement system requires aggregates of multifunctional characteristics to meet various demands. For asphalt wearing courses these characteristics not only include strength and durability but also adequate skid resistance. Aggregates having all these properties are often not locally available and have to be imported, thereby increasing delivered costs.

Limestone aggregates are readily available in northern Alabama. However, their use in asphalt wearing course mixes is not currently permitted by the Alabama Highway Department (AHD) because of potential long-term skid resistance problems. Therefore, the use of crushed gravel, slag, and other types of noncarbonate aggregates is required. However, some siliceous aggregates, particularly gravel, have the following disadvantages: low resistance to water damage (stripping and raveling), high asphalt absorption (high asphalt requirement), and partially crushed nature (low strength and stability). Crushed limestone generally does not exhibit these undesirable characteristics. However, its potential lack of long-term skid resistance must be evaluated before its use in asphalt wearing courses.

P. S. Kandhal, National Center for Asphalt Technology, 211 Ramsay Hall, Auburn University, Auburn, Ala. 36849. F. Parker, Jr., Highway Research Center, 238 Harbert Engineering Center, Auburn University, Auburn, Ala. 36849. E. A. Bishara, Auburn University, 211 Ramsay Hall, Auburn, Ala. 36849.

In a recent study sponsored by AHD, limestone aggregates were evaluated in asphalt wearing courses (*1*). Laboratory tests showed that limestone aggregates were beneficial in increasing the stability of the mix and its resistance to moisture damage. In two field evaluations, mixes with approximately 30 percent limestone provided better skid resistance than control mixes with 100 percent siliceous aggregate. Figure 1 is from one of these evaluations after approximately 3,000,000 vehicle passes. It shows how skid resistance of the pavement, as measured with the locked-wheel trailer (SN) and the British pendulum tester (BPN), varied with time. At a third field site there was no discernible difference in skid resistance. It was important, therefore, that additional sources of limestone aggregates be evaluated to determine their possible use in wearing courses to take advantage of their durability and stability.

OBJECTIVES

This study was undertaken to achieve the following objectives:

1. Review available literature pertaining to the use of limestone aggregates in asphalt wearing courses.
2. Conduct a nationwide survey through a questionnaire to obtain information about states' experiences with the use of limestone aggregates in asphalt wearing courses.
3. Fingerprint approved sources of limestone and crushed gravel by running various physical tests and by petrographic examination.
4. Analyze data to determine correlations between British pendulum number (BPN) and other aggregate properties.
5. Classify aggregates into three levels (low, medium, or high) of skid resistance on the basis of laboratory tests.

BACKGROUND AND LITERATURE REVIEW

Skid resistance characteristics of the asphalt wearing course are principally determined by the properties of aggregates used because aggregates constitute more than 90 percent of the asphalt paving mix.

According to Sherwood and Mahone (*2*) and Gandhi et al. (*3*), limestone aggregates tend to polish more readily than other commonly used aggregates. Sherwood and Mahone (*2*) found that the majority of Virginia limestones tested in their study tended to become slick when subjected to heavy traffic. However, it has also been established by other investigators (*4–6*) that many limestones differ significantly in polish sus-

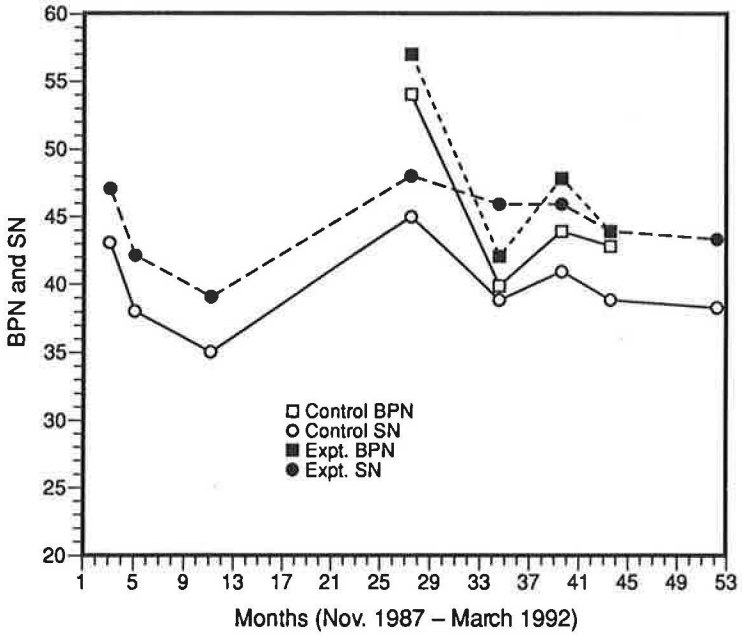

FIGURE 1 Comparison of control and experimental mix frictional performance.

ceptibility. These differences have been attributed primarily to the noncarbonate or acid insoluble constituents in the rock.

Polish susceptibility may be evaluated using a number of different testing techniques. These techniques include (*a*) the British wheel/pendulum method, (*b*) circular track wear method, (*c*) percent acid insoluble residue, (*d*) locked-wheel skid trailer, (*e*) stopping distance on paved surfaces, and (*f*) petrographic analysis.

British Wheel/Pendulum Method

The British wheel/pendulum method (ASTM D3319 and ASTM E303) has been used extensively by researchers including a recent evaluation by Diringer (*7*) in New Jersey. In this method, polish susceptibility is indicated by the so-called polish value (PV), which is a measure of the state of polish reached by a test specimen subjected to accelerated polishing. Diringer's results (*7*) were in agreement with New Jersey's experience from previous studies (*8,9*), where it was documented that crushed gravel mixes yielded superior skid resistance, whereas carbonate rock mixes provided marginal skid resistance over the long term.

Gandhi (*10*) tested various types of aggregates in Puerto Rico for polishing value. He concluded that correlations between the polish value and other aggregate properties such as specific gravity, absorption, abrasion value, initial friction value, percent insoluble residue, and sand size residue were very poor.

Circular Track Wear Method

The circular track wear method (*11*) was used by Dahir and Mullen (*12*). In this method, pavement samples, manufactured from the aggregate to be evaluated, are placed in a circular track and subjected to wear from small-diameter pneumatic tires. Pavement specimens could usually be brought to terminal polish in about 16 hr. Skid resistance values are determined by using the British pendulum tester.

Percent Acid Insoluble Residue Method

Dahir and Mullen (*12*) also used the insoluble residue test (ASTM D3042) in their study of four carbonate aggregates. In this test the insoluble residue reflects the amount of noncarbonate material in limestone (carbonate) aggregates. A large amount of noncarbonate material may indicate higher polish resistance. Dahir and Mullen (*12*) concluded that the acid insoluble residue percentages for the four carbonate aggregates indicated that skid resistance improved with increased residue content and that sand-size residue was probably more important than total residue. Using the polarizing microscope method, the authors found that the sand-sized insoluble residue consisted of hard siliceous particles, mostly quartz. Similar findings have been reported by other investigators (*13–19*). Sherwood (*20*) and Gray and Renninger (*13*) showed that the amount and nature of the acid insoluble mineral grains contained in limestones were primarily responsible for their variable wearing characteristics.

Locked-Wheel Skid Trailer Method

The locked-wheel skid trailer method (ASTM E274) is a field technique that measures the pavement skid resistance. The trailer is usually towed at 40 mph, water is sprayed on the pavement surface, and the trailer wheels are locked to measure skid resistance. When the test wheel is locked, the resistance offered by the pavement surface is measured by a torque-measuring device in the trailer. This resistance is converted into a numerical value called skid number (SN).

Dahir et al. (*21*) used various polishing methods and friction measurement techniques, such as the locked-wheel skid trailer method and the British pendulum tester, to determine the

correlations between laboratory and field skid resistance test results. They found that the general level of skid-resistance characteristics of surface aggregates may be determined in the laboratory and that the aggregates may be ranked similarly by both approaches.

Stopping Distance Method

The stopping distance method (ASTM E445/E445M) is a field technique that characterizes the pavement surface skid resistance by the so-called stopping distance number (SDN). In this method a passenger vehicle with four wheels is used. The pavement in the test lane is wetted. The test vehicle is brought above the desired test speed and is permitted to coast onto the wetted section until the proper speed is attained. The brakes are then promptly and forcefully applied to cause a quick lockup of the wheels and to skid to a stop. The distance required to stop is recorded.

Sherwood and Mahone (*2*) used skid test data and coefficient of friction measurements, measured by different test methods, compiled for 23 years to propose the acid insoluble residue test for differentiation between skid resistance of different aggregates. For the sake of uniformity the authors converted all the skid test data and reported them as 40-mph stopping distance skid numbers using conversion curves developed by Dillard and Allen (*22*). The authors found that a simple relationship existed between the total acid insoluble residue percentages of Virginia limestones and their polish resistance (as indicated by the stopping distance skid number).

Petrographic Analysis Method

Dahir and Mullen (*12*) used the petrographic analysis method to determine the percentages of minerals and their hardness from thin sections of aggregates. The authors concluded that within the various aggregates tested in their study, a mixture of different minerals with different hardness in the same aggregate had a positive influence on skid resistance.

Most carbonate rocks tested by Gandhi et al. (*3*) were pure limestones. Their results showed that polishing of aggregates did not depend entirely on mineral composition. Other factors, such as texture of the rock (grain size, shape, and grain to grain relationship), degree of alteration, cementation, nature of cementating material, nature of impurities present, and porosity, could have considerable influence on polishing.

QUESTIONNAIRE

To obtain information about other states' experiences and current practices with the use of limestone aggregates in asphalt wearing courses, a questionnaire was sent to highway officials in the 50 states and the Canadian provinces.

The detailed results of this questionnaire, based on responses given by 43 states and Ontario, Canada, are given elsewhere (*23*). Figure 2 shows the responses concerning the use of limestone as coarse aggregate in the wearing course.

Seven states responded that they do not use limestone in asphalt wearing course mixes. Limestone aggregate did not meet their specifications or was not available in their region.

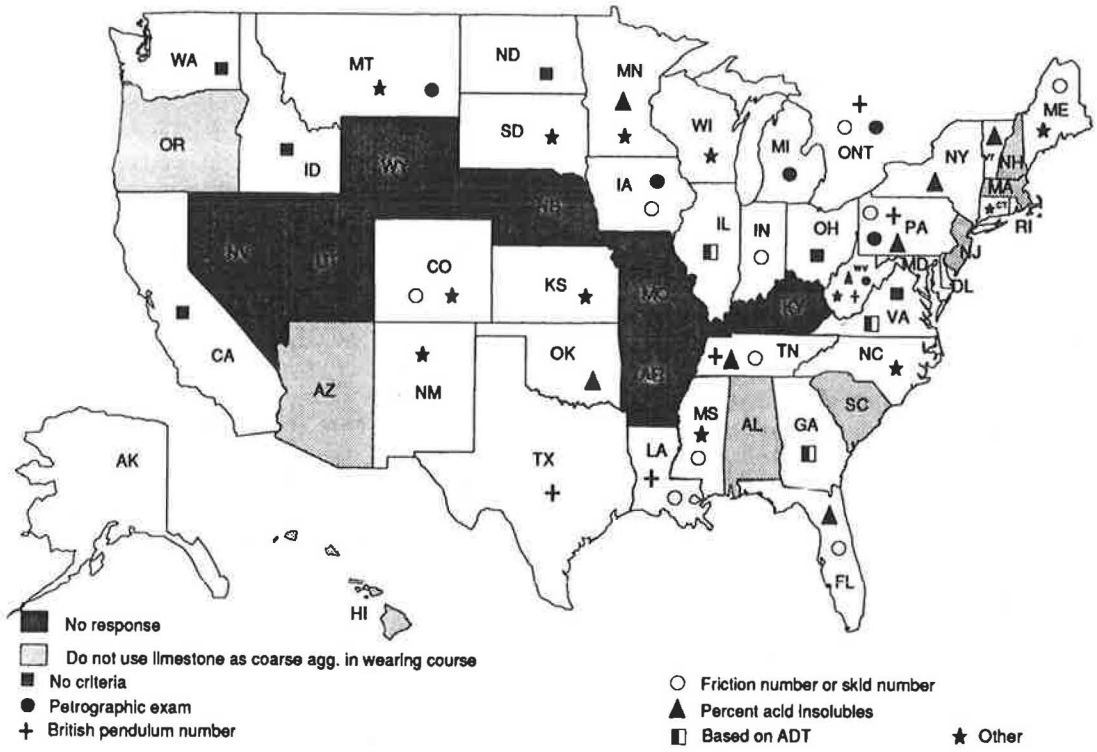

FIGURE 2 Response to the questionnaire on the use of limestone as coarse aggregate.

Eight states use the acid insoluble residue test in evaluating limestone aggregates for polish susceptibility. The skid trailer is used by nine states. Five states use the British pendulum and five states use petrographic analysis. Some states restrict the use of limestone aggregate based on the average daily traffic, and some use more than one criterion as shown in Figure 2.

MATERIALS AND TESTING METHODOLOGY

Materials

Two types of aggregates were used in this study: limestone and gravel. These aggregates were obtained from sources in Alabama approved for use in hot mix asphalt. Physical properties (obtained from AHD) are given in Tables 1 and 2. Thirty-two limestone and 12 gravel aggregates from AHD-approved sources were used. However, there are other approved sources of gravel that are not listed on the approved source list. The limestone aggregate serial number was assigned an A code and the gravel a B code.

Testing Methodology

Aggregate fractions passing the 12.7-mm (½-in.) sieve and retained on the 9.5-mm (⅜-in.) sieve were used for preparing test samples for the British pendulum test. Aggregate fractions passing the 9.5-mm (⅜-in.) sieve and retained on the 4.75-mm (No. 4) sieve were also used for the insoluble residue test and for the loss by ignition test.

The tests conducted are described in the following subsections.

Accelerated Polishing of Aggregates Using the British Wheel (ASTM D3319)

This test method simulates the polishing action of vehicular tires under conditions similar to those occurring on coarse aggregates used in asphalt pavements. A polish value is determined that may be used to classify coarse aggregates by ability to resist polishing under traffic.

Polishing wheel specimens consisting of bare aggregate particles were prepared to fit on the periphery of the accelerated polishing wheel. A rubber-tired wheel rubs against the polishing wheel when both are rotating. Silicon carbide grit and water are fed to accelerate the polishing action. Five replicate samples for each quarry were polished in this manner.

Measurement of Surface Frictional Properties Using the British Pendulum Tester (ASTM E303)

This test method is used to determine the relative effects of the British polishing wheel on coarse aggregates in terms of

TABLE 1 Physical Properties of Limestone Aggregates

SOURCE #	Bulk Specif. Gravity	Absorption %	L.A. Abrasion % Wear	Sod.Sulf. Soundness % Sound
A-1	2.800	0.7	40.0	99.8
A-2	2.600	1.3	24.9	99.7
A-3	2.815	0.5	26.9	99.6
A-4	2.678	0.8	22.8	99.8
A-5	2.565	1.6	27.8	99.7
A-6	2.663	0.9	36.8	97.9
A-7	2.695	0.7	19.8	99.6
A-8	2.672	0.9	20.8	99.1
A-9	2.707	0.8	22.0	98.7
A-10	2.600	1.2	29.0	99.9
A-11	2.729	0.6	28.3	99.7
A-12	2.694	0.5	22.3	99.1
A-13	2.776	0.5	19.5	99.9
A-14	2.703	0.4	24.8	99.8
A-15	2.722	0.4	23.1	99.8
A-16	2.805	0.5	24.5	99.6
A-17	2.629	1.8	22.8	97.4
A-18	2.686	0.6	21.8	99.4
A-19	2.664	1.0	24.2	99.6
A-20	2.804	0.6	17.9	99.1
A-21	2.608	1.0	32.8	98.4
A-22	2.667	0.9	20.0	99.2
A-23	2.647	0.8	25.6	99.7
A-24	2.633	0.8	20.2	99.8
A-25	2.516	2.0	19.1	99.9
A-26	2.654	0.9	27.1	99.6
A-27	2.680	0.7	21.8	99.7
A-28	2.718	0.7	19.6	99.6
A-29	2.707	1.6	22.4	99.6
A-30	2.682	0.6	20.8	99.5
A-31	2.658	0.7	24.0	99.7
A-32	2.808	0.6	21.5	99.8

TABLE 2 Physical Properties of Gravel Aggregates

SOURCE #	Bulk Specific Gravity	Absorption %	L.A. Abrasion % Wear	Sod. Sulf. Soundness % Sound
B-1	2.399	3.7	23.6	99.1
B-2	2.318	4.5	15.5	100.0
B-3	2.330	5.0	16.7	98.9
B-4	2.376	4.1	13.5	99.7
B-5	2.480	2.2	39.0	99.4
B-6	2.444	3.0	15.5	99.3
B-7	2.597	0.6	24.8	99.9
B-8	2.316	4.5	15.5	99.8
B-9	2.567	1.2	36.1	99.0
B-10	2.467	2.7	33.2	98.5
B-11	2.601	0.6	29.4	99.4
B-12	2.342	4.1	17.3	99.1

polish value. A dynamic pendulum impact-type tester was used to measure the energy loss when a rubber slider edge is propelled over a test surface. The test surface is wet before testing to simulate worst conditions and for correlation with field tests such as the locked-wheel skid trailer. BPNs are dimensionless values that represent the frictional properties of the tested surface. BPN values of all test specimens were obtained by removing the specimens from the polishing wheel at set intervals (3, 6, and 9 hr) and testing with the British pendulum. This was done to evaluate the rate of polishing with time.

Percent Insoluble Residue in Carbonate Aggregates (ASTM D3042)

This test gives the percentage of noncarbonate (insoluble) material in carbonate aggregates, which may indicate the polish susceptibility or friction properties of aggregate used in asphalt pavements.

A 500-g sample of aggregate is placed in a glass beaker and is reacted with several increments of hydrochloric acid solution until effervescence is stopped completely. The aggregate residue is washed over a 75-μm (No. 200) sieve, dried, and sieved again. The weight of the plus 75-μm (No. 200) residue is determined and expressed as a percentage of the original sample weight. The gradation of the insoluble residue was not analyzed to determine the sand size fraction, which many believe is critical for skid resistance.

Percent Loss on Ignition of the Mineral Aggregate (Tennessee Department of Transportation Method)

This test gives the percentage of weight loss when aggregates are subjected to a very high ignition temperature. It is an indicator of the relative percentages of carbonate and noncarbonate material in an aggregate.

This test is used by the Tennessee Department of Transportation to restrict the carbonate content of aggregate used in surface mixes. The basic principle of the test is same as that of the acid insoluble residue test. A 300-g sample of aggregate is heated in a muffle furnace at 950°C for a minimum of 8 hr. The samples are weighed before and after heating. The loss in the weight of the sample provides an indication of the carbon dioxide driven from the calcium or magnesium carbonate and is expressed as percent of the original weight.

Petrographic Analysis

This analysis was performed by a geologist in the Geology Department at Auburn University and identifies the constituent minerals of an aggregate and their characteristics. The analysis is done using different approaches for limestone and gravel aggregates. It consists of descriptions of thin sections made from quarry rock samples for limestone aggregates and visual inspection for gravel aggregates. The analysis determines the relative percentage of each mineral type present in an aggregate. The results of petrographic analysis are given elsewhere (*23*).

PRESENTATION AND ANALYSIS OF RESULTS

As mentioned earlier, the BPN is a measure of the frictional characteristics of test specimens subjected to accelerated polishing reported for various polish times. It is reported from an average of three to five specimens depending on the survivability of specimens during polishing. The relationship between the BPN value and polish time follows a hyperbolic function (*1,24*):

$$\text{BPN} = \text{BPN0} - \frac{t}{a + bt} \tag{1}$$

where BPN is the British pendulum number value at time t (hours), BPN0 = British pendulum number value at time 0 (initial BPN), and a and b are constants calculated from following equations:

$$a = \frac{t1\ t2}{t2 - t1}\left(\frac{1}{\text{dBPN1}} - \frac{1}{\text{dBPN2}}\right) \tag{2}$$

$$b = \frac{1}{t2 - t1}\left(\frac{t2}{\text{dBPN2}} - \frac{t1}{\text{dBPN1}}\right) \tag{3}$$

where dBPN1 and dBPN2 are differential BPNs for polish times $t1$ and $t2$, respectively. These values are defined as follows:

$$dBPN1 = BPN1 - BPN0$$

$$dBPN2 = BPN2 - BPN0$$

As the polish time approaches infinity, the BPN value described by Equation 1 approaches the so-called limiting BPN value (BPNL):

$$\lim_{t\to\infty} BPN = BPN0 - \lim_{t\to\infty} \frac{t}{(a + bt)} \quad (4)$$

Hence,

$$BPNL = BPN0 - \frac{1}{b} \quad (5)$$

The limiting BPN value can be estimated from Equation 5 provided both BPN0 and b are known. The former is obtained experimentally and the latter is calculated from Equation 3 and requires measuring BPN values after two polishing intervals.

Results of the average BPN values measured at 0-hr polish time (BPN0) and 9-hr polish time (BPN9) and corresponding estimated limiting BPN values (BPNL) are given in Tables 3 and 4 for limestone and gravel aggregates, respectively. Also included in Table 3 are the values of ΔBPN (BPN0 − BPN9), percent loss by ignition (%LI) and percent insoluble residue (%IR). As shown in Table 3, values of BPN9 for the 32 limestone aggregates tested in this study range from 24 to 36. The range of BPN9 for gravel aggregates (12 sources) is from 27 to 34 (see Table 4). Therefore, values of BPN9 for both limestone and gravel aggregates tested in this study are quite comparable.

Using correlation analysis (SAS program), simple statistics and a correlation matrix among all parameters of the study were developed (see Tables 5 and 6). The top number in each cell is the coefficient of correlation between the two variables defining the cell. The bottom number in each cell is developed from hypothesis testing and indicates the significance of the correlation; lower numbers imply greater significance. The

TABLE 3 Test Results for Limestone Aggregates

SOURCE #	BPN0	BPN9	BPNL	ΔBPN	% LI	% IR
A-1	47	32	29	15	45.68	3.48
A-2	44	33	32	11	34.76	20.51
A-3	43	30	28	13	44.59	0.68
A-4	41	28	27	13	42.29	1.95
A-5	44	33	32	11	37.90	13.04
A-6	43	29	28	14	40.38	1.29
A-7	42	29	28	13	42.36	0.57
A-8	42	31	30	11	39.59	8.79
A-9	44	35	35	9	38.58	6.33
A-10	41	32	29	9	39.18	7.30
A-11	44	27	18	17	44.07	0.27
A-12	38	30	28	8	41.28	2.00
A-13	44	30	26	14	42.68	0.80
A-14	38	28	27	10	38.36	0.85
A-15	40	29	21	11	43.32	2.49
A-16	44	32	30	12	44.45	1.31
A-17	43	31	30	12	38.19	1.57
A-18	42	30	29	12	42.45	0.5
A-19	45	31	30	14	37.00	15.88
A-20	41	27	22	14	41.42	9.73
A-21	46	32	31	14	42.00	0.00
A-22	45	35	32	10	39.14	2.54
A-23	39	29	29	10	39.78	6.8
A-24	43	35	33	8	40.12	7.53
A-25	48	36	34	12	30.72	29.13
A-26	41	29	28	12	41.05	3.50
A-27	46	33	32	13	40.30	3.21
A-28	42	27	24	15	41.66	5.97
A-29	38	26	25	12	46.21	0.83
A-30	45	35	34	10	39.76	0.39
A-31	45	32	26	13	38.52	0.52
A-32	40	24	22	16	42.98	0.01

Notations: BPN0 = British pendulum number value at 0 hour
BPN9 = British pendulum number value at 9 hours
BPNL = limiting British pendulum number value
ΔBPN = BPN0 - BPN9
% LI = percent loss by ignition
% IR = percent acid insoluble residue (plus No. 200)

TABLE 4 Test Results for Gravel Aggregates

SOURCE #	BPN0	BPN9	BPNL	ΔBPN
B-1	35	30	30	5
B-2	39	30	27	9
B-3	41	30	22	11
B-4	39	32	31	7
B-5	45	34	31	11
B-6	37	27	26	10
B-7	36	29	27	9
B-8	40	29	25	11
B-9	37	29	26	8
B-10	41	32	31	9
B-11	37	33	32	4
B-12	40	31	16	9

numbers are expressions of probability, in decimal form, that the correlations are not significant. For the purpose of this study, the correlation coefficient will be considered low if below 0.50, fair if between 0.50 and 0.80, and good if above 0.80.

In addition to correlations for BPN0, BPN9, ΔBPN, %LI, and %IR, correlations for %SIL, %DOL, %CAL, BSG, and %ABS are shown in Table 5. The terms %SIL, %DOL, and %CAL indicate, respectively, the percentages of silica, dolomite, and calcite determined in the petrographic analysis of the limestone aggregates. The terms BSG and %ABS are, respectively, the aggregate bulk specific gravity and percent absorption. Correlations in Table 6 include the variables %CHERT, %QUARTZ, and %SANDSTONE. These terms indicate, respectively, the percentages of chert, quartz, and sandstone determined in the petrographic analysis of the gravel aggregates.

Relationship Between BPN9 and BPNL

Since polish time of 9 hr was the maximum examined in this study, it was important to determine the correlations between BPN9 and BPNL values for both limestone and gravel aggregates.

Coefficients of correlation between the BPN9 and the BPNL are 0.85 and 0.42 for limestone and gravel aggregates, respectively. This relationship is shown in Figure 3 for limestone

TABLE 5 Correlation Matrix for Limestone Aggregates

	BPN0	BPN9	BPNL	ΔBPN	%LI	%IR	%SIL	%DOL	%CAL	BSG	%ABS
BPN0	1.00000 0.0	0.68086 0.0001	0.47390 0.0061	0.26863 0.1371	-0.32151 0.0728	0.33094 0.0643	0.18528 0.3100	-0.16447 0.3684	0.14727 0.4212	-0.22019 0.2259	0.24363 0.1790
BPN9		1.00000 0.0	0.85382 0.0001	-0.52260 0.0022	-0.55744 0.0009	0.41408 0.0185	0.22777 0.2099	-0.42502 0.0153	0.41040 0.0196	-0.50825 0.0030	0.30436 0.0903
BPNL			1.00000 0.0	-0.57126 0.0006	-0.54913 0.0011	0.38450 0.0298	0.26959 0.1357	-0.46572 0.0072	0.44732 0.0103	-0.53302 0.0017	0.39167 0.0266
ΔBPN				1.00000 0.0	0.35887 0.0437	-0.15934 0.3837	-0.08388 0.6481	0.36752 0.0385	-0.36830 0.0381	0.41212 0.0191	-0.11667 0.5248
%LI					1.00000 0.0	-0.76887 0.0001	-0.55098 0.0011	0.53073 0.0018	-0.48082 0.0053	0.75538 0.0001	-0.54729 0.0012
%IR						1.00000 0.0	0.70531 0.0001	-0.25302 0.1623	0.17667 0.3334	-0.55340 0.0010	0.59373 0.0003
%SIL							1.00000 0.0	-0.30032 0.0949	0.19037 0.2967	-0.56062 0.0008	0.59261 0.0004
%DOL								1.00000 0.0	-0.99357 0.0001	0.80860 0.0001	-0.42818 0.0145
%CAL									1.00000 0.0	-0.76567 0.0001	0.37033 0.0369
BSG										1.00000 0.0	-0.71040 0.0001
%ABS											1.00000 0.0

TABLE 6 Correlation Matrix for Gravel Aggregates

	BPN0	BPN9	BPNL	ΔBPN	%CHERT	%QUARTZ	%SANDSTONE	BSG	%ABS
BPN0	1.00000 0.0	0.56103 0.0577	-0.06461 0.8419	0.70702 0.0101	0.00102 0.9975	0.04598 0.8872	-0.26746 0.4007	-0.32175 0.3078	0.29681 0.3488
BPN9		1.00000 0.0	0.41870 0.1755	-0.18874 0.5569	-0.34461 0.2727	0.32888 0.2966	0.08039 0.8039	0.13735 0.6704	-0.14996 0.6418
BPNL			1.00000 0.0	-0.43435 0.1583	-0.44244 0.1498	0.40696 0.1892	0.19023 0.5537	0.44806 0.1441	-0.41849 0.1758
ΔBPN				1.00000 0.0	0.29562 0.3509	-0.22641 0.4792	-0.38598 0.2153	-0.49904 0.0986	0.48022 0.1141
%CHERT					1.00000 0.0	-0.98450 0.0001	-0.06178 0.8487	-0.87639 0.0002	0.88947 0.0001
%QUARTZITE						1.00000 0.0	-0.11424 0.7237	0.87484 0.0002	-0.89155 0.0001
%SANDSTONE							1.00000 0.0	-0.01129 0.9722	0.03537 0.9131
BULK S.G.								1.00000 0.0	-0.99001 0.0001
%ABS									1.00000 0.0

aggregates. The lower correlation between BPNL and BPN9 in the case of gravel aggregates may be a result of the use of a smaller number of sources compared with limestone aggregates.

Relationship Between BPN9 and BPN0

It was important to evaluate the relationship between the frictional value (BPN) at 9 hr and that at zero time to determine the effect of polishing. As shown in Table 5, the correlation coefficient between BPN9 and BPN0 for limestone is 0.68. The corresponding coefficient for gravel aggregates (Table 6) is 0.56. These results indicate that the BPN value measured at a certain time is partially dependent on the initial BPN value.

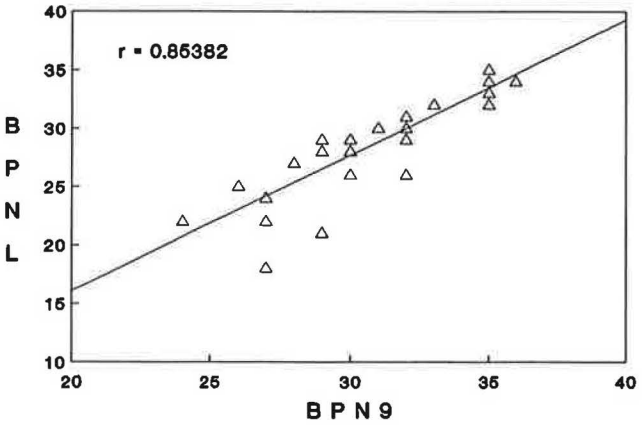

FIGURE 3 BPN9 versus BPNL values for limestone aggregates.

Categorization of BPN9 Values for Both Limestone and Gravel Aggregates

To divide the BPN9 values into low, medium, and high categories, the full range of BPN9 values for both limestone and gravel aggregate sources examined in this study was arbitrarily subdivided into three about equal ranges. This procedure resulted in the following categories and ranges (see Figures 4 and 5): low BPN9, below 28; medium BPN9, 28 to 32; and high BPN9, above 32.

AHD permits the use of all gravel aggregates. The lowest BPN9 for gravel aggregates used in this study is 27. If BPN9 is used as an acceptance criterion, the limestone aggregates with medium and high BPN9 (28 to 32 and 33 to 36, respectively) should also be permitted. However, their performance

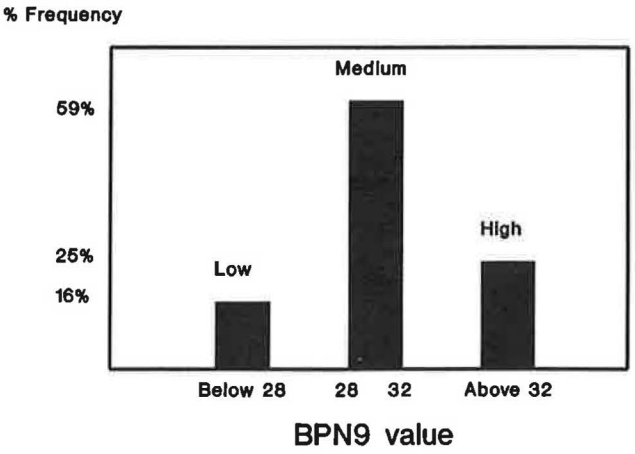

FIGURE 4 Categories of limestone aggregates based on BPN9 values.

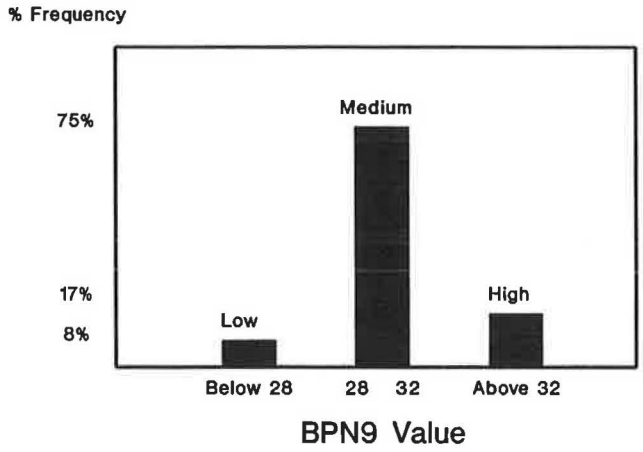

FIGURE 5 Categories of gravel aggregates based on BPN9 values.

should be confirmed in the field. Figure 6 shows the changes in BPN values with respect to time for typical limestone aggregates from low, medium, and high categories. Curves shown in the figures are theoretical plots of the BPN-time relationship based on the hyperbolic function given in Equation 1. There was good agreement between the experimental observations and the theoretical function for both types of aggregates in all these categories. Accordingly, it is expected that the hyperbolic function will provide a good tool for estimating aggregate's BPN value after different polishing times.

Results of Insoluble Residue

Results of the percentage insoluble residue for all the limestone aggregate sources examined in this study are given in Table 3. These values range from 0.00 to 29.13 percent. The correlation coefficient between the percentage insoluble residue (%IR) and other parameters is given in Table 5. A positive correlation coefficient of 0.41 is found between the percentage insoluble residue and the BPN9. The relationship between the two parameters is given by

$$BPN9 = 29.7 + 0.02(\%IR) \quad (6)$$

There is a general trend that as the percentage of insoluble residue increases, the value of BPN9 also increases, but the degree of correlation is poor. This is likely due to variability in the composition and gradation of the residue material: both influence friction.

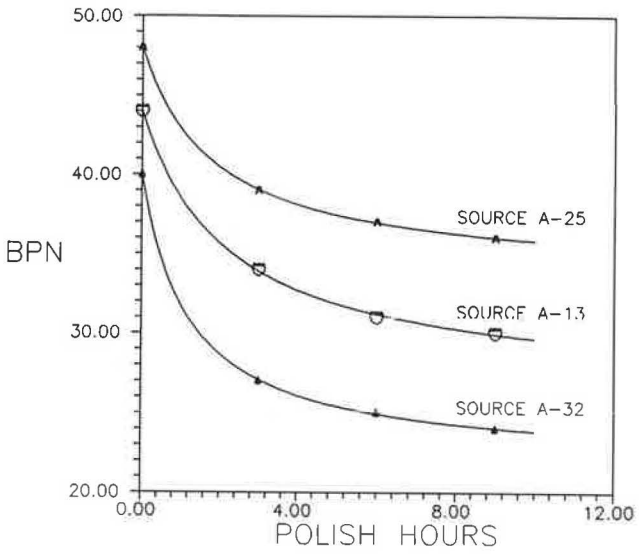

FIGURE 6 Polish hours versus BPN values for three limestone aggregates.

Results of Percentage Loss by Ignition

Results of the percentage loss by ignition for all the limestone aggregate sources examined in this study are given in Table 3. These values range from 30.73 to 46.22 percent. The correlation coefficient between the percentage loss by ignition (%LI) and BPN9 is given in Table 5. A negative correlation coefficient of -0.56 is found between the percentage loss by ignition and the BPN9. The relationship between the two parameters is given by

$$BPN9 = 52.0 - 0.5(\%LI) \quad (7)$$

There is a general trend that as the percentage loss by ignition decreases, the value of BPN9 increases, but there is a relatively low degree of correlation.

The correlation results given in Table 5 also show that a high negative correlation of -0.77 exists between the percentage insoluble residue and the percentage loss by ignition. This high correlation is probably a result of the fact that the two methods use the same concept of measuring the amount of carbonates in the aggregates.

CONCLUSIONS AND RECOMMENDATIONS

On the basis of the test data obtained and analyzed in this study the following conclusions are drawn and recommendations made:

1. The BPN or polish values were found to follow a hyperbolic relationship with polishing time. The relationship can possibly be used to predict the ultimate or limiting BPN value (BPNL) at infinite polish time.
2. A wide range of BPN values after 9 hr of polish (BPN9) exists for limestone aggregates (24 to 36). This may be a result of the different constituents of the rocks such as calcite, silica, dolomite, and other minerals. It may also be due to differences in crystalline structure that result in different densities, porosity, fracture shape, surface texture, and so forth.
3. There is a general trend that as the percentage of insoluble residue increases the value of BPN9 also increases. However, the poor degree of correlation obtained suggests that the BPN value cannot be statistically predicted from percent insoluble residue.
4. There is also a general trend that as the percentage loss by ignition decreases the value of BPN9 increases. However, the low correlation obtained suggests that the BPN value

cannot be statistically predicted from the percentage loss by ignition.

5. The coefficient of correlation between values of percentage loss by ignition and those of percentage insoluble residue was determined to be −0.77. This fairly good correlation between the two parameters exists because both measure the amount of carbonates in different ways.

6. The results of this laboratory study have made it possible to establish categories of potentially low, medium, and high skid resistance levels of limestone aggregates for Alabama. On the basis of 9-hr BPN values, these categories have ranges of 24 to 27, 28 to 32, and 33 to 36 for low, medium, and high levels, respectively.

7. AHD permits the use of all gravel aggregates. The lowest BPN9 for gravel aggregates used in this study is 27. If BPN9 is used as an acceptance criterion, the limestone aggregates with medium and high BPN9 (28 to 32 and 32 to 36, respectively) have the potential to provide skid resistance comparable with gravel aggregates used at the present time.

8. A field evaluation of limestone aggregate sources falling into various categories based on 9-hr BPN values (BPN9) is being conducted. Short sections utilizing 75 to 85 percent limestone aggregates are being constructed and will be evaluated periodically with locked-wheel skid trailer. The various sources can then be categorized finally on the basis of field measurements rather than 9-hr BPN values measured in the laboratory.

ACKNOWLEDGMENTS

This research project was sponsored by the Alabama Highway Department and the Auburn University Highway Research Center.

REFERENCES

1. Manglorkar, D., P. S. Kandhal, and F. Parker. *Evaluation of Limestone Aggregate in Asphalt Wearing Courses*. Research Report, Project ST2019-10. Highway Research Center, Auburn University, 1991.
2. Sherwood, W. C., and D. C. Mahone. *Predetermining the Polish Resistance of Limestone Aggregates*. Virginia Highway Research Council, Charlottesville, 1970.
3. Gandhi, P. M., B. Colucci, and S. P. Gandhi. Polishing of Aggregates and Wet Accident Rate in Flexible Pavements. Presented at the 70th Annual Meeting of the Transportation Research Board, Washington, D.C., 1991.
4. Shelburne, T. E., and R. L. Sheppe. *Highway Research Board Research Report 5-B: Skid Resistance Measurements of Virginia Pavements*. HRB, National Research Council, Washington, D.C., 1948.
5. Nichols, F. P., J. H. Dillard, and R. L. Alwood. Skid Resistant Pavements in Virginia. *Highway Research Board Bulletin 139*, HRB, National Research Council, Washington, D.C., 1956, pp. 35–59.
6. Nichols, F. P. Further Studies on Skid Resistance of Virginia Pavements. *Proc., First International Skid Prevention Conference*, Part 2, 1959, pp. 461–468.
7. Diringer, K. T. *Aggregates and Skid Resistance*. New Jersey Department of Transportation, 1990.
8. Afferton, K. C. *Further Evaluation of Skid Resistance Characteristics of Carbonate Rock Aggregates*. New Jersey Department of Transportation, 1978.
9. Quinn, J. J. *Evaluation of Skid Resistant Thin Bituminous Overlays*. New Jersey Department of Transportation, 1972.
10. Gandhi, P. M. *Evaluation of Skid Resistance Characteristics of Aggregates Used for Highway Construction in Puerto Rico*. Puerto Rico Department of Transportation and Public Works, 1978.
11. Mullen, W. G., S. H. M. Dahir, and B. D. Barnes. Two Laboratory Methods for Evaluating Skid-Resistance Properties of Aggregates. In *Highway Research Record 376*, HRB, National Research Council, Washington, D.C., 1971.
12. Dahir, S. H. M., and W. G. Mullen. Factors Influencing Aggregate Skid Resistance Properties. In *Highway Research Record 376*, HRB, National Research Council, Washington, D.C., 1971, pp. 136–148.
13. Gray, J. E., and F. A. Renninger. Limestones with Excellent Nonskid Properties. *Crushed Stone Journal*, Vol. 35, No. 4, 1960, pp. 6–11.
14. Balmer, G. G., and B. E. Colley. Laboratory Studies of the Skid Resistance of Concrete. *Journal of Materials*, ASTM, Vol. 1, No. 3, 1966, pp. 326–559.
15. Shupe, J. W., and R. W. Lounsbury. Polishing Characteristics of Mineral Aggregates. *Proc., First International Skid Prevention Conference*, Virginia Council of Highway Investigation and Research, Charlottesville, Part 2, 1959, pp. 590–599.
16. Burnett, W. C., J. L. Gibson, and E. J. Kearney. Skid Resistance of Bituminous Surfaces. In *Highway Research Record 236*, HRB, National Research Council, Washington, D.C., 1968, pp. 49–60.
17. Colley, B. E., A. P. Christensen, and W. J. Nowlen. Factors Affecting Skid Resistance and Safety of Concrete Pavements. In *Special Report 101*, HRB, National Research Council, Washington, D.C., 1969, pp. 80–99.
18. Shapiro, L., and W. W. Brannock. *U.S. Geological Survey Bulletin 1144A: Rapid Analysis of Silicate, Carbonate and Phosphate Rocks*. 1962.
19. Sherwood, W. C., and D. C. Mahone. Predetermining the Polish Resistance of Limestone Aggregates. In *Highway Research Record 341*, HRB, National Research Council, Washington, D.C., 1970.
20. Sherwood, W. C. *A Study of the Crystallization and Mineral Content of Some Virginia Limestones with Possible Relationship to Their Skid Resistance Performance*. Progress Report 1, Virginia Highway Research Council, 1959.
21. Dahir, S. H., W. E. Meyer, and R. Hegmon. Laboratory and Field Investigation of Bituminous Pavement and Aggregate Polishing. In *Transportation Research Record 584*, TRB, National Research Council, Washington, D.C., 1976.
22. Dillard, J. H., and T. M. Allen. Comparison of Several Methods of Measuring Road Surface Friction. *Proc., First International Skid Prevention Conference*, Part 2, 1959, pp. 381–410.
23. Kandhal, P. S., and E. A. Bishara. *Evaluation of Limestone Aggregates in Asphalt Wearing Courses—Phase II*. Report IR-92-03. Auburn University Highway Research Center, March 1992.
24. Kandhal, P. S., and M. A. Khatri. Evaluation of Asphalt Absorption by Mineral Aggregates. *Asphalt Paving Technology*, Vol. 60, 1991.

The opinions, findings, and conclusions expressed here are those of the authors and not necessarily those of the Alabama Highway Department or Auburn University.

Publication of this paper sponsored by the Committee on Mineral Aggregates.

Aggregate Type and Traffic Volume as Controlling Factors in Bituminous Pavement Friction

WILLIAM H. SKERRITT

The New York State Department of Transportation's (NYSDOT's) Pavement Friction Inventory program has collected friction data on 155 pavement sites since testing began in 1980. The data gathered were analyzed and the adequacy of the current high-friction aggregate specification, in place since 1970, was determined. Data from another 66 sites, gathered as part of a previous NYSDOT study, were included. Together, the 221 sites tested represent most combinations of coarse aggregate rock types and traffic volumes normally encountered in New York State. The coefficient of friction for a pavement at terminal polish, as determined by a drag-force trailer in accordance with ASTM E274, was found to be controlled mostly by coarse aggregate rock type and daily traffic volume, expressed as lane average annual daily traffic (LAADT). Mineral aggregates used in New York State were divided into three rock-type categories—homogeneous, sandy, and blended—each having a distinct polishing mode. Semilog plots of friction number versus LAADT were constructed for each rock type, showing whether each rock type is performing adequately and, if not, under what traffic conditions its use must be restricted.

The purpose of the study reported here was to analyze pavement friction data and determine the adequacy of New York's current high-friction aggregate specification. Data from 155 pavement sites were gathered as part of an ongoing Pavement Friction Inventory (PFI) program administered by the Materials Bureau of the New York State Department of Transportation (NYSDOT). Data from another 66 sites had been gathered previously by the NYSDOT Engineering Research and Development Bureau and were included in the analysis.

Friction properties of bituminous pavement surfaces were derived from their macro- and microtextural roughness. Macrotexture is roughness due to aggregate size, shape, and gradation. Microtexture [which depends on the petrology or rock physical characteristics of exposed individual particles (*1–4*)] and the lane average annual daily traffic (LAADT) have been good predictors of pavement friction (*5,6*). NYSDOT has relied on a high-friction aggregate (HFA) specification (given later in the paper) that defines which aggregates are to be used in terms of rock type, acid-insoluble residue (AIR) content, and minimum blending percentages. The department's PFI program monitors performance of aggregates meeting the HFA specification, using a matrix of aggregate rock types and daily traffic volumes as encountered throughout the state (Table 1).

Materials Bureau, New York State Department of Transportation, 1220 Washington Avenue, Bldg. 7A, Room 200, State Office Building Campus, Albany, N.Y. 12232.

SITE SELECTION AND FRICTION MEASUREMENT

The PFI was established in 1978 in response to a Federal Highway Administration requirement to monitor pavement friction performance. NYSDOT's monitoring program is based on testing pavement sections representative of highway construction throughout the state. Selection of a PFI site involves field evaluation of potential sections, pavement coring, and petrographic analysis of aggregate extracted from these cores to determine proportions of the various rock types present in the coarse fraction. Field evaluation avoids any pavement having problems that might affect friction measurements, such as flushing or raveling. Also, close examination of the pavement flushing indicates whether aggregates are uniformly distributed throughout the potential test section. Depending on the HFA type used, petrographic analysis includes appropriate determinations of constituent rock types, percentage of noncarbonate materials in blended aggregate, and AIR. Acceptable test sites are fitted into the inventory matrix according to their aggregate classification and LAADT, as indicated in Table 1. All PFI sites have been and will continue to be scrutinized in this manner.

All friction testing is performed with the NYSDOT two-wheeled drag-force trailer, using a procedure conforming to ASTM E274 with a standard ribbed test tire (ASTM E249). Tests are run at 64 kph (40 mph) and 89 kph (55 mph) on roughly tangent pavement sections over a distance of 0.48 km (0.3 mi). The department considers paving materials and surface texture to be adequate when measured friction number (FN) [wet at 64 kph (40 mph)] is 32 or higher. This number was selected as a minimum design target value because it corresponds to the friction assumed by AASHTO in calculating stopping distances.

AGGREGATE CATEGORIES

Aggregates may be separated into three categories on the basis of their polishing characteristics: homogeneous, sandy, and blended (Table 1). Each responds to traffic wear in its own way.

Homogeneous Rock Types

Homogeneous rock types contain mineral constituents having roughly the same Moh's hardness (a scratch hardness rating

TABLE 1 Sites in the PFI Matrix

Aggregate Type	Lane AADT					
	-1K	1K-2K	2K-5K	5K-10K	10K-20K	20K-30K
HOMOGENEOUS						
Traprock	0	3	1	2	2	2
Granite	5	1	1*	0*	0*	0*
Limestone						
Dolomite						
Wappinger	0	2	2	2	2	1
Lockport	2	7	9	1	0*	0*
Other	3	2	2	0	0	0
SANDY						
Sandstone	3	6	6	0	0	0
Siliceous Limestone	4	7	3	0*	0*	0*
Siliceous Dolomite	3	4	13	4	2	0*
BLENDS						
Limestone/Non-Carb.	18	21	21	8	4	0*
Dolomite/Non-Carb.	0	o	0	1*	1*	0*
Gravel	2	4	2	0*	0*	0*

*More sites being sought

on a scale of 1 to 10, reflecting a mineral's resistance to wear) and include traprock, granite, limestone, and dolomite. Uniform Moh's hardness results in even particle wear in the pavement surface. The two carbonate rocks included in this category, limestone and dolomite, have low AIRs. Of the two, dolomite is allowed by the current HFA specification to be used alone in top courses in NYSDOT projects. Since the HFA specification does not allow use of limestone alone as the coarse aggregate, no such sites were tested.

Sandy Rock Types

These rock types contain quartz sand either as the major constituent or as a significant component and include sandstone, siltstone, quartzite, siliceous limestone, and siliceous dolomite. The last two are carbonate rocks having high AIRs.

Aggregate Blends

These contain two or more rock types, both carbonate and noncarbonate. Since the noncarbonate rock types capable of meeting NYSDOT quality requirements have Moh's hardnesses much greater than carbonates and are consequently more resistant to wear and polish, they provide most of the friction in these blends.

ANALYSIS OF TEST DATA AND DISCUSSION

Friction of new pavements comes mostly from macrotexture, since the aggregate is still coated with asphalt. As traffic wears the surface, aggregate is exposed and polished. Eventually, all coarse aggregate particles at the surface are abraded to an equilibrium condition referred to as "terminal polish" (*1*,*2*,*7*) (Figure 1). It generally takes 2 to 3 years of exposure to traffic before that condition is reached (*5*,*6*). Testing normally begins on PFI sites 2 or more years after construction, and the data show no decline in FN. A non-PFI site, tested shortly after construction and for the next 2 years because of anticipated inadequate friction performance, showed rapid decline in driving lane friction within the first year (Figure 2). Many sites were tested annually 8 to 10 times, and all were tested at least twice. The data show that FN for any given site fluctuates about an average. Thus, the coefficient of friction for each site is expressed as an arithmetic average of all FN. Only the FNs determined at 64 kph (40 mph) were used in the analysis because they can be related to the established design minimum FN of 32.

Data for each rock type were plotted as average FN at 64 kph (40 mph) versus LAADT on a semilog grid. When all other variables are eliminated, traffic volume shows an inverse relationship to friction in all aggregate categories. Table 2 gives FNs for pavement sites where both driving and passing lanes were tested at terminal polish. When both lanes have the same mix, contain the same aggregates, and are constructed under essentially the same conditions, the only remaining significant variable is traffic volume. Under such conditions, the driving lane, which invariably carries more traffic than the passing lane, always has a lower FN, regardless of aggregate type.

The amount of AIR in a carbonate aggregate and the amount of noncarbonate particles in an aggregate blend are significant factors in pavement friction (*7*). These considerations were incorporated into the HFA specification tested in this study.

Homogeneous Rock Types

Initial analyses included these aggregates because they involve the fewest variables. In Figure 3 data from sites containing

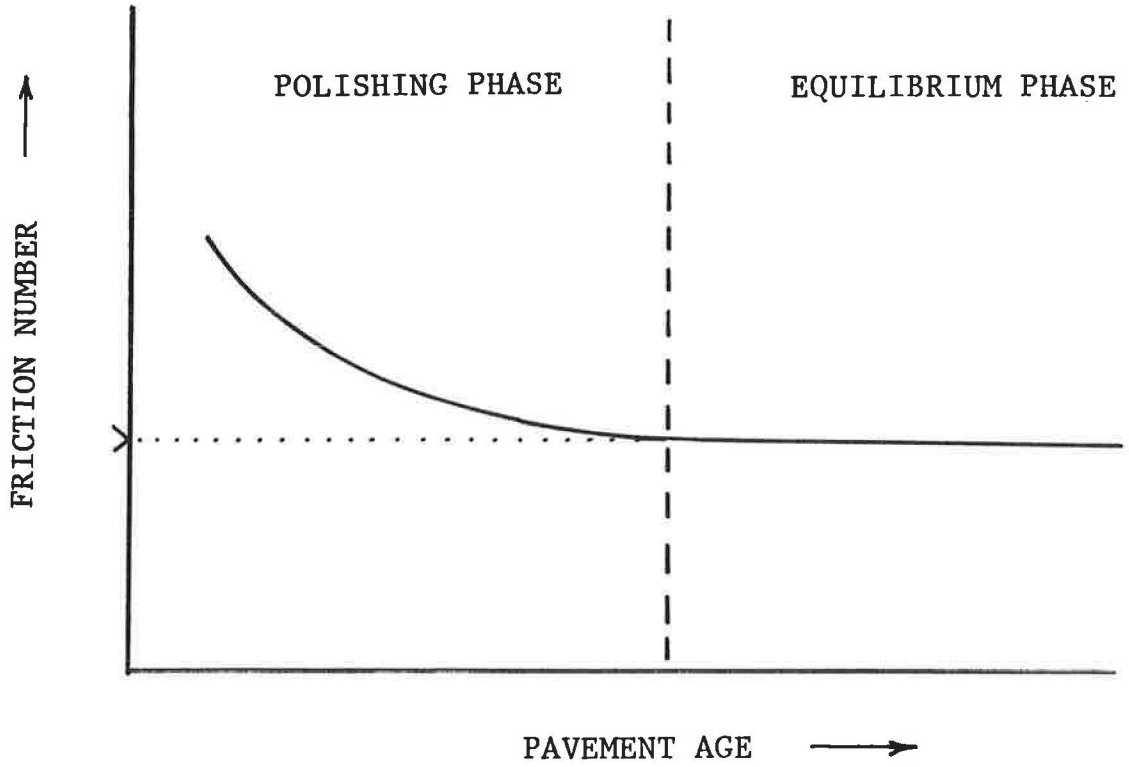

FIGURE 1 Generalized pavement polishing model in which a "terminal polish" condition is reached, first shown in laboratory studies (*1*,*2*).

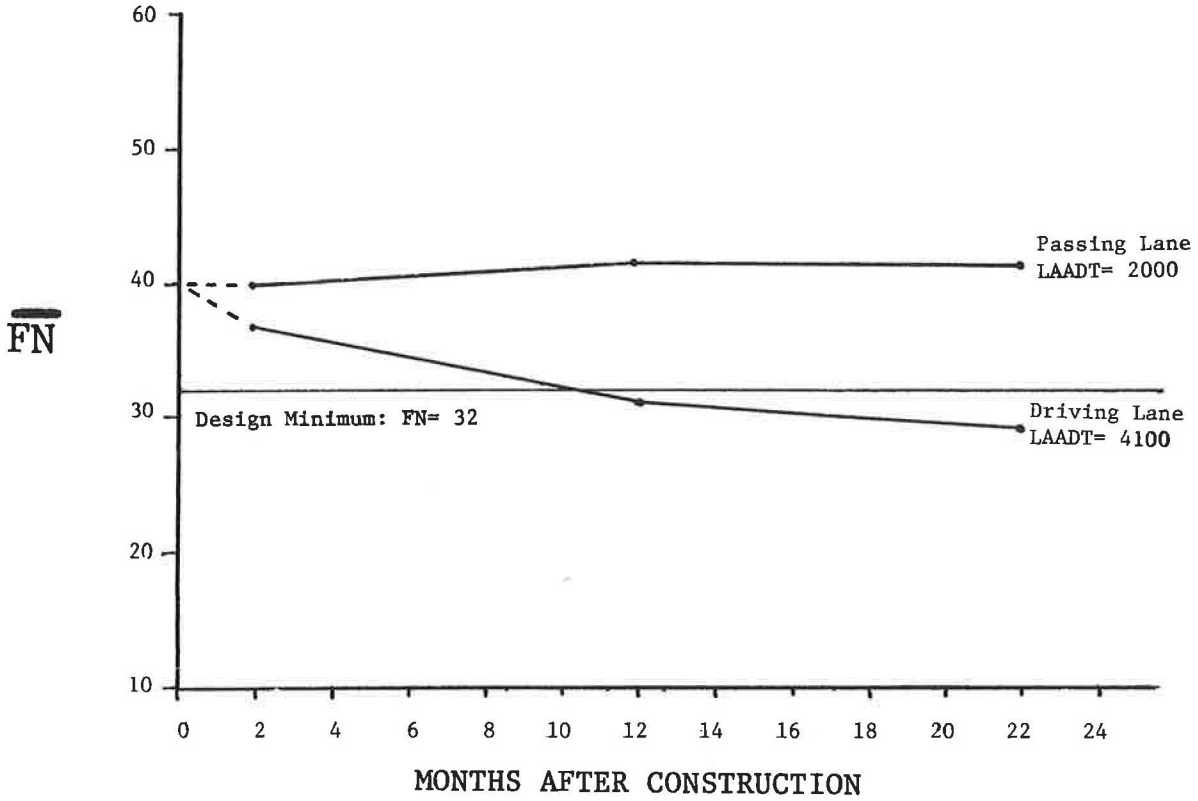

FIGURE 2 Average FN at 64 kph (40 mph) versus LAADT for a pavement made of blended aggregate containing 10 percent noncarbonate particles.

TABLE 2 FNs for Sites Where Driving and Passing Lanes Were Tested

Site	Lane	LAADT	Avg. Friction Number at 64 kph (40 mph)	Coarse Aggregate
A	Driving	3,800	52	Sandstone
	Passing	2,500		
B	Driving	1,700	46	Siliceous Dolomite
	Passing	800	51	(22% AIR)
C	Driving	10,800	42	Siliceous Dolomite
	Passing	6,500	47	(35% AIR)
D	Driving	18,000	28	Blended Aggregate
	Passing	12,200	37	(18% Noncarbonate)
E	Driving	4,100	29	Blended Aggregate
	Passing	2,000	42	(10% Noncarbonate)

traprock were combined with data from sites containing granite, because both rock types have similar Moh's hardnesses (6 to 7) and are made up of interlocking mineral crystals. The data clearly correlate well, with a straight best-fit line showing that 11 FNs are lost for every log-cycle increase in LAADT. A similar plot of sites containing Wappinger dolomite (Figure 4), a nonsiliceous stone quarried extensively in southeastern New York just north of New York City, also shows a good correlation. The best-fit line for the Wappinger dolomite has a negative slope of 18 FNs per cycle. In both plots, lines were drawn parallel to the best-fit lines, above which 90 percent of the data fall. These "90 percent lines" were used to test and predict HFA specification conformance for these aggregates. Figure 3 shows the 90 percent line for traprocks and granites intersecting the "FN 32 design minimum" line at about 33,000 daily vehicle passes, indicating that these aggregates can be expected to provide adequate friction up to that traffic volume. Fortunately, it is unlikely that an LAADT above 33,000 will be encountered in New York State. On the other hand, Figure 4 shows that some Wappinger dolomite sites are already below the design minimum FN of 32. The 90 percent line intersects the FN 32 design minimum line at

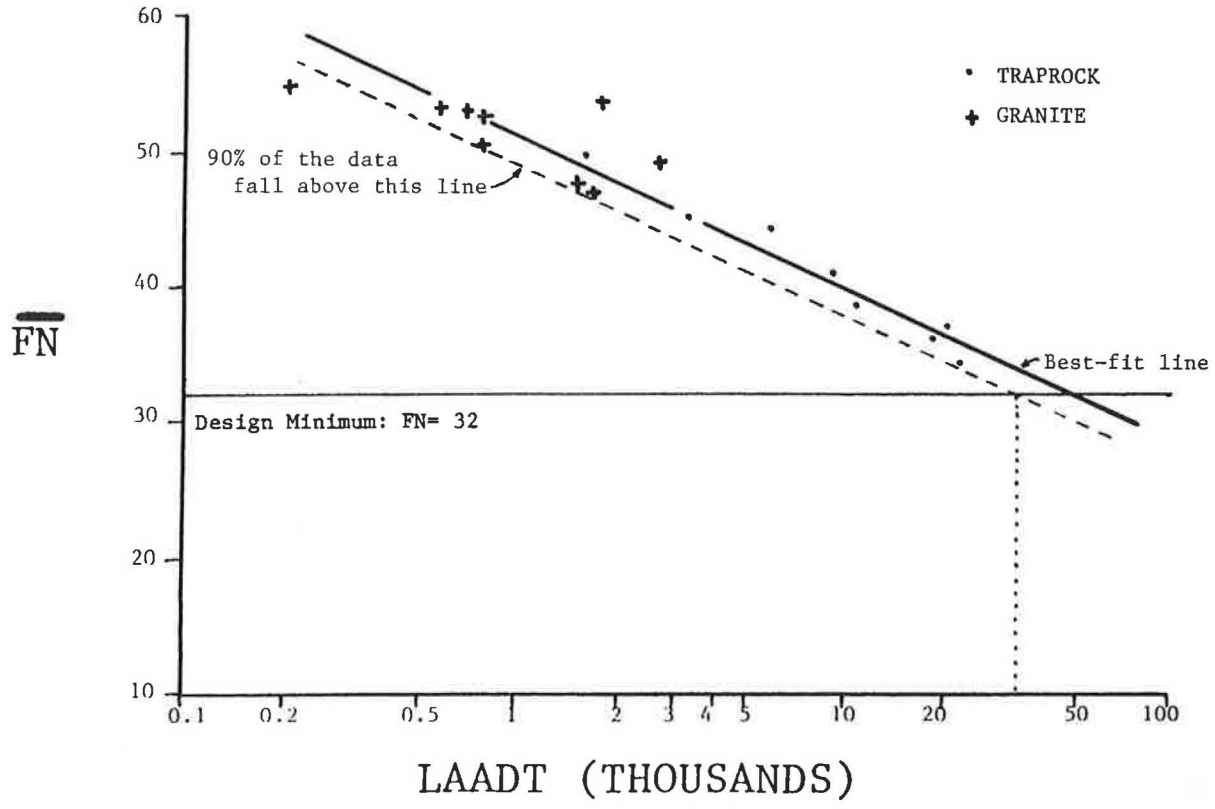

FIGURE 3 Average FN at 64 kph (40 mph) versus LAADT for sites containing traprock or granite. The 90 percent line intersects the FN 32 design minimum line at an LAADT of 33,000.

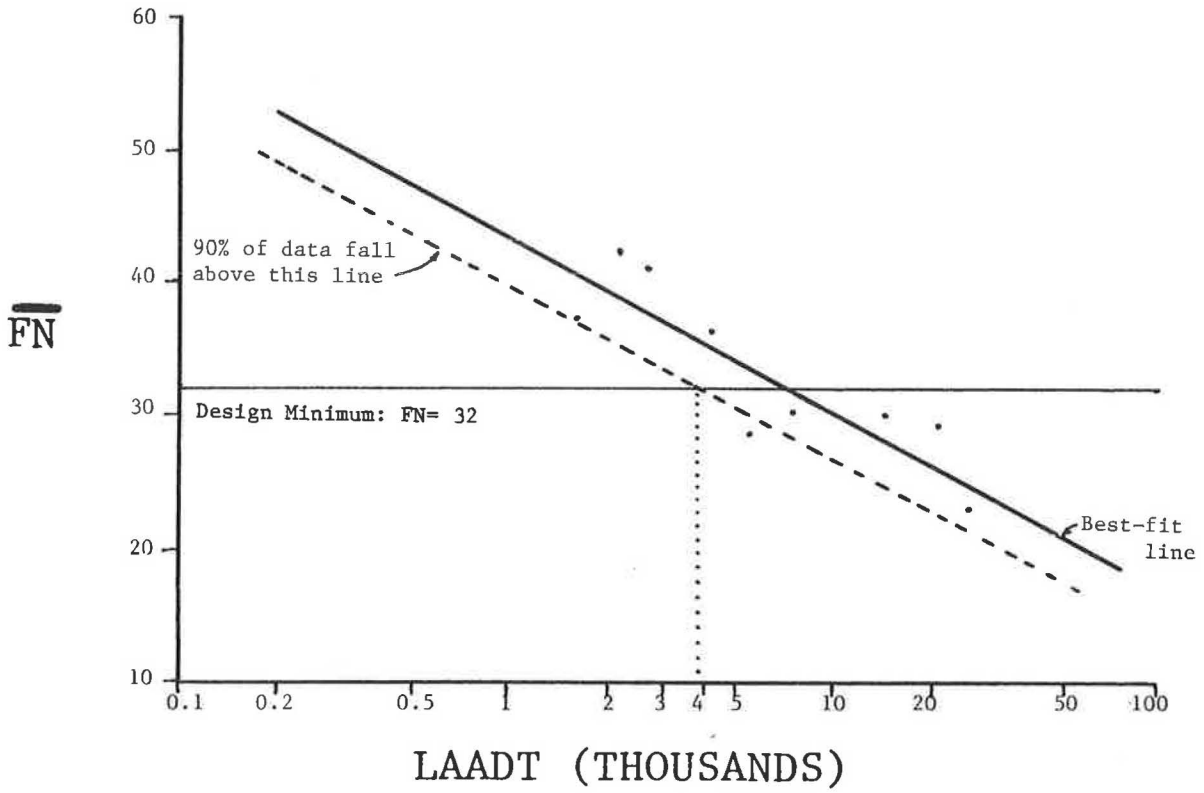

FIGURE 4 Average FN at 64 kph (40 mph) versus LAADT for sites containing Wappinger dolomite. The 90 percent line intersects the FN 32 design minimum line at an LAADT of 4,000.

an LAADT of 4,000, indicating that the Wappinger dolomite can be expected to provide adequate friction only in pavement lanes carrying 4,000 or fewer vehicles daily.

Sandy Rock Types

These rock types all contain significant amounts of sand-sized (+74 micron) quartz grains and include sandstone, siltstone, quartzite, siliceous limestone (all those tested contained more than 20 percent quartz sand), and siliceous dolomite (defined for this study as containing 15 percent or more quartz sand). Dolomites having AIRs of 15 percent or more consistently produce FNs above 40, even at high LAADTs, whereas dolomites having AIRs of less than 15 percent produce lower FNs as LAADTs increase [e.g., Wappinger dolomite (Figure 4)]. In a bituminous pavement surface, sandy rock types show a pattern of wear resulting in a continuing renewal of microtexture. As aggregate particles abrade, sand grains are displaced from particle surfaces, exposing fresh grains. Figure 5 shows a plot of sandstone sites, including sandstone, siltstone, and quartzite. These three rock types are related, differing from one another in grain size (fine versus coarse) or in degree of induration (how well grains within each particle are bonded). Although it is known from comparison of driving and passing lanes that sandstones respond to differences in traffic volume (Table 2), not enough data are available over a wide enough range of LAADTs to determine a clear trend. The renewable nature of the sandstone particle surface suggests that there may be a friction level below which a sandstone aggregate will not fall, regardless of traffic volume. Figure 5 shows that 90 percent of the sandstone data fall above an average FN of 50.

Figure 6 shows an array of data for siliceous limestones and siliceous dolomites similar to that of the sandstones, but expanded vertically. AIRs of these siliceous carbonates vary from 15 to more than 50 percent. This variable helps account for some of the data scatter, since higher AIRs tend to produce higher friction numbers (*1*). The data show, however, that these siliceous carbonate rocks can be expected to produce average FNs above 40 over a wide range of traffic volumes.

Aggregate Blends

This category includes not only combinations created in a bituminous mix plant but also naturally occurring blends, such as gravel and cherty limestone in which chert (a form of quartz) occurs in distinct nodules within a limestone matrix. Differential wearing characteristics of these blends cause friction to develop in a manner unlike homogeneous or sandy rock types. As pavements containing blended aggregate wear, softer rock types such as limestone and dolomite (having Moh's hardnesses of 3 to 4) abrade and become less prominent than harder, more resistant noncarbonate rocks such as granite and sandstone (having Moh's hardnesses of 6 to 7). This differential wearing creates a macrotexture that, in combination with the microtexture of noncarbonate rock particles, pro-

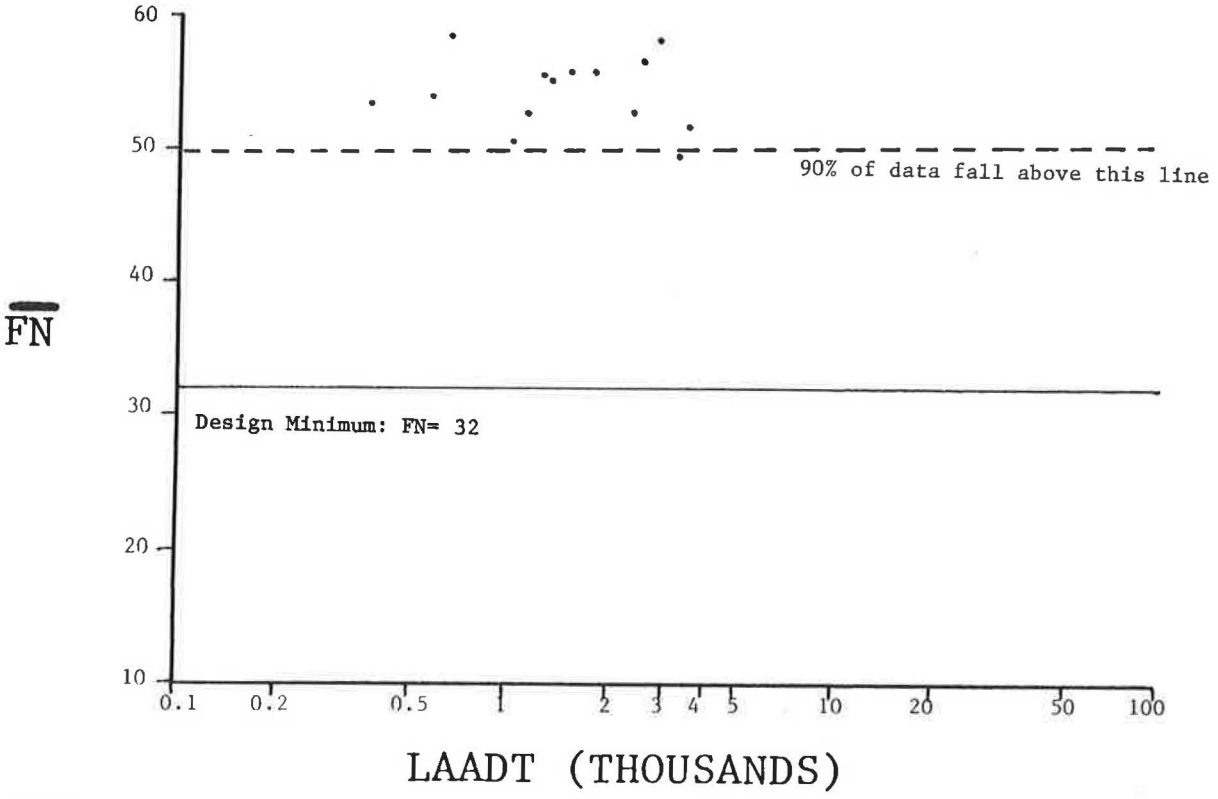

FIGURE 5 Average FN at 64 kph (40 mph) versus LAADT for sites containing sandstone.

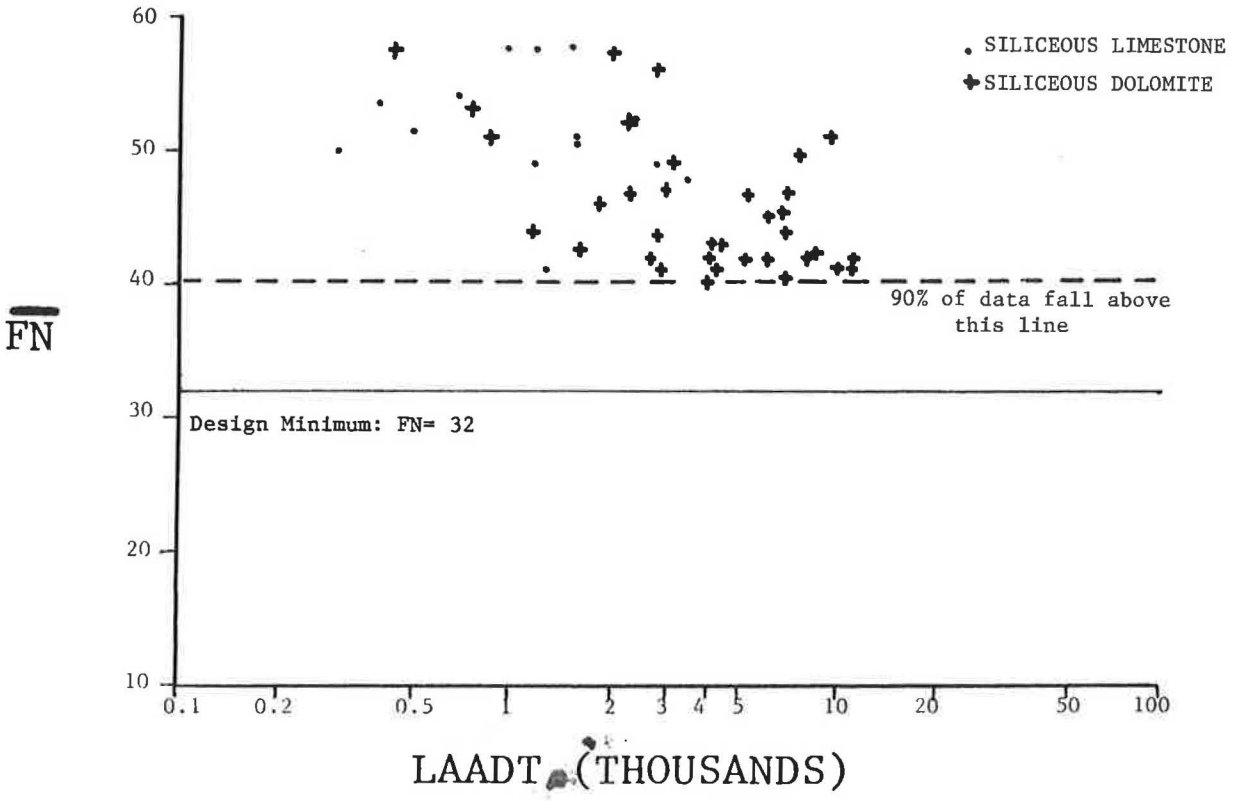

FIGURE 6 Average FN at 64 kph (40 mph) versus LAADT for sites containing siliceous limestone or siliceous dolomite.

vides the desired friction. A minimum level of noncarbonate in blends, perhaps the 20 percent required by the HFA specification, must be achieved throughout the range of LAADTs to be encountered. Two sites independent of the PFI given in Table 2 have blended aggregates containing less than 20 percent noncarbonate particles. Comparisons of driving and passing lanes show FNs both above and below the design minimum FN of 32. These blends are unacceptable both from the standpoint of the HFA specification and their measured friction. Figure 7 shows a plot of sites with blended aggregates. Data scatter can be largely accounted for by the fact that the percentage of noncarbonate particles varies from 18 to more than 70 percent. Friction tends to increase as the amount of noncarbonate in the blend increases (7). In spite of the scatter, the best-fit line shows the data having a negative slope. Only 5 percent of the data points fall below the FN 32 design minimum line, indicating that within the range of traffic volumes encountered in areas of the state where blended aggregates are used, the 20 percent noncarbonate requirement is generally adequate. When friction is plotted against percent noncarbonate, the data scatter is comparable with that in Figure 7. These plots show that both traffic volume and noncarbonate percentage are important and that neither can be overlooked.

NYSDOT HIGH-FRICTION AGGREGATE SPECIFICATIONS

Current NYSDOT high-friction aggregate specifications were revised in 1992 on the basis of this study:

HIGH-FRICTION AGGREGATE SPECIFICATION FOR STANDARD BITUMINOUS MIXES

Coarse aggregates shall meet one of the following high-friction requirements:

1. Coarse aggregates shall be crushed limestone that has an acid insoluble residue content of not less than 20%, excluding particles of chert and similar siliceous rocks unless approved by the Director, Materials Bureau, or crushed dolomite.
2. Coarse aggregates shall be crushed sandstone, granite, chert, traprock, ore tailings, slag, or other similar materials.
3. Coarse aggregates shall be crushed gravel or blends of two or more of the following types of materials: crushed gravel, limestone, dolomite, sandstone, granite, chert, traprock, ore tailings, slag, or other similar materials. These aggregates shall meet the following requirements:

   For Type 6F Mixes—Not less than 20% (by weight with adjustments to equivalent volumes for materials of different specific gravities) of the total coarse aggregate particles (plus 1/8 inch material) shall be noncarbonate. Noncarbonate particles are defined as those having an acid insoluble residue content not less than 80%. In addition, not less than 20% of the plus 1/4 inch particles shall be noncarbonate.

   For Types 7F and 8F Mixes—Not less than 20% (by weight with adjustments to equivalent volumes for materials of different specific gravities) of the total coarse aggregate particles (plus 1/8 inch material) shall be noncarbonate.

HIGH-FRICTION AGGREGATE SPECIFICATION FOR HEAVY-DUTY AND RUT-AVOIDANCE BITUMINOUS MIXES

(These mixes will be used on pavements having LAADTs over 4000 daily vehicle passes)

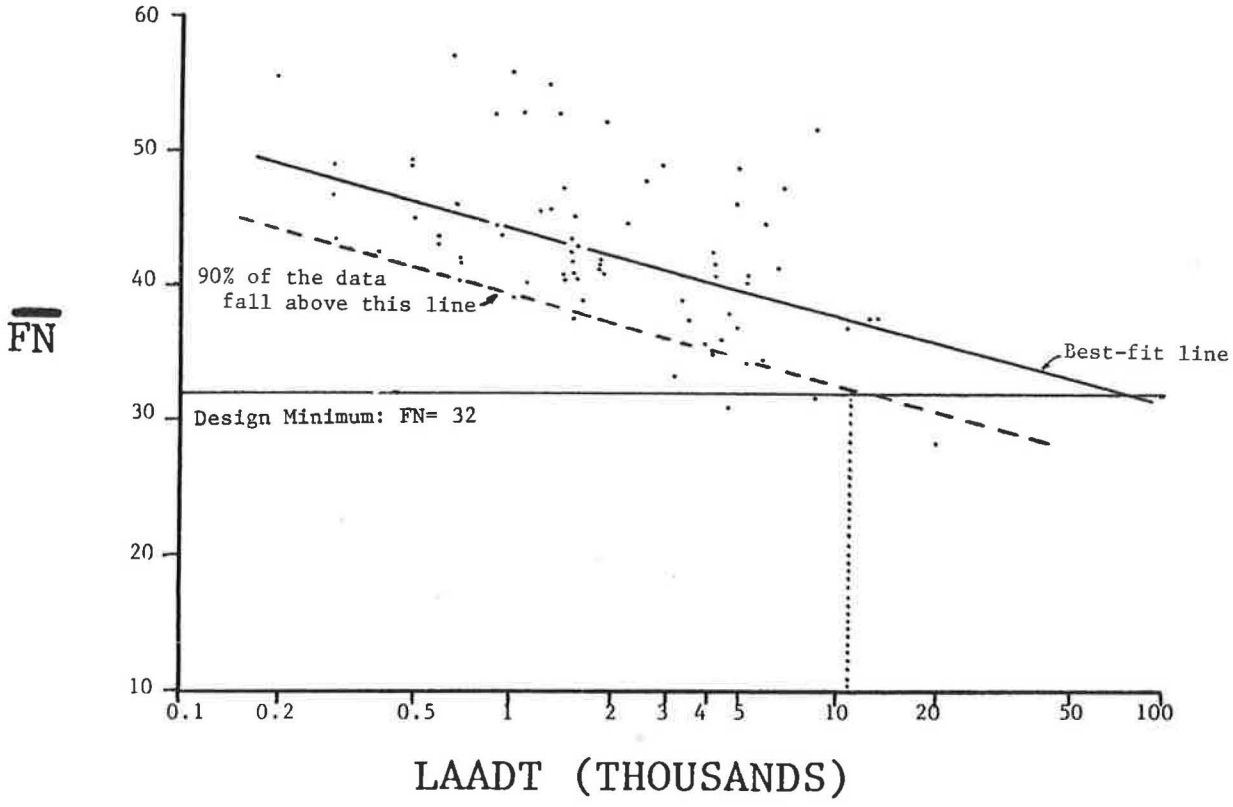

FIGURE 7 Average FN at 64 kph (40 mph) versus LAADT for sites containing blended aggregates. The 90 percent line intersects the FN 32 design minimum line at an LAADT of 11,000.

Coarse aggregates shall meet one of the following high-friction requirements:

1. Coarse aggregates shall be crushed limestone that has an acid insoluble residue content of not less than 20%, excluding particles of chert and similar siliceous rocks unless approved by the Director, Materials Bureau.
2. Coarse aggregates shall be crushed sandstone, granite, chert, traprock, dolomite (excluding Wappinger Dolomite), ore tailings, slag, or other similar materials.
3. Coarse aggregates shall be crushed gravel or blends of two or more of the following types of materials: crushed gravel, limestone, dolomite (including the Wappinger Dolomite), sandstone, granite, chert, traprock, ore tailings, slag, or other similar materials. These aggregates shall meet the following requirements:

   For Types 6FHD and 6FRA Mixes—Not less than 20% (by weight with adjustments to equivalent volumes for materials of different specific gravities) of the total coarse aggregate particles (plus 1/8 inch material) shall be noncarbonate. Noncarbonate particles are defined as those having an acid insoluble residue content not less than 80%. In addition, not less than 20% of the plus 1/4 inch particles shall be noncarbonate.

   For Type 7FHD and 7FRA Mixes—Not less than 20% (by weight with adjustments to equivalent volumes for materials of different specific gravities) of the total coarse aggregate particles (plus 1/8 inch material) shall be noncarbonate.

CONCLUSIONS

On the basis of an analysis of friction data from 155 pavement sites in the NYSDOT PFI program and from an additional 66 sites previously tested by the department, the following conclusions are drawn:

1. Bituminous pavements reach a terminal polish state within 2 to 3 years, after which the coefficient of friction can be expressed as an average of all measurements. This conclusion was largely inferred from the PFI data and bolstered by data from an independent site (Figure 2).
2. Pavement friction is inversely related to daily traffic volume, expressed as LAADT. Data from homogeneous rock types demonstrate this relationship best, but comparisons of driving and passing lanes show that it also holds true for both sand and blended aggregates (Table 2).
3. Aggregate rock types can be categorized as homogeneous, sandy, or blended, and on the basis of this classification an aggregate's wearing and polishing characteristics can be predicted.
4. Traprocks, granites, sandstones, siliceous carbonates (as defined for this study), and aggregate blends containing 20 percent or more noncarbonate particles can be expected to provide adequate friction throughout the range of traffic volumes normally encountered (traprocks and granites, LAADTs up to 30,000; sandstones and siliceous carbonates, no upper limit on LAADT; aggregate blends, LAADTs up to 10,000).
5. Wappinger dolomite, with an AIR below 15 percent, can be expected to provide adequate friction only in pavements with LAADTs under 4,000. NYSDOT has restricted the use of Wappinger dolomite in pavements having LAADTs of 4,000 or more.

ACKNOWLEDGMENTS

PFI testing is conducted by the General Engineering Section of the NYSDOT Materials Bureau. The General Engineering Section is also responsible for the management of friction test data and has assisted greatly in this analysis.

REFERENCES

1. Gray, J. E., and F. A. Renninger. The Skid-Resistant Properties of Carbonate Aggregates. In *Highway Research Record 120*, HRB, National Research Council, Washington, D.C., 1966, pp. 18–34.
2. Kearney, E. J., and G. W. McAlpin. Skid Resistance of Bituminous Surfaces. In *Highway Research Record 236*, HRB, National Research Council, Washington, D.C., 1968, pp. 49–60.
3. Burnett, W. C., J. L. Gibson, and E. J. Kearney. Development of Specifications for Skid Resistant Asphalt Concrete. In *Highway Research Record 396*, HRB, National Research Council, Washington, D.C., 1972, pp. 12–20.
4. *Skid Accident Reduction Program*. Instructional Memorandum 21-2-73. FHWA, U.S. Department of Transportation, 1973.
5. Tam, K. K., R. Raciborski, and D. F. Lynch. Performance of 18 Bituminous Test Sections on a Major Urban Freeway During 11 Years of Service. In *Transportation Research Record 1217*, TRB, National Research Council, Washington, D.C., 1990, pp. 64–79.
6. Abdul-Malak, M.-A. U., A. H. Meyer, and D. W. Fowler. Research Program for Predicting the Frictional Characteristics of Seal-Coat Pavement Surfaces. In *Transportation Research Record 1217*, TRB, National Research Council, Washington, D.C., 1990, pp. 53–64.
7. Miller, R. W., and W. P. Chamberlin. *Skid Resistance of Bituminous Pavements Built with Carbonate Aggregates*. Research Report 77. Engineering Research and Development Bureau, New York State Department of Transportation, April 1980.

Publication of this paper sponsored by Committee on Mineral Aggregates.

Evaluation of Domestic Incinerator Ash for Use as Aggregate in Asphalt Concrete

NORMAN W. GARRICK AND KUO-LIANG CHAN

The potential use of incinerator ash in asphalt concrete paving was evaluated. Laboratory tests were conducted on ash from a waste-to-energy incinerator. Tests were conducted to assess whether asphalt concrete mix with ash was suitable both in terms of physical performance and environmental safety. It was determined that a mix with acceptable parameters on the Marshall tests could be produced with an aggregate consisting of up to 32 percent incinerator ash. This mix requires a higher asphalt content than a normal mix and appears to be prone to stripping. The results of the toxicity tests on the leachate were inconclusive; however, they suggest that there might be a problem since a significant amount of lead was detected in the leachate. It was concluded that an asphalt concrete mix with ash might be suitable for use in base course or for low-quality surface applications. However, a significant quantity of undesirable material must first be removed to get an aggregate of acceptable quality. Only about one-third of the material in the bottom ash is suitable for use in an asphalt concrete mix.

The northeastern United States is in danger of being buried under a mountain of discarded paper, wood, metal, plastic, and other detritus of modern life. Incineration is one of many strategies being used to deal with the refuse disposal problem. As can be expected, there are problems associated with burning trash on a large scale. Foremost among these is the question of how best to dispose of the potentially toxic residue that is generated by incineration. Many people have suggested that this material might be suitable for use in construction as a structural fill, an aggregate for asphalt concrete and portland cement concrete, or a replacement for some of the cement in concrete. Various facets of this idea have been studied since at least the 1940s.

In Connecticut, this issue is particularly topical since the use of waste-to-energy incinerators is an important component of the state's solid waste management plan (*1*). This project was conducted to investigate the feasibility of using incinerator ash from a refuse-derived fuel (RDF) incinerator in asphalt concrete paving. The project was conducted in two parts: a literature review of work that has been done to date and a laboratory study of incinerator ash from one local RDF incinerator. Unlike most previous studies, the laboratory tests in this project were conducted to evaluate not only the physical properties of the asphalt concrete mix but also the potential toxicity of leachate from the mix.

Department of Civil Engineering, University of Connecticut, Storrs, Conn. 06269-3037.

LITERATURE REVIEW

Commercial incineration of domestic refuse in the United States dates back to the turn of the century; however, the first significant wave of construction of incinerators did not come about until the 1940s. To get around war-related shortages, residues from some of these plants were used for embankment and subbase construction at various sites in Pennsylvania and New York during the war years (*2*).

In the 1960s and 1970s, with the push to construct large, centrally located incinerators, interest in the technology of residue utilization was revived as an answer to the problem of ash disposal. Many projects were conducted to study the issue, but the most comprehensive review was given in a series of reports published by FHWA in the mid-1970s (*2–4*).

FHWA described the different types of incinerator plants and the properties of the incinerator ash that are likely to affect the performance of the ash as a construction material (*3*). FHWA classified incinerator residue as well burned out, intermediately burned out, or poorly burned out depending on the amount of volume reduction and the organic content of the material remaining after ignition. The criteria used for this method of classification are summarized in Table 1.

The degree of burnout is affected by the composition and moisture content of the incoming refuse and the overall efficiency of the plant. If the refuse is relatively dry, most modern plants can be operated to give a well-burned-out residue with about 90 percent reduction in volume and 70 to 80 percent reduction in weight. FHWA found that only the well-burned-out residue is a likely candidate for use in asphalt concrete.

FHWA's laboratory evaluation showed that it was necessary to mix the incinerator residue with conventional aggregate. The best results were obtained when the incinerator residue made up no more than 40 to 55 percent of the total aggregate (*5*). Asphalt concrete mixes made with incinerator residue were found to require a higher asphalt content than conventional mixes (up to 10 percent compared with the usual 4 to 6 percent).

Since 1970 test sections made from asphalt concrete mix with incinerator residue have been constructed at various sites, including Houston (1974); Harrisburg, Pennsylvania (1975); Washington, D.C. (1977); and Lynn, Massachusetts (1980) (*5*). Mix with residue was used for both surface and base course in Harrisburg and Lynn but was used only in the base course of the Houston and Washington projects. In all cases the test sections were reported to be in good condition after many years of service. However, some surface raveling was reported in Harrisburg despite the fact that lime had been

TABLE 1 FHWA's Classification of Incinerator Ash (3)

Category	Description
WELL BURNED-OUT	Usually produced by continuous fed incinerators with high degree of grate agitation. Residue is about 10 % by volume and 20 to 30 % by weight of the refuse input.
INTERMEDIATE BURNED-OUT	Usually produced by continuous fed incinerators with little or no agitation or breaking down of the burning refuse. Residue is about 20 % by volume and 25 to 35 % by weight of the refuse input.
POORLY BURNED-OUT	Produced by batch fed incinerator or poorly operated continuous fed incinerators. Residue is about 30 to 40 % by volume and 30 to 40 % by weight of the refuse input.

added to inhibit asphalt stripping. It was also reported that the large quantity of dust generated by the residue during mixing with asphalt slowed down the rate of production at the hot mix plant.

Collins reports on one project in which incinerator residue was processed before being used as an aggregate (*5*). The process consists of first grinding the residue to a particle size of 1/4 in. or less. The ground material is heated at 1,600°F to remove combustibles and is fused at 2,000°F. After air cooling, the fused mass is crushed to give the desired gradation. In 1976, this Eco-rock, as it is called, was used in asphalt concrete mix for paving a road in Harrisburg, Pennsylvania. This road was still reported to be in good condition after 10 years of service. Furthermore, its skid resistance was found to be better than average. A large-scale Eco-rock plant, built in 1984 by the Environmental Protection Agency and the city of Philadelphia, was never activated.

THE CONNECTICUT STUDY

Description of Residue

The residue used in this study was from an RDF incinerator in Hartford, Connecticut. Depending on the operating condition of the plant, the residue produced was 12 to 15 percent by weight of the incoming refuse. This represents a very high degree of combustion. The residue can be collected in four separate streams in this plant: bottom ash, grate shiftings, economizer ash, and fabric filter ash. The bottom ash was about 85 percent of the residue, the fabric filter about 14 percent, and the grate shiftings and economizer ash was less than 1 percent. Only the bottom ash was used in this study. The other streams were unsuitable as aggregates in asphalt concrete because of their small particle size.

The bottom ash arrived at the laboratory as a wet sludge that had to be oven dried. After drying, all particles larger than 1 in. and all unburnt paper were removed from the sample. Particles larger than 1 in. constituted about 21 percent by weight of the bottom ash, whereas the paper made up only about 1.5 percent. Thus the material that was actually used in this project consisted of only about 78 percent of all the bottom ash generated.

Description of Project

The first stage of this project was the evaluation of the physical properties of the residue. Properties evaluated include gradation, specific gravity, water absorption, and particle toughness (by the Los Angeles abrasion test). The second stage of the project was the determination of an asphalt mix composition that would meet conventional specifications for road paving. The major objective of this process was to select the mix with as large a proportion of residue as was feasible; therefore, the first trial was a mix with the aggregate being 100 percent residue. In subsequent mixes, the residue was gradually replaced with a local aggregate (traprock) until a mix was obtained that met the specifications.

In the third stage of the project, the indirect tensile strength and the moisture susceptibility of the selected asphalt concrete mix were determined. Finally, leachate tests were conducted on samples of this mix to assess the likelihood of any potential hazard to the environment.

Properties of Residue

The data in Table 2 indicate that the largest fraction of the residue (after the removal of oversized particles and large pieces of paper) consists of mineral matter such as sand, stone, brick, and fused ash. Many particles in this fraction appear to be quite porous. Aside from the mineral matter, much of the rest of the residue is either glass or metal. Glass and, to some extent, metal could pose some problem in an asphalt mix because they are likely to be prone to stripping. The organic matter is present as fairly fine particles (minus No. 16 sieve).

The gradation of the residue is given in Table 3. The values in this table indicate that the residue meets the specifications for the Connecticut mix (Class 1), which is used on high-type facilities. Results of the specific gravity and absorption determination are given in Table 4. The residue was determined to have lower specific gravity and a higher degree of water absorption than most conventional aggregates (values for the traprock are given for comparison).

It is also of interest to compare the coarse (retained on No. 4 sieve) and fine (passing No. 4 sieve) fractions of the residue

TABLE 2 Composition of the RDF Incinerator Residue Versus Typical FHWA Well-Burned Residue

Components	Hartford RDF Residue (by weight)	FHWA Well-burned Residue (by weight)
Metal	23.0%	17.1%
Glass	35.0%	39.9%
Mineral Matter(sand,brick etc)	40.0%	39.5%
Organic Matter(wood,paper etc)	2.0%	3.5%

itself. The fine fraction is less dense and more absorbent—reflecting the fact that it contains a large amount of unburned organics (mostly paper), which could not easily be removed. The composition of the coarse fraction is very different, consisting mostly of metal, glass, and ceramics particles.

The percentage loss on the Los Angeles abrasion test for the coarse fraction of the residue was 44.7 percent, higher than the 40 percent maximum specified by the Connecticut Department of Transportation (ConnDOT) for its highest quality aggregate. This result is indicative of a material that is not as tough as one would desire in an aggregate to be used in a paving mix, but it is not unexpected given the large number of glass particles in the residue.

Mix Design

The purpose of this procedure was to obtain a mix that met conventional asphalt mix specifications but contained as high a proportion of residue as possible. The first trial was a mix in which the aggregate consisted totally of incinerator residue. This mix proved to be unsuitable because the Marshall stability value was low (650 lb) and the air void content was excessively high (23.5 percent) (see Table 5). (These results are for the mix with optimum asphalt content in the Marshall mix procedure.)

In the second trial the aggregate was 60 percent traprock and 40 percent residue. This proportion was used for all sieve sizes. The Marshall results were virtually unchanged from those for the first trial. The Marshall stability value actually decreased slightly to 600 lb, and the air voids improved to 21.5 percent.

It was felt that the undesirable results of these two trials were most likely attributable to the presence of unburnt organic matter of fine particle size. Thus, in the third trial, residue particles finer than the No. 8 sieve were excluded. For this trial, the incinerator ash was used as the coarse fraction (retained on the No. 8 sieve), and the traprock was used as the fine fraction. The residue made up 48 percent of the total aggregate weight—a larger proportion than in the mix for the second trial. Nonetheless, this change resulted in a significant improvement in the Marshall properties of the mix. The Marshall stability increased to 1,050 lb, a value greater than the minimum specified for ConnDOT Class 1 mix. The air voids improved significantly to 13.5 percent; however, this value was still significantly higher than that allowed by the specifications.

To obtain a lower air voids content, the amount of residue of fine particle size was further reduced for the fourth trial. This was achieved by changing the cutoff point from the No. 8 to the No. 4 sieve. As before, the coarse fraction (in this case, the fraction retained on the No. 4 sieve) was incinerator residue only, whereas the fine fraction was traprock. The residue portion of the total aggregate weight was reduced to 32 percent by this change.

TABLE 3 Average Gradation of the RDF Incinerator Residues (Chunks Larger than 1 in. Not Included)

Sieve Size	Residue % Passing Sieve	CONNDOT SPEC LIMITS (Class 1)
1 in (25.4 mm)	100	100
1/2 in (12.7 mm)	85	70-100
3/8 in (9.51 mm)	72	60-82
#4 (4.76 mm)	46	40-65
#8 (2.38 mm)	30	28-50
#16 (1.19 mm)	18	-
#30 (0.60 mm)	12	-
#50 (0.30 mm)	7	6-26
#100 (0.15 mm)	4	-
#200 (0.075 mm)	3	3-8

TABLE 4 Specific Gravity and Absorption: RDF Incinerator Residue Versus Traprock

Property	Traprock		RDF Residue	
	Coarse	Fine	Coarse	Fine
Bulk Spec. Gravity	2.89	2.84	2.29	1.52
Apparent Spec. Gravity	2.97	3.03	2.52	1.75
Absorption, %	1.0	2.3	3.9	8.6

TABLE 5 Marshall Results for Four Trial Ash Mixes and for Traprock Mixes (Optimum Asphalt Content Only)

Test	Trap	Trial 1 100% Residue	Trial 2 40% Residue	Trial 3 48% Residue	Trial 4 32% Residue
Asphalt Content, %	4.9	7.0	7.0	6.5	6.2
Stability lb, 60 C	2200	650	600	1050	1150
Unit Wgt lb/cu. ft.	157.8	102.3	103.4	139.2	141.6
Flow 0.01 in	11.0	11.5	13.0	11.0	12.0
Air Void %	5.0	23.5	21.5	13.4	7.2
VMA, %	16.3	28.5	27.5	19.5	18.6

The air voids for this mix decreased significantly to 7.2 percent; this value was slightly greater than the maximum specified for Class 1 mixes. However, all the other Marshall parameters for this mix met the minimum ConnDOT specification for Class 1 mixes. Thus it was decided to use this mix proportion as the basis for the comprehensive testing program.

Properties of Asphalt Concrete Mix

These tests were conducted on the Trial 4 mixes of optimum asphalt content. It was determined that the optimum asphalt content of these mixes was 6.2 percent. This value is substantially higher than the asphalt content of about 4.9 percent for a traprock mix. In other words, the use of incinerator residue increases asphalt demand by about 20 percent over that required by an all-traprock mix.

Results of the indirect tensile test (77°F) and of the stripping tests are given in Table 6. The results show that the indirect tensile strength of the residue mixes was about 20 percent lower than that of the traprock mix. It is difficult to say how these results would compare with other aggregates since many factors affect the indirect tensile strength. Therefore, results from other studies cannot be used for comparison.

The residue mixes also performed poorly in the stripping test, which was conducted according to the Tunnicliff procedure (*6*). The tensile strength ratio (TSR) for these mixes suggests that they might be susceptible to water damage (TSR of 0.75 is generally considered to be acceptable). This result is attributable to the large amount of glass in the residue. It might be possible to solve this problem by adding lime to the asphalt concrete mix.

Leachate Tests

Both the extraction procedure toxicity (EP Tox) and the toxicity characteristic leaching procedure (TCLP) tests were run on samples of loose residue mix and traprock mix. In both procedures a leachate is extracted from the sample with a specified aqueous extraction fluid (*7,8*). The leachate is an-

TABLE 6 Properties of Trial 4 Residue Mixture

Mix Type	Indirect Tensile Strength (ITS), psi	Water Sensitivity Tensile Strength Ratio (TSR)
Trap	103	0.85
Residue	80	0.70

TABLE 7 Leachate Test Results (EP Tox and TCLP) for Trial 4 Residue Mix and Traprock Mix

Element	Maximum Value, ppm	Traprock Mix		Residue Mix	
		E.P Tox ppm	TCLP ppm	E.P Tox ppm	TCLP ppm
Ba	100.00	0.0490	0.2470	0.1540	0.2040
Cd	1.00	0.0030	0.0030	0.0040	0.0190
Cr	5.00	0.0060	0.0110	0.0040	0.0260
Pb	5.00	0.0082	0.0258	2.3750	10.5000
Ag	5.00	0.0000	0.0170	0.0000	0.0230
As	5.00	0.0004	0.0009	0.0016	0.0024
Se	0.99	0.0027	0.0017	0.0023	0.0018

alyzed to determine the concentration of eight toxic metals; the specimen is classified as being hazardous if the concentration of any of these eight metals exceeds established threshold levels. The TCLP test is considered to be slightly more severe than the EP Tox test.

The results of the leachate tests in Table 7 show that lead is the only metal present in any appreciable amount in the leachate of the residue mix. The level of lead exceeds the threshold limit in the TCLP test but not in the EP Tox test.

It is difficult to draw firm conclusions about the potential toxicity of compacted pavements from these results, since the tests were not specifically designed for that purpose. Nevertheless, the results raise some concern, because many states severely restrict the use of substances such as these, which, in essence, fail the EP Tox or TCLP tests.

SUMMARY AND CONCLUSION

The results of the study indicate that an aggregate of marginal quality can be obtained from the bottom ash portion of the residue from this RDF plant. However, a large quantity of unsuitable material must first be removed from the residue. The components that must be removed include (*a*) oversized objects (larger than 1 in.), (*b*) unburned paper particles larger than the No. 4 sieve, and (*c*) fines passing the No. 4 sieve. Thus, only about 35 percent (by weight) of all the residue generated by the plant can be used as asphalt concrete aggregate.

An asphalt mix with acceptable Marshall parameters was made with an aggregate that is 32 percent residue and 68 percent traprock. As expected, the optimum asphalt content of this mix was higher (by 20 percent) than that of a corresponding traprock mix. In addition, the residue mix had lower tensile strength and showed a greater tendency to strip in the presence of water than did the traprock mix. A relatively high concentration of lead was detected by two separate procedures for analyzing the toxicity of the residue mix.

The results taken together do not provide a strong basis for recommending the use of the unprocessed residue in the wearing course of an asphalt concrete pavement. On the basis of the properties of the mix and of the residue itself, the performance of such a mix is likely to be marginal at best. This mix could possibly be suitable for use in the base course or in low-quality surface applications. However, the results of the leachate tests raise the question whether a pavement from such a mix would be environmentally inert.

Very little attention has been paid to using processed residues as asphalt concrete aggregates. The undesirable properties of the residue that were identified in this report could conceivably be improved if the ash were stabilized by vitrification or some other process. Further research is required in this area.

ACKNOWLEDGMENT

This project was sponsored by the Environmental Research Institute at the University of Connecticut and the Connecticut Department of Environmental Protection. The environmental tests were conducted by Environmental Research Institute personnel.

REFERENCES

1. Weir, B. A., G. E. Hoag, K. J. Walsh, H. E. Klei, and A. J. Perna. Leachate Characterization of Ash from a Refuse Derived Fuel (RDF) Incinerator. Presented at AIChE National Meeting, Philadelphia, Pa., Aug. 1989.
2. Pindzola, D., and R. J. Collins. *Technology for Use of Incinerator Residue as Highway Material—Identification of Incinerator Practices and Residue Sources.* Report FHWA-RD-75-81 (Interim Report). FHWA, U.S. Department of Transportation, 1975.
3. Collins, R. J., R. H. Miller, and S. K. Ciesielski. *Guidelines for Use of Incinerator Residue as Highway Construction Material.* Report FHWA-RD-77-150. FHWA, U.S. Department of Transportation, 1977.
4. Teague, D. J., and W. B. Ledbetter. *Three Year Performance of Incinerator Residue in a Bituminous Base.* Report FHWA-RD-78-144 (Interim Report). FHWA, U.S. Department of Transportation, 1978.
5. Collins, R. J. Synthesis of Waste Utilization in Highway Construction. Presented at the 67th Annual Meeting of the Transportation Research Board, Washington, D.C., 1988.
6. Tunnicliff, D. G. *NCHRP Report 274: Use of Antistripping Additives in Asphaltic Concrete Mixtures—Laboratory Phase.* TRB, National Research Council, Washington, D.C., 1982.
7. *Test Method for Evaluating Solid Wastes. Physical/Chemical Methods* (2nd edition). SW-846. U.S. Environmental Protection Agency, Cincinnati, Ohio, 1982.
8. *Methods for Chemical Analysis of Water and Wastes.* EPA-600/4-79-010. U.S. Environmental Protection Agency, Cincinnati, Ohio, 1979.

Publication of this paper sponsored by Committee on Mineral Aggregates.

Mineralogy of Aggregates in Relation to the Frictional Performance of Seal Coat Pavement Overlays: A Petrographic Study

MOHAMED-ASEM U. ABDUL-MALAK, D. W. FOWLER, AND A. H. MEYER

A petrographic study was conducted to identify the mineralogical and textural properties of aggregates that may influence the frictional performance of seal coat pavement overlays constructed with these aggregates. Twenty aggregate samples were petrographically examined, and their frictional performance in seal coat overlays was monitored over about 4 years. The petrographic and field results were used to formulate a probabilistic prediction model describing field performance. Statistically significant petrographic variables included the percentage of grain-supported texture particles, the amounts of dolomitic and other carbonate grains in aggregate particles, the percentage of noncarbonate matrix in particles, and the level of prevailing void content. A construction-related variable, the design spreading rate of aggregate particles, also showed significance in explaining some of the observed variation in frictional performance.

A petrographic study was conducted as part of a research project at the University of Texas at Austin. The ultimate aim of this project was to formulate statistical models for predicting the frictional performance of seal coat pavement overlays. The methodology (*1*,*2*) involved establishing 59 seal coat test sections in all the four environmental regions of Texas and monitoring their frictional performances over time. The following factors, believed to have an influence on performance and identified in the literature and Texas districts surveys (*1*), were considered: aggregate physical and mineralogical properties, construction variables, traffic, and environment and weather variables.

Construction data had construction application rates and types of aggregates and asphalt. Aggregate samples obtained from construction sites were tested in the laboratory for their basic properties, polish susceptibility, resistance to weathering action, and resistance to abrasion and impact actions. Twenty of the samples were also examined for their mineralogical and petrographical properties. In this examination, the mineralogical constituents were estimated, and the textural characteristics were evaluated.

The frictional performance data were graphed to detect the sources of variations and then grouped according to the different variables considered. The grouping gave insights into which variables controlled the observed differences in frictional performance. The grouping was followed by extensive statistical modeling, which pinpointed the significant variables. In this paper, only the results pertaining to the observed effects of aggregate's petrographic properties on frictional performance are presented.

M.-A. U. Abdul-Malak, Faculty of Engineering and Architecture, American University of Beirut, Beirut, Lebanon. D. W. Fowler and A. H. Meyer, Department of Civil Engineering, The University of Texas at Austin, Austin, Tex. 78712-1076.

OBJECTIVES OF THE PETROGRAPHIC STUDY

The petrographic examination was performed

1. To determine the physical properties of an aggregate that may be observed by petrographic methods and that may have a bearing on the performance of the aggregate in seal coat surfaces;
2. To identify, describe, and classify the constituents of the aggregate sample; and
3. To determine the relative amounts of the constituents of the samples when the constituents differ significantly in a property, such as hardness, that may be expected to influence the frictional behavior of the aggregate when used in these surfaces.

BACKGROUND

Rocks can be classified into three major groups: igneous, sedimentary, or metamorphic. Igneous rocks are formed by cooling and solidification of magma. Metamorphic rocks are formed by transformations of preexisting rocks while they remain in the solid state. Most of the aggregates of this study were sedimentary rocks. Hence, the formation, composition, and texture of this type of rock were reviewed to develop a procedure for identifying the mineralogical and petrographic properties that may be relevant to the study.

Formulation of Sedimentary Rocks

Sedimentary rocks are formed either by the accumulation of weathered mineral and rock fragments or by precipitation. However, postdepositional changes are common in these rocks and affect both the texture and composition (*3*). These changes occur at relatively low temperatures and are termed diagenetic, which includes compaction, solution, and authigenesis and replacement (*3*,*4*). The most common authigenic minerals replacing calcite in limestones are quartz, chert, and dolomite.

Composition of Sedimentary Rocks

Limestone, dolomite, sandstone, and chert are the most common sedimentary rocks. Common minerals in these rocks include carbonate minerals such as calcite and dolomite and noncarbonates such as quartz, chert, pyrite, and feldspar. The calcite and dolomite minerals are soluble in dilute hydrochloric acid and have hardness values of 4 or less according to Mohs's scale of hardness; calcite has a hardness of 3, whereas dolomite is slightly harder with a hardness of 3.5 to 4.0. The noncarbonate minerals are insoluble and their hardness ranges from 6 to 7.

Texture of Sedimentary Rocks

Texture refers to a rock's crystallinity, grain size, and the mutual relationship of the individual components (*4,5*). Some rocks are composed of single size grains, whereas others are made up of large crystals scattered through a matrix of smaller ones.

The material in aggregates with a wide range of particle sizes is subdivided into grains and matrix. These terms refer to the relative size of the particles and their deposition in the aggregate. If grains compose more than two-thirds of an aggregate, the grains will be in contact, resulting in a grain-supported texture. In this texture, the matrix simply fills in the potential pores between the grains. On the other hand, if the grains are much fewer, loosely packed, and scattered in the matrix, they appear to be suspended in the matrix, resulting in a matrix-supported texture.

In limestones, the matrix may be composed of microcrystalline calcite or spary calcite. Calcite grains may be fossils, oids, pellets, or intraclasts, all of which consist of calcite spar or mud with different internal structures.

EXAMINATION PROCEDURE AND RESULTS

Examination Procedure

A simple petrographic procedure was developed that included those mineralogical and textural properties identified. Table 1 was designed to facilitate organization of the information from the examination. The second part of the table was adapted from Dunham's limestone classification (*4*) and modified so that it can also be used for the examination of rocks other than sedimentary. Dunham suggested the use of a polarizing microscope for examining thin sections of aggregate particles, whereas in this study the mineralogical and textural properties of aggregates were evaluated by examining aggregate particles under a stereomicroscope. A total of 20 handful-sized aggregate samples, representing the limestone rock asphalt (LMRA), limestone (LMST), siliceous gravel (SIGR), and sandstone (SDST) aggregate groups were examined. The LMRA aggregate group is characterized by natural impregnation of asphalt into the pores of the rock. The impregnated asphalt and the asphalt coating on the precoated samples were extracted (*6*) before these samples were examined as follows:

1. Acid-etch the handful-sized sample to reveal the depositional texture of the carbonate particles and remove dust coating. Etch by placing the sample in a container and adding enough dilute hydrochloric acid (concentration of 5 to 10 percent) to cover the particles being examined. The container is gently swirled for approximately 20 sec, then rinsed thoroughly with water. Caution should be taken for potential spattering when examining calcareous particles.
2. The aggregate sample is then subdivided into groups, each having particles with certain textural and mineralogical characteristics that may be related similarly to the overall expected performance. To accomplish this, each aggregate particle is examined on all of its sides using a stereomicroscope

TABLE 1 Summary of Mineralogical and Petrographic Properties

Aggregate Number: 51 **Color:** Dark gray to dark tan
Group: 2 of 2 **Sphericity:** Low
Percentage: 30 % **Roundness:** Angular
Name: Crushed sandy limestone

TEXTURE			
Matrix-supported texture		**Grain-supported texture**	
Less than 10% grains	**More than 10% grains**	Matrix present between grains	Lacks matrix

Voids	Matrix		Grains	
	Carbonate	Non-carb.	Carbonate	Non-carb.
	Mud		Dolomite	Quartz
0 %	Total= 80 %		Total= 5 %	Total= 15 %

Grain size	Roundness	Sphericity
Fine	Subangular to subrounded	High

at a magnification of 10 to 45 and then placed in a group that best represents its overall textural and mineralogical characteristics. A balance should be sought between a reasonable number of groups and properly representing the expected performance. It is suggested that the number of groups be limited to five, preferably three for crushed limestones.

3. The data for each subdivided group are summarized in separate tables. The first part of each table has information on the approximate percentage of total sample, name, color, roundness, and sphericity of group particles. On the basis of roundness and the curvature of the corners of a particle, six classes can be distinguished: very angular, angular, subangular, subrounded, rounded, and well rounded. Sphericity, a measure of how closely the particle shape approaches that of a sphere, is characterized as low, medium, or high.

4. In the second part, each group is classified according to its overall textural appearance into either a matrix- or grain-supported texture.

5. The textural evaluation is taken one step further by classifying matrix-supported textures into either less than 10 percent grains or more than 10 percent grains. Grain-supported textures are subdivided into either matrix present between grains or no matrix present (by the end of this step, a particular group will have been assigned to one of the four textural classifications of Table 1).

6. Once a texture class is selected, the aggregate group is described in terms of its overall average percentage of voids and the percentage and mineralogy of its matrix and grains. The mineral constituents of the matrix and grains categories are then divided into carbonates and noncarbonates. The percent subtotal in this third part of the table must add up to 100 (i.e., percent void + percent carbonate matrix + percent noncarbonate matrix + percent carbonate grains + percent noncarbonate grains = 100). In each class under the matrix and grains categories, the different minerals are expressed in terms of their percentages of the percent subtotal for that class.

7. The grains are characterized with respect to their size, roundness, and sphericity. Grain size is evaluated from very fine to very coarse, whereas grain roundness and sphericity are evaluated in the same manner as those of the aggregate particles in the first part of the table.

8. Photomicrographs of the texture representing each of the groups encountered in a particular aggregate are taken.

Examination Results

The results describing a group of limestone particles in Aggregate 51 are included in Table 1. Table 2 summarizes information on the different groups encountered in each aggregate sample. The results for each group in a particular aggregate sample were used to calculate weighted results that represent the sample as a whole. For each of the variables included in Table 1, this was done by multiplying the results obtained in each of the groups by the respective percentages of the groups to the whole sample. The weighted results, given in Table 3, were used in the statistical analysis. The meanings of the variables in this table are as follows:

MST = percent matrix-supported texture particles,
GST = percent grain-supported texture particles,
TM = percent total matrix,

TABLE 2 Summary of Aggregate Sample Groups

Aggregate Number	Description	Group Name *	Percentage
1	Crushed limestone	Mudstone Wackestone Packstone	55 40 5
6	Partially crushed mixed gravel	Mudstone Packstone Quartz & Chert Quartzite	50 41 6 3
7	Crushed limestone	Packstone Mudstone Wackestone	65 20 15
9	Partially crushed mixed gravel	Granite gneiss Wackestone Calcareous sandstone	80 10 10
12	Partially crushed mixed gravel	Granite gneiss Sandstone Calcareous sandstone Quartz	40 35 15 10
15	Crushed limestone	Packstone - 1 Packstone - 2	60 40
16	Partially crushed mixed gravel	Chert Dolomitic wackestone Quartz	90 5 5
18	Crushed limestone	Mudstone Wackestone Packstone	55 40 5
22	Partially crushed mixed gravel	Chert Sandstone	65 35
25	Crushed Sandstone	Sandstone	100
31	Crushed Sandstone	Sandstone	100
32	Crushed limestone & dolomitic limestone	Mudstone Packstone Dolomitic wackestone	55 35 10
36	Crushed limestone	Mudstone Packstone Wackestone	55 25 20
37	Crushed limestone	Mudstone Wackestone Packstone	80 15 5
38	Crushed limestone	Mudstone Wackestone Packstone	75 15 10
39	Partially crushed mixed gravel	Mudstone Chert Sandstone	73 24 3
50	Crushed limestone & dolomitic limestone	Wackestone Packstone Dolomitic wackestone Mudstone	45 35 10 10
51	Crushed calcareous sandstone & sandy limestone	Calcareous sandstone Sandy limestone	70 30
52	Crushed calcareous sandstone	Calcareous sandstone	100
53	Crushed dolomite & dolomitic limestone	Dolomite Dolomitic mudstone	75 25

* See text for definitions/descriptions of specific terms

CM = percent carbonate matrix,
NCM = percent noncarbonate matrix,
TG = percent total grains,
CG = percent carbonate grains,
DG = percent dolomite grains,
NGG = percent noncarbonate grains,

TABLE 3 Weighted Mineralogical and Petrographical Results for the Aggregate Samples Examined

AGMT	Agg. No.	Texture		Matrix			Grains				Mineralogy		Voids			Particle Shape	
		MST	GST	TM	CM	NCM	TG	CG	DG	NCG	CC	NCC	VC	VCG	VCM	SPH	RND
LMRA	15	0	100	14.00	14.00	0.00	69.00	62.00	13.20	7.00	76.00	7.00	17.00	17.00	0.00	LTM	ATSA
LMST	1	95	5	85.00	85.00	0.00	14.75	13.00	0.55	1.75	98.00	1.75	0.25	5.00	0.00	LTM	ANGU
	7	35	65	51.30	51.30	0.00	44.70	43.70	4.00	1.00	95.00	1.00	4.00	5.00	2.14	LOW	ANGU
	18	95	5	80.50	80.50	0.00	14.50	13.50	0.00	1.00	94.00	1.00	5.00	5.00	5.00	LTM	ATSA
	32	65	35	63.25	63.25	0.00	16.00	15.00	0.80	1.00	78.25	1.00	20.75	25.00	18.46	LTM	ATSA
	36	75	25	73.25	73.25	0.00	25.50	25.30	0.00	0.20	98.55	0.20	1.25	5.00	0.00	LOW	ATSA
	37	95	5	84.00	84.00	0.00	10.00	9.20	0.00	0.80	93.20	0.80	6.00	10.00	5.80	MED	ANGU
	38	90	10	84.50	84.50	0.00	12.25	12.25	0.00	0.00	96.25	0.00	3.25	10.00	2.50	LOW	ATSR
	50	65	35	57.80	57.80	0.00	30.45	29.10	1.50	1.35	86.90	1.35	11.75	10.00	12.70	LTM	ANGU
	53	25	75	36.25	36.25	0.00	58.75	57.70	56.75	1.00	94.00	1.00	5.00	5.00	5.00	LOW	ANGU
SIGR	6	56	44	63.75	57.75	6.00	36.25	32.34	0.00	3.91	90.09	9.91	0.00	0.00	0.00	MED	WRTA
	9	10	90	9.00	9.00	0.00	90.00	2.90	1.00	87.10	11.90	87.10	1.00	0.55	5.00	LOW	ATSR
	12	10	90	20.00	3.00	17.00	80.00	0.00	0.00	80.00	3.00	97.00	0.00	0.00	0.00	LTM	ANGU
	16	100	0	94.25	3.75	90.50	5.50	0.74	0.75	4.75	4.50	95.25	0.25	0.00	0.25	LOW	ATSR
	22	65	35	65.50	0.00	65.50	29.50	0.00	0.00	29.50	0.00	95.00	5.00	5.00	5.00	MED	ATSR
	39	94	6	92.00	67.00	25.00	8.00	4.50	0.25	3.50	71.50	28.50	0.00	0.00	0.00	LTM	ATSA
SDST	25	0	100	25.00	0.00	25.00	75.00	0.00	0.00	75.00	0.00	100.00	0.00	0.00	0.00	LOW	ANGU
	31	0	100	25.00	0.00	25.00	75.00	0.00	0.00	75.00	0.00	100.00	0.00	0.00	0.00	LOW	ANGU
	51	30	70	38.00	38.00	0.00	62.00	8.50	8.50	53.50	46.50	53.50	0.00	0.00	0.00	LOW	ANGU
	52	0	100	30.00	30.00	0.00	70.00	2.00	0.00	68.00	32.00	68.00	0.00	0.00	0.00	LOW	ANGU

CC = percent carbonate content,
NCC = percent noncarbonate content,
VC = percent void content,
VCG = percent void content in grain-supported texture particles,
VCM = percent void content in matrix-supported texture particles,
SPH = particle sphericity, and
RND = particle roundness.

The meanings of the abbreviations under the sphericity and roundness variables are as follows: LTM, low to medium; MED, medium; ANGU, angular; ATSA, angular to subangular; ATSR, angular to subrounded; and WRTA, well rounded to angular.

The noncarbonate content weighted results when compared with those of the insoluble residue test (ASTM D3042-79) performed on all examined samples indicated a coefficient of correlation of 0.99. This gives confidence in the results of the subjective evaluation of mineralogical content attempted in this study. Future work may involve a more objective method of mineralogical evaluation, such as the X ray diffraction procedure.

Textures and Minerals Encountered

The rocks examined were from all of the three basic rock types and exhibited a wide variety of textures. The sedimentary rocks were carbonates, sandstones, and cherts. The igneous and metamorphic rocks included quartzite, quartz, granite gneiss, and a minor amount of volcanic rocks.

The carbonate rocks were mudstones, wackestones, packstones, dolomitic limestones, sandy limestones, and dolomites. The matrix was predominantly microcrystalline calcite mud, with partial recrystallization of the mud to spary calcite in some. The carbonate grains observed were composed of calcite spar, calcite mud, or dolomite. However, siliceous, pyrite, pyrolusite, clay, and limonite grains as well as stylolite formations were also found. In addition, these rocks had a wide range of visible porosity, which is considered to generally increase frictional properties. This phenomenon may be compared with that of the synthetic lightweight aggregates whose vesicular structure contributes to the well-documented, excellent frictional properties (*1*).

Mudstones are matrix-supported limestones with less than 10 percent grains. Some mudstones were dense and firm, comprising well-compacted microcrystalline calcite, whereas others had a considerable amount of voids. Wackestones are also matrix-supported limestones but with more than 10 percent grains. These were found with a wide range of percent voids in their structures. Packstones, which are grain-supported limestones, had the widest range of percent voids in this study. Some were firmly dense, whereas others were so porous that they were described as very soft and friable. The latter were frequently composed of calcite and dolomite grains that were not well compacted.

The presence of dolomite grains, which have a hardness slightly greater than that of calcite grains, is expected to enhance the frictional properties of the carbonate rocks. When dolomite grains were more than a trace in a limestone, the rock was referred to as a dolomitic limestone. Similarly, when quartz grains were found in sizeable amounts, the limestone was referred to as a sandy limestone.

Dolomites were also observed that were predominantly composed of dolomite grains with calcite mud filling the pores between them. Thus, they were classified as grain supported.

The other types of sedimentary rocks examined were sandstones and cherts. Sandstones were commonly composed of abundant quartz, feldspar, or carbonate grains cemented together with calcite or silica and perhaps some minor hematite and other impurities. Therefore, they were considered to have an excellent grain-supported texture. When the grains were cemented with calcite, the rock was referred to as a calcareous

sandstone. This rock is believed to have excellent differential wear, which has great influence on frictional properties. Chert is a microcrystalline quartz formed by either the accumulation of organism sediment or precipitation from solution. Although cherts are hard and, thus, are expected to aid in frictional resistance, they were classified as matrix-supported because of the lack of surface texture.

In the metamorphic and igneous groups, quartzite and granite gneiss were identified. Quartzite is a metamorphosed quartz sandstone. It was composed of quartz grains with silica cement that had grown in optical continuity around each fragment. Granite gneiss, also referred to as metagranite, is a metamorphic rock containing mostly quartz with some feldspar and mica in a conspicuously foliated, banded, or aligned pattern. Both rocks were considered to have a granular texture and lacked matrix.

Last was quartz, a hard rock with no surface texture. It was considered to be matrix-supported with less than 10 percent grains.

ANALYSIS OF FIELD DATA

Collected Data

Field data were gathered on all established test sections. The data for each test section consisted of a survey of construction variables performed at the construction site, traffic data collected annually, results of field testing, and long-term and periodical weather data.

For each test section, a survey was made of the coarse aggregate material and asphalt type and the rates at which both materials were to be placed [the design distribution rate of asphalt and the spreading rate of aggregate (AGSR)]. The AGSR ranged from 77 to 142 m^2 of surface for each cubic meter of aggregate (70 to 130 yd^2/yd^3). The annual average daily traffic (ADT) counts varied between 300 and 3,500 vehicles per lane.

The skid resistance test has been conducted twice a year in accordance with ASTM E274. The measured friction is expressed as a friction number (FN). Six sets of skid resistance measurements that spanned about 3.5 years were used in the analysis to follow.

Detailed climatological data have also been sought. Specifically, the data have been concerned with the testing seasons (dry or wet) and the amount of rainfall that occurred before and during field testing. These data were statistically analyzed to explain as much of the field performance variability as possible.

Grouping of Field Frictional Data

The friction data for the test sections and replicates built with the 20 aggregates examined petrographically were used. The data were grouped according to the major variables describing aggregate texture and mineralogy.

First, the data for the 20 aggregates were divided into two groups on the basis of percentage of particles with a grain-supported texture (Figure 1). Most of the aggregates with more than 50 percent GST particles had performance levels above the zone of minimum friction. This zone was assumed to be confining FNs in the range of 30 to 40. The data for the group with less than 50 percent GST particles were widely scattered but generally showed a decrease in frictional resistance. Groupings according to content of minerals with Mohs's hardness values greater than 5 revealed further explanations for the observed variations. Aggregates with more than 50 percent GST particles but less than 10 percent hard minerals experienced a decrease in frictional resistance (Figure 2), whereas the majority of the aggregates with less than 50 percent GST particles but more than 90 percent hard minerals had the highest FNs (Figure 3).

Second, the data for the 20 aggregates were grouped according to percentage of hard minerals (*2*). The group with less than 30 percent hard minerals showed a general decrease

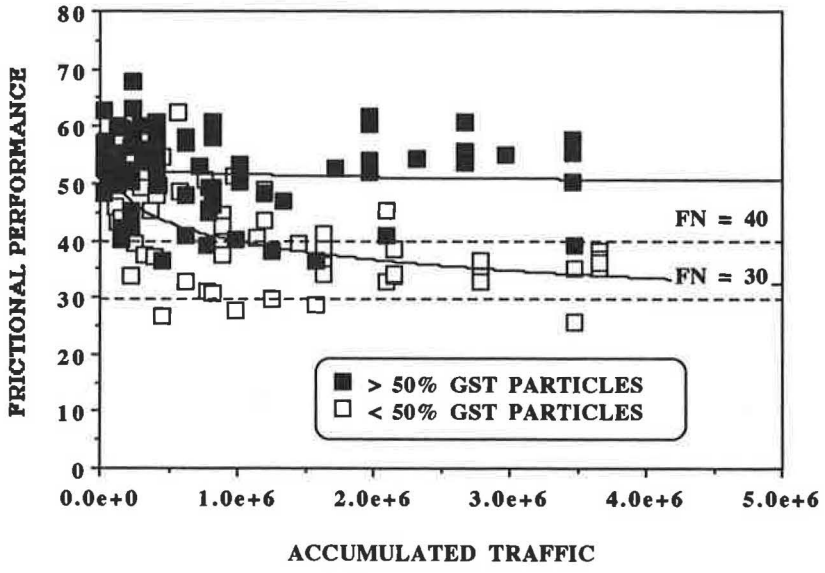

FIGURE 1 Frictional performance of aggregates considered in the petrographic examination, grouped according to their textural classification.

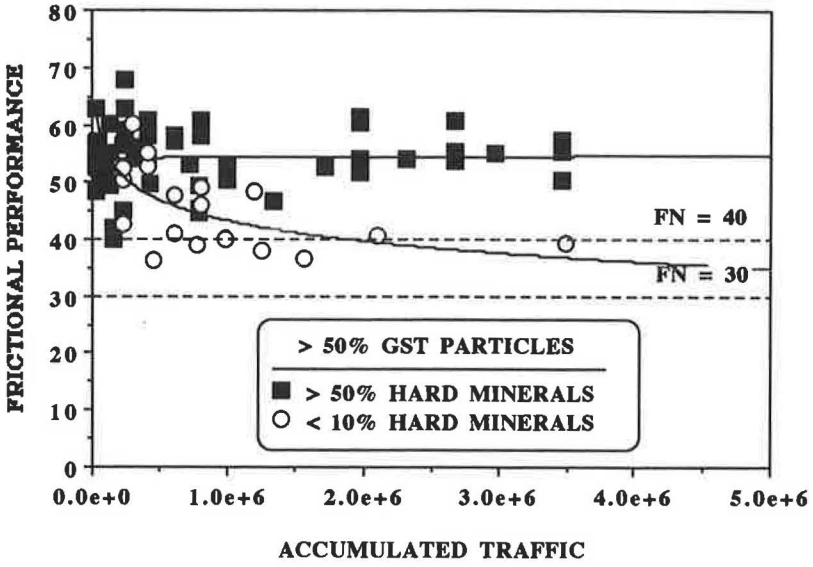

FIGURE 2 Frictional performance of aggregates with more than 50 percent GST particles, grouped according to percentage of hard minerals.

in performance. For this group, aggregates with more than 30 percent GST particles varied widely in performance. This variation is largely explained by the ADT, void content, and the mineralogy of the grains (Figure 4).

Finally, all aggregates with a considerable amount of carbonate minerals were grouped according to their petrographic properties (Figure 4), and two major observations were made. First, the level of performance of aggregates with a large amount of MST particles improved as the percentage of voids increased. Second, the level of performance of aggregates with a considerable amount of GST particles was associated with the level of traffic and the hardness of the grains. The dolomitic grains gave a level of performance higher than that given by the calcite grain. Aggregates with GST particles consisting of quartz grains cemented by carbonate minerals gave the highest levels of performance.

STATISTICAL MODELING OF PETROGRAPHIC AND FIELD DATA

Probabilistic Prediction Model

When the friction data of the petrographically examined aggregates were used along with the traffic, construction, and weather variables, a regression model with a good adjusted

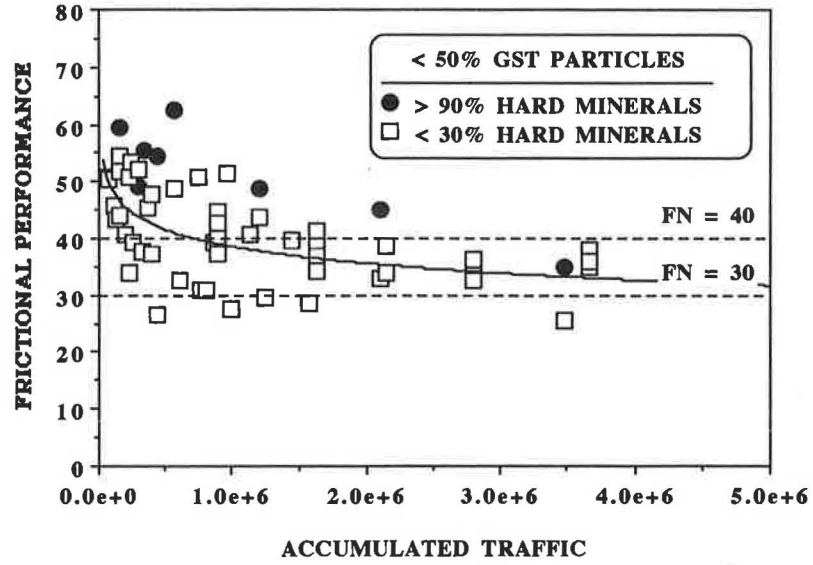

FIGURE 3 Frictional performance of aggregates with less than 50 percent GST particles, grouped according to percentage of hard minerals.

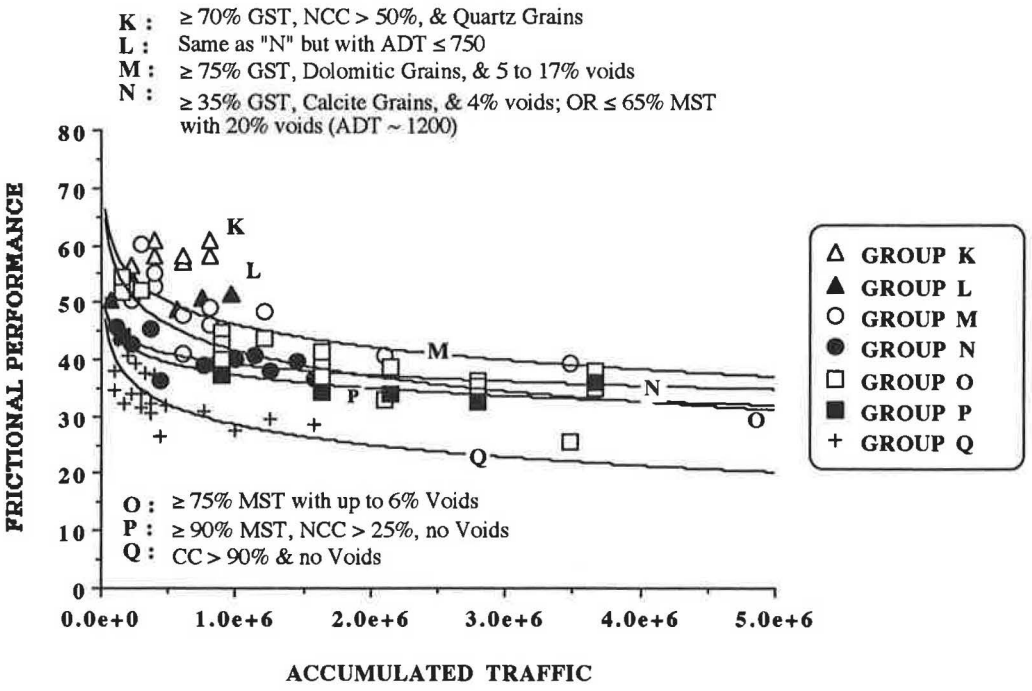

FIGURE 4 Frictional performance of aggregates with considerable amount of carbonate minerals.

R^2 of about 0.67 resulted. On the basis of 139 observations, the model, with the statistically significant variables, has the following form:

$$FN = 52.47 - 2.55(LGCUTR) + 0.0125(GST \times LGCUTR) - 0.02(CG \times LGCUTR) + 0.184(DG) + 0.1174(NCM) + 0.48(VC) + 0.17(AGSR) \quad (1)$$

with a standard error on the order of 5.37.

Whereas FN decreased with the logarithmic function of cumulative traffic (LGCUTR), the slope of this relationship changed upwardly depending on the percentage of grain-supported texture (GST) particles in an aggregate. However, for the carbonate grains (CG), as opposed to hard ones, the slope was observed to negatively adjust for this property. This indicated that although the texture was good (GST), it did not greatly enhance the performance because the grains were carbonate. When the grains were dolomite (DG), the FN increased. In addition, the percentage of noncarbonate matrix (NCM) positively affected performance in spite of the lack in noncarbonate grains. Aggregate 16, which exhibited poor laboratory polish properties but had a high percentage of NCM, showed a better performance than the carbonate aggregates with similar laboratory polish characteristics. Moreover, the void content (VC) had a positive effect on performance, particularly on the carbonate aggregates with considerable amount of matrix-supported texture (MST) particles. Although environmental region did not come out as an important variable in this model, it is believed that, since most of the somewhat porous, MST carbonate aggregates were located in the warm, moist region of Texas, it contributed to the VC variable showing significance in this model. Finally, the construction design aggregate spreading rate (AGSR) was found to be a significant variable in the model.

Example Application of the Prediction Model

Predicted values of frictional performance (to be observed in the future) for given values of the predictor variables can be obtained by substituting values of the predictor variables into the prediction model. A confidence interval for the mean value and a prediction interval for the specific value of frictional performance can then be constructed (*7*). The mean performance estimate of LMST Aggregate 53, with an AGSR of 130 m^2 of surface for each cubic meter of aggregate, was predicted using the formulated probabilistic model described above. Figure 5 shows the close prediction obtained using this petrographic model as well as the boundaries of error associated with it.

CONCLUDING REMARKS AND LIMITATIONS

The results of the petrographic examination of aggregates attempted in this study appeared to have explained a sizeable portion of the performance variability experienced with the monitored seal coat pavement overlays. The variables showing statistical significance in the model included the percentage of grain-supported texture particles, the amounts of dolomitic and other carbonate grains in aggregate particles, the percentage of noncarbonate matrix present in particles, and the level of prevailing void content. However, the proposed model, based on only 139 observations, may need to be re-

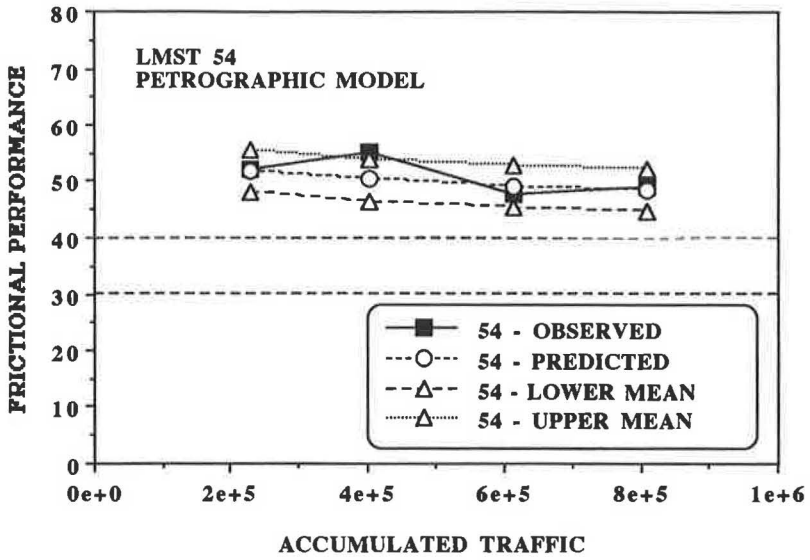

FIGURE 5 Predicted versus observed performance for LMST Aggregate 54 petrographic probabilistic model.

fined and validated to include a wider range of aggregates and service conditions.

ACKNOWLEDGMENT

This study was conducted by the Center for Transportation Research at the University of Texas at Austin under the sponsorship of the Texas Department of Highways and Public Transportation in cooperation with the Federal Highway Administration. The authors express their appreciation to Margaret Hanson and Tom Patty of Erlin, Hime Associates for their assistance in the petrographic examination. Thanks are also extended to the University Research Board of the American University of Beirut, which made it possible for the first author to conduct follow-up research on this subject.

REFERENCES

1. Abdul-Malak, M. U., A. H. Meyer, and D. W. Fowler. Research Program for Predicting the Frictional Characteristics of Seal-Coat Pavement Surfaces. In *Transportation Research Record 1217,* TRB, National Research Council, Washington, D.C., 1989, pp. 53–64.
2. Abdul-Malak, M. U. *Implication of Aggregates in the Construction and Performance of Seal Coat Pavement Overlays.* Ph.D. dissertation. The University of Texas at Austin, Austin, 1990.
3. Greensmith, J. T. *Petrology of the Sedimentary Rocks* (7th edition). Unwin Hyman, London, 1989.
4. Williams, H., F. J. Turner, and C. M. Gilbert. *Petrography: An Introduction to the Study of Rocks in Thin Sections.* W. H. Freeman and Company, San Francisco, Calif., 1982.
5. Dietrich, R. V., and B. J. Skinner. *Rocks and Rock Minerals.* John Wiley and Sons, New York, 1979.
6. Test Method Tex-210-F-1986: Determination of Asphalt Content of Bituminous Mixtures by Extraction. In *Manual of Test Methods,* Texas State Department of Highways and Public Transportation, Austin, March 1986.
7. Kachigan, S. K. *Statistical Analysis: An Interdisciplinary Introduction to Univariate and Multivariate Methods.* Radius Press, New York, 1986.

Publication of this paper sponsored by Committee on Mineral Aggregates.

Comparison of Some Engineering Properties of Expanded Polystyrene with Those of Soils

D. NEGUSSEY AND M. JAHANANDISH

The engineering behavior of expanded polystyrene (EPS) was investigated for potential applications as an alternative geomaterial. Background on European experience with EPS in road construction over the past 20 years is provided. Tests were performed on EPS samples of two densities in constrained and unconfined deformation with loads applied in stress-controlled mode. Strength and deformation behavior and lateral stress coefficients for soils and EPS are compared. The results indicate that the engineering properties of EPS can be quantified in a manner similar to those of earth materials. For some applications that involve infrastructure rehabilitation and construction of transportation facilities, EPS offers unique advantages over soils. EPS needed for subsurface construction may contain recycled portions, and this would be an important environmental incentive for using EPS as a geomaterial.

Expanded polystyrene (EPS) is a synthetic material that is widely used to manufacture disposable utensils and for product packaging. Most applications of EPS involve a short service life and one-time use with virtually no recycling. EPS is not a readily biodegradable waste product. There appears to be a good deal of interest in reducing EPS solid waste.

EPS has peculiar characteristics that would be desirable for subsurface construction applications. It is very light compared with soil and concrete and has energy absorption and insulation properties. EPS has been used as superlightweight fill and for foundation insulation to reduce frost cover requirements. Reported applications of EPS in subsurface construction have mostly been related to roads. There have been some large and small unpublished applications in the United States. Norway has been the pioneer in EPS applications, and much of the experience to date has been guided more by rule of thumb and field observation.

Sorlie et al. (*1*) presented the Norwegian road construction experience with lightweight soil substitute materials. They suggest that EPS should have a compressive strength of 100 kPa at 5 percent deformation and an air resistance number of better than 70 to limit moisture pickup. Inflammability, dissolving by petroleum fluids, and increased icing potential at near-freezing temperatures are practical problems that require design consideration. A fire-resisting variety of EPS can be specified at an additional cost of 5 to 10 percent above standard quality (*2*). Potential damage of EPS by spilled fuel can be mitigated by providing a membrane cover in addition to and below concrete slabs that are normally placed on top of EPS fills for improved load distribution (*3*). Icing problems can be minimized by using a thicker pavement structure and by restricting moisture access (*1*).

A 4.5-m EPS fill is reported to have been used as lightweight fill on soft ground for a temporary overpass bridge in Norway (*4*). Creep deformations at stress levels of up to 60 percent of yield were negligible. Transient heavy wheel loads did not induce residual stresses.

Satisfactory performance of EPS as fill above rigid pipes to promote induced trench conditions has been reported (*5*). This application is of special interest because EPS replaces the more commonly used organic materials, which degrade in time. Furthermore, EPS for trench fill may consist entirely of sorted or recycled waste material.

Rygg and Sorlie (*3*) report on three applications in Norway that involved repair of a road across a bog, new road construction on a bog, and road embankment adjoining a bridge abutment, all using EPS. These case histories indicate successful use of EPS for road rehabilitation and construction over difficult foundation soils.

EPS fills that remain submerged for extended durations are found to retain about 4 percent water by volume in the first year and about 9 percent in 9 to 12 years (*6*). Even in cases of significant groundwater lowering, this level of moisture retention does not compromise the superlightweight advantages of EPS. However, adequate cover must be provided to prevent EPS breakout in times of submergence due to flooding or general rise in groundwater level.

Norwegian experiences with EPS road fills over the past 20 years indicate aging effects to be insignificant within the design life of transportation facilities. The performance of roads built on EPS fill is reported to have been satisfactory (*7*).

Future trends envisioned for EPS in transportation include high embankments with steep side slopes for concrete form work, floating bridges, and fill for buried structures (*8*). EPS has also been used for slope stabilization along troublesome transportation corridors in mountainous country. The option of using recycled EPS or EPS with recycled fraction in subsurface construction is a new concept that would be worth exploring. Familiarity with EPS behavior and comparison with geomaterials should help promote broader applications in transportation and other geotechnical construction.

Department of Civil and Environmental Engineering, Syracuse University, Syracuse, N.Y. 13244.

TEST MATERIALS

EPS

Production of EPS blocks begins from EPS pellets that contain a blowing agent. The specific gravity, G_s, of polystyrene in amorphous or crystalline form is about 1.1 (*9*). The pellets are first subjected to steam to form prepuffs. Initial pellet size and duration of steam exposure determine the prepuff and final block density. The prepuff to pellet volume ratio is in the range of 40 to 1. Approximately 10 percent of recycled EPS reclaimed from plant waste is shredded and mixed with the prepuffs. The shredded EPS and prepuffs are poured into a Teflon-lined molding box. Steam is injected through small perforations along the molding box inside boundaries to induce additional expansion and fusion of the prepuffs. EPS blocks of typically 1.25 × 0.6 × 4 m or 1.25 × 0.6 × 8 m are formed by this process. Commercially available densities range from 15 to 50 kg/m³, with 20 and 30 kg/m³ varieties being more common. Depending on quantity and location, the more common 20 and 30 kg/m³ densities may cost between $25/m³ and $50/m³, with the higher-density EPS costing more. Cylindrical EPS blocks 76 mm in diameter and 150 mm in height were provided for the investigation by Thermal Foams/ Syracuse, Inc.

Clay

A soft inorganic clay of medium plasticity was tested to compare with the EPS behavior. The clay is used for making pottery and has a water content of 30 percent and liquid and plastic limits of 41 and 24 percent, respectively. The specific gravity was determined to be 2.8 and the portion finer than 2μ amounted to 46 percent by weight. The dry density of the clay sample was about 1520 kg/m³.

Sand

Results of tests on silica sand are also compared with the behavior of EPS. The sand has a D_{50} of 0.55 mm and is uniform, having a uniformity coefficient, C_u, of 1.9. Quartz is the predominant mineral in silica sand, and individual grains are mostly subangular. The fines content of silica sand is less than 1 percent, and the specific gravity is 2.6. The dry density of the sand sample was about 1550 kg/m³.

EQUIPMENT

Constrained deformation tests were performed using a laterally instrumented oedometer 76 mm in diameter and 38 mm in height. Details of the oedometer are shown in Figure 1. Along the outside of a thin section near the midheight of the oedometer, strain gauges are mounted to sense lateral strain due to bending and hoop stresses. The instrumented ring adapts to a base fitted with a central porous stone and an outer O-ring seal. A retaining ring clamps the ring to the base to seal. Drainage connection is provided along the base block. A spacer with a top O-ring seal and narrow section along the thin section fits inside the oedometer. With the spacer block in place and restrained vertically, the instrumented ring can be pressurized. The response of the strain gauges was calibrated against precise changes in pressure set by a deadweight tester. The instrumented section provides a sensitivity of about 1 Mv/volt. The output is linear to lateral pressures in excess of 700 kPa.

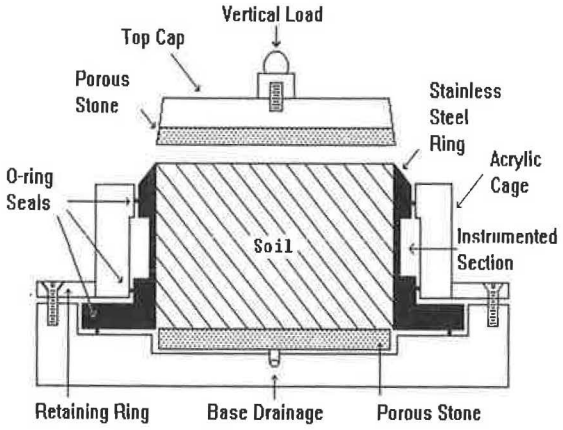

FIGURE 1 Oedometer with lateral pressure sensors.

PROCEDURE

EPS test samples 38 mm high and 76 mm in diameter were cut from EPS rods of the same diameter using a hot nichrome wire. An EPS rod was placed in a glass tube of a slightly larger diameter and having smooth cut perpendicular ends. With the block held in position and the glass end as guide, test samples were cut. The weight and dimensions of cut samples were recorded. Samples for confined tests were installed in the oedometer, and those for unconfined tests were placed directly in the loading frame. In both cases vertical loading was applied pneumatically in steps, and the applied load was sensed by a load cell positioned above the top cap. Vertical movement was monitored by a displacement transducer.

Confined compression tests were also performed on the clay and sand soils in the instrumented oedometer. The consolidation test on the clay soil was performed under constant rate of displacement. The clay soil was also tested in unconfined compression. Procedures followed for the latter tests were in accordance with ASTM standards.

RESULTS

Test results from one-dimensional compression of a low-density EPS (21.0 kg/m³) in Figure 2 show a behavior very similar to consolidation of clay soils. Segments of reloading, loading, and unloading are evident. A yield stress at an apparent maximum past pressure of about 80 kPa can be identified. Before yield, void ratio state changes are moderate as would be in an overconsolidated stress range. Postyield, void ratio states traverse in a path much similar to virgin compression, and associated deformations are relatively large. Unloading and reloading are associated with smaller rates of void ratio change.

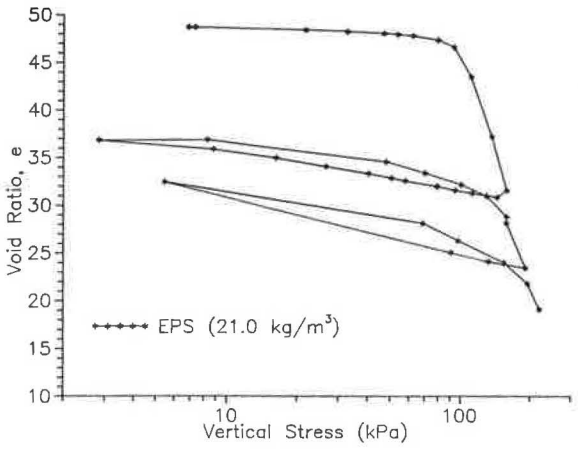

FIGURE 2 Characteristic behavior of EPS under one-dimensional deformation.

The state of maximum past pressure is recalled on reloading, and the material shows evidence of having a "memory."

One-dimensional compression test results for EPS samples of 21.0 and 30.4 kg/m³ are compared in Figure 3. The upper curve represents a portion of the results shown in Figure 2 for the lower-density EPS. The lower curve represents results for the higher-density EPS, and the yield stress is about 155 kPa. Neither sample had a prior history of loading. The observed differences in apparent maximum past pressures are due to different product initial densities. In the manufacture of EPS blocks, densities are controlled by duration of expansion time rather than applied pressure. Yet initial density effects are much like prestress effects in soils.

Constrained deformation test results for EPS are compared with those for silica sand and normally consolidated clay soil in the familiar semilog space [see Figure 4(a)]. Because the void ratio contrast between EPS and soils is very large, the comparison is based on strain rather than void ratio. The results indicate that EPS behavior compares favorably with the behavior of soils in the stress range before yield. For loading past yield, the EPS compression is much more severe even when compared with that of the clay.

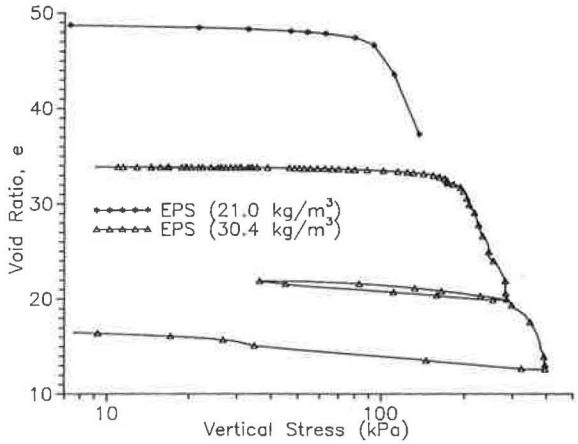

FIGURE 3 One-dimensional deformation behavior of EPS at two densities.

When the constrained deformation of EPS and the soils is compared in vertical stress and strain space [see Figure 4(b)], the soil response curves show a tendency to stiffen with strain. As expected, the sand develops much less strain and stiffens more rapidly than the clay. The EPS maintains a relatively constant modulus up to yielding near 155 kPa and almost 4 percent strain. Initial moduli for the sand, clay, and EPS are approximately 25,000 kPa, 3,000 kPa, and 4,000 kPa, respectively. Being on the higher side, the EPS modulus compares favorably with the clay. The postyield EPS response is characterized by a much lower modulus than the preyield. Even though confined, the EPS response curve simulates a behavior typical of unconfined compression.

A plot of restraining lateral stress against applied vertical stress to the soils and the EPS is shown in Figure 5. Lateral stresses are highest in the clay and are least in the EPS. K_o values for the clay, sand, and EPS are about 0.55, 0.43, and 0.15, respectively. In terms of customary approximations of K_o with reference to friction angle, the observed values for the soils are in a general range common for normally consolidated clay and loose sand, respectively. However, the EPS response up to yield approximates a low Poisson's ratio material and closer to very stiff to hard clay or very dense sand. With further loading beyond yield, lateral stresses in the EPS (and hence K_o states) decrease as would be the case for a

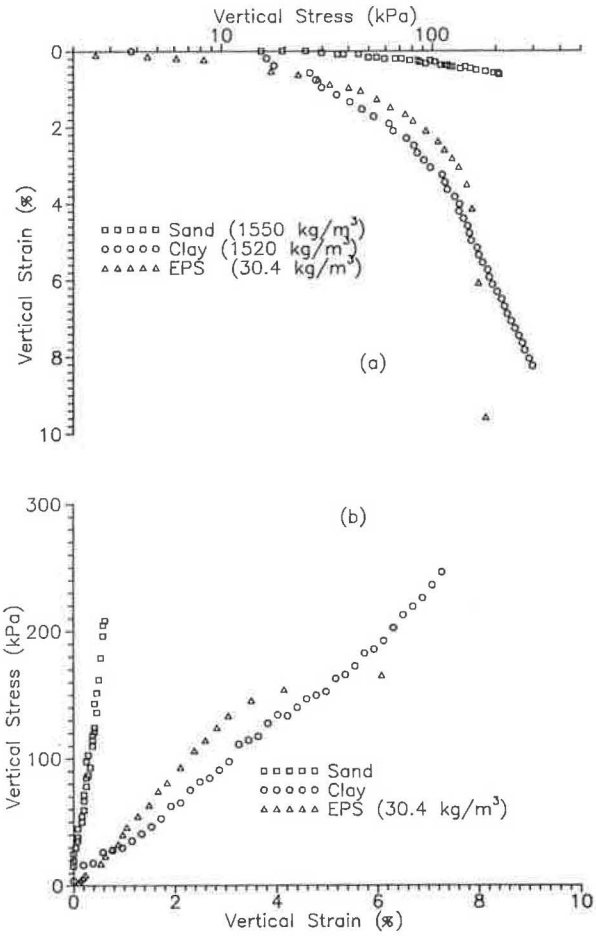

FIGURE 4 Comparison of one-dimensional deformation behavior of EPS with that of soils.

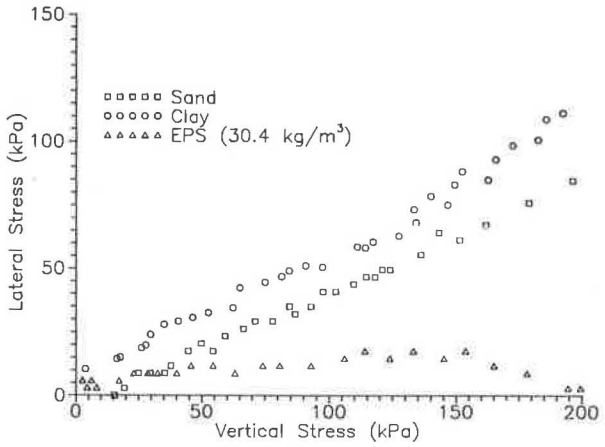

FIGURE 5 Induced lateral stresses under constrained deformation in EPS and soils.

material possessing a negative Poisson's ratio. This implies that lateral restraint is not essential to maintain features of constrained deformation in EPS and lends support to the observation that constrained and unconfined deformation responses of EPS are alike [see Figure 4(b)].

Test results of constrained deformation and unconfined compression of EPS (30.4 kg/m³) are compared in Figure 6(a) in natural vertical strain against applied vertical stress space. These results are also presented in the customary semilog space of void ratio and vertical stress in Figure 6(b). The yield state in unconfined compression corresponds closely to the apparent maximum past pressure in the constrained test. As implied by the earlier interpretation of a low Poisson's ratio for EPS, constrained modulus and Young's modulus are about the same. Loading, unloading, and reloading responses are also similar for constrained and unconstrained conditions. Virgin compression in constrained mode resembles postyield unconfined loading response. A preferred shear plane does not develop, and lateral spreading does not occur in response to unconfined loading.

The unconfined compression strength of EPS increases with density (Figure 7). Compared with the soft clay unconfined compression strength, the low-density (21.0 kg/m³) EPS is much stronger and would be equivalent to a firm clay. The unconfined compression strength of the denser EPS (30.4 kg/m³) is closer to that of stiff to hard clay. There is generally small additional increase in strength between 5 and 10 percent strain, but this may depend on strain rate and load duration. EPS compression strength is usually reported at 5 percent strain. In practice, applied loads must be distributed with a concrete pad or soil cover to prevent stress concentrations and punching failure to realize the indicated high strengths.

Figure 8(a) shows unconfined compression results in which EPS continues to support a stepwise increasing load past yield and at large strains. Postyield deformations are nonrecoverable and time dependent. Hysteresis loops are relatively small both at states below and past yield [Figure 6(a)]. Thus damping and energy absorption features of EPS are most favorable with virgin loading. As noted earlier, there was no evidence of a shear plane or lateral spreading at any stage of loading or deformation. The initial and final diameter of the sample was about the same even though very large vertical strains occurred.

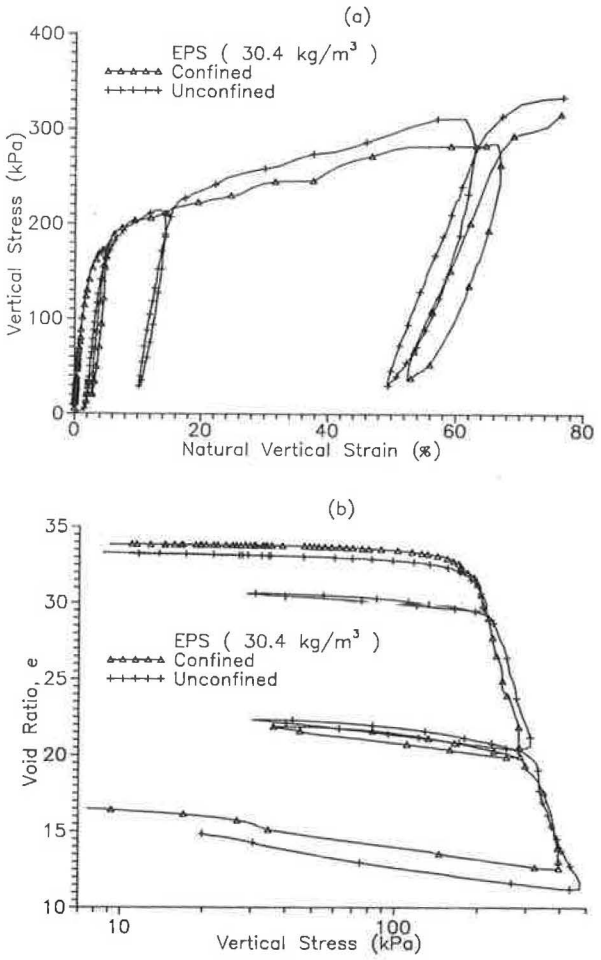

FIGURE 6 Comparison of EPS compression behavior under constrained and unconstrained lateral deformation.

Results in Figure 8(b) also show that EPS deformations have time dependence and that the degree of dependence is a function of stress level, stress history, and void ratio. These results are for unconfined compression, but the similarity of confined and unconfined compression behavior of EPS was shown in Figures 6(a) and 6(b). Each load increment was

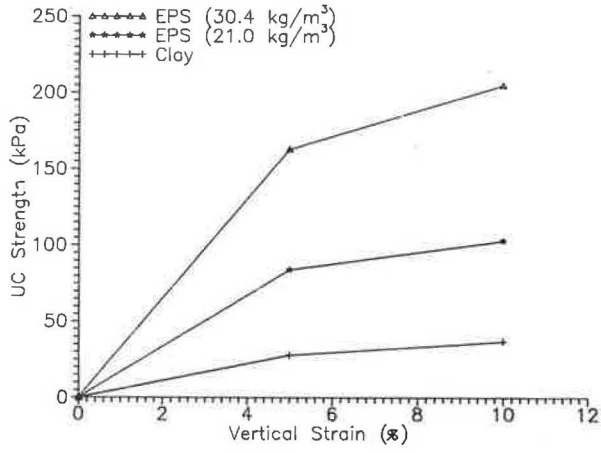

FIGURE 7 Comparison of unconfined compression strengths of EPS and clay.

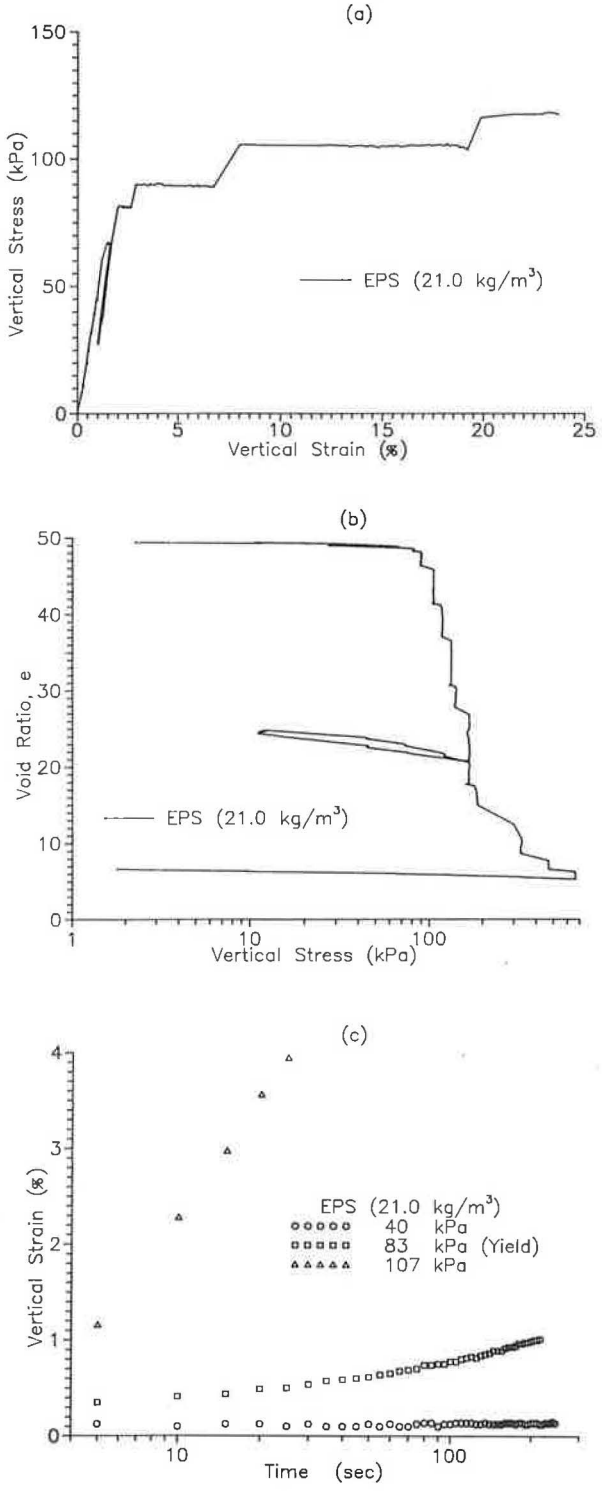

FIGURE 8 Time-dependent behavior of EPS.

sustained until time-dependent deformations subsided. States of stress near and postyield show evidence of time dependence in that deformations occur without change in stress state. Time-dependent deformations are small in the stress range below yield and along unloading and reloading segments when unloading is initiated before arresting time-dependent deformations; in subsequent loading, time-dependent deformations commence when the previous maximum stress level is reestablished. The magnitude of creep deformations diminish with decreasing void ratio states.

Isolated observations of time-dependent deformations at three selected stresses are presented in Figure 8(c) for EPS (21 kg/m³). The selected stresses are at about 50 percent of yield, yield at 83 kPa, and in postyield at 107 kPa. Elapsed times are referenced to load application. The curves resemble conventional primary and secondary creep stages for all three load steps. A tertiary type of creep stage may be inferred for the load steps corresponding to yield and postyield but not for the 50 percent of yield or lowest load stage. For the first load step, the resulting strain over the entire load duration is reasonably small. Essentially all of the deformation in this stage occurs in the first few seconds and during primary creep. Deformations in the secondary creep stage are relatively insignificant, and the stress level of 40 kPa is in the range of practical interest for geotechnical applications. A higher EPS density has been shown to result in a higher yield stress, and the corresponding stress threshold for time-dependent deformations should be higher.

Some of the observed engineering properties of EPS offer benefits superior to soils for certain subsurface applications. Fire hazard and chemical attack possibilities will require careful consideration and attention to storage arrangements and construction practice. Delivery of EPS to project sites and handling during construction will be easy. This should make EPS use more attractive in projects where site access is difficult. Environmental concerns and anticipated increased engineering activity in infrastructure rehabilitation and development over the coming years will offer challenges and opportunities to adapt new construction materials such as EPS. In a manner similar to geotextiles and geomembranes, geofoams (EPS for geotechnical applications) may be the next wave of cost-effective and environmentally compatible construction materials.

CONCLUSIONS

1. EPS is a superlightweight material with a wide range of possible applications in geotechnical and infrastructure engineering.
2. The stress-strain response and yield of EPS are well conditioned and bear close resemblance to some aspects of soil behavior.
3. Young's modulus and yield of EPS compare favorably with those of natural soils in the stress and strain range of practical interest for most geotechnical applications.
4. The yield stress for EPS is a function of initial density induced by the manufacturing process and can be specified.
5. EPS behaves as a low Poisson's ratio material and has similar confined and unconfined compression response.
6. During confined compression, induced lateral stresses are very low, and hence EPS has a low K_o property.
7. Time-dependent deformations of EPS assume significance at stress levels approaching yield and postyield but are reasonably small at working stress levels of about half of yield.
8. EPS for subsurface construction may be derived, in part, from recycling.
9. EPS has been used in Europe for geotechnical applications over the past 20 years, and the experience to date has been positive.

ACKNOWLEDGMENTS

The authors thank Syracuse University for providing funds and facilities that enabled this investigation and Thermal Foams/ Syracuse, Inc., for supplying EPS samples. The comments and suggestions for improvement made by the technical reviewers are acknowledged with gratitude.

REFERENCES

1. Sorlie, A., R. G. Dahlberg, G. Refsdal, and O. E. Ruud. National Report: Norway. *16th World Road Congress,* Vienna, Austria, 1979.
2. Flaate, K. Super Light Material in Heavy Construction. *Geotechnical News,* Vol. 22, 1987, pp. 22–23.
3. Rygg, N. O., and A. Sorlie. Polystyrene Foam for Lightweight Road Embankment. *10th International Conference on Soil Mechanics and Foundation Engineering,* Stockholm, Sweden, Vol. 2, 1981, pp. 247–252.
4. Skuggedal, H., and R. Aaboe. Temporary Overpass Bridge Founded on Expanded Polystyrene. *10th European Conference on Soil Mechanics and Foundation Engineering,* Florence, Italy, Vol. 2, 1991, pp. 559–561.
5. Vaslestad, J. Load Reduction on Buried Rigid Pipes. *10th European Conference on Soil Mechanics and Foundation Engineering,* Florence, Italy, Vol. 2, 1991, pp. 771–774.
6. Van Dorp, T. Expanded Polystyrene Foam as Light Fill and Foundation Material in Road Structures. *International Congress on Expanded Polystyrene,* Milan, Italy, 1988.
7. Aaboe, R. *Plastic Foam in Road Embankments: Experience with Expanded Polystyrene as a Light Weight Fill Material in Road Embankments.* Norwegian Road Research Laboratory, Oslo, Norway, 1985.
8. Refsdal, G. *Plastic Foam in Road Embankments: Future Trends for EPS Use.* Norwegian Road Research Laboratory, Oslo, Norway, 1985.
9. Rudd, J. F. Physical Constants of Polystyrene. In *Polymer Handbook* (J. Brandrup and E. H. Immergut, eds.), 3rd edition, John Wiley, New York, 1989.

DISCUSSION

JOHN S. HORVATH
Civil Engineering Department, Manhattan College, Bronx, N.Y. 10471.

I am actively involved in researching the application of rigid plastic foams to a wide variety of geotechnical problems. Such materials are now recognized as geosynthetics under the newly created product category of "geofoams." An inventory of geofoam materials and functions identified to date is summarized elsewhere (*1*). EPS has been and still is the most widely used geofoam (*2,3*). Among the reasons are its relative cost, environmental effects related to manufacture, finished product size, and material properties. A summary of basic EPS material properties of interest to geotechnical engineers is presented elsewhere (*4*).

In the light of this ongoing research, I would like to comment on or question several items in this paper:

1. The most significant comment is a general one concerning the soil samples used for comparison with EPS behavior. It is well established that the load-deformation behavior of soil is highly dependent on stress history, aging, relative density (for sand), and other factors in addition to particle size distribution. Information concerning specimen preparation and conditioning was lacking for the soils tested. Consequently, the conclusions drawn concerning whether EPS is behaviorally "better" or "worse" than soil are misleading. The conclusions of the paper in this regard are strictly applicable to two specific types of soil, each at a stress state that is undefined.

2. Whereas recycling is an admirable goal, the contribution of EPS to the domestic solid waste stream in the United States should be kept in perspective. Recently published work detailing the scientific exhumation and evaluation of actual landfills in the United States has demonstrated that all polystyrene products combined occupy less than 0.25 percent of landfill volumes. In comparison, paper occupies approximately 40 percent. Furthermore, the potential for using postconsumer recycled EPS for geofoam is complicated by the fact that in the United States, flame-retardant expandable polystyrene beads are used routinely to produce EPS for construction products such as geofoam (this is not true in some other countries, Norway being one example) but normal beads for other products. If flame-retardant EPS is commingled with normal EPS, the flame retardancy of the end product is compromised. Because the two types of EPS are visually indistinguishable, separation of the postconsumer recycled EPS is difficult unless special measures (e.g., coloring) were to be implemented industrywide during manufacture. As noted in the paper, recycling of in-plant scrap produced during manufacturing is already practiced by the EPS industry.

3. On the basis of recent (1992) correspondence with both the Norwegian Road Research Laboratory and the world's largest manufacturer of expandable polystyrene beads for EPS (BASF), the air-resistance test is no longer used for EPS geofoam quality control because it was found to provide inconsistent results.

4. Final, trimmed dimensions of EPS blocks in the United States are usually 610 by 1209 by 2438 mm (2 by 4 by 8 ft). Molding lengths are 4.9 m (16 ft) or 7.3 m (24 ft).

5. Current definitions of EPS compressive strength or yield strength are based on tests performed at a relatively rapid strain rate. Industry practice at present is to define EPS compressive strength as the stress at 10 percent strain, not 5 percent (*5*). The 5 percent strain criterion is used in Norway and perhaps elsewhere. However, it is correct that the difference in compressive stress between 5 percent strain and 10 percent strain in the typical short-term test is relatively small. This is because the elastic range ends and yielding begins for EPS at a compressive strain between 1 and 2 percent depending on product density. As will be discussed later, the compressive strength defined using such short-term tests does not provide insight into behavior under the more typical geotechnical loads of long duration.

6. Was the inside of the instrument oedometer lined with any low-friction material or substance? Axial strains of EPS specimens in excess of 50 percent were implied for some of the one-dimensional compression tests, and friction along the wall of the oedometer, which would reduce the actual axial compressive stress on the test specimen, is of concern.

7. It was stated that constant-rate-of-strain loading rather than the traditional incremental loading was used for the one-

dimensional compression tests on the clay specimen. What was the strain rate?

8. Incremental loading was used for both the one-dimensional and unconfined compression tests on EPS specimens. What was the duration of each load increment? As noted previously, estimation of yield stress for EPS is highly dependent on the load duration.

9. With reference to Figures 8(a) and 8(b), what were the durations of each load increment for which creep effects were observed? What criteria were used to select a time for which the strain rate appeared to be zero? EPS is a thermoplastic material, and time-dependent deformations will continue for some as-yet-unknown duration at all stress levels. The question becomes whether such time-dependent deformations are acceptable in a given application. Tests of EPS creep behavior in unconfined compression indicate that test durations of 10,000 hr or more are required to draw correct inferences as to whether tertiary creep effects will occur at a given stress level (*5*). By comparison, load durations of only about 0.1 hr are shown in Figure 8(c). Figure 9 shows the creep behavior for an EPS specimen with a density close to that used for the results shown in the authors' Figure 8(c). The "yield strength" of the specimen in Figure 9 in the standard short-term test (strain rate of 10 percent/min) was slightly greater than 100 kPa. For stresses greater than about 50 percent of yield, the long-term creep would likely be excessive for many engineering applications.

10. The qualitative similarity between EPS and soil with regard to the shape of the load-deformation curves is not a unique aspect of EPS. Rather, EPS and soil both exhibit rather classical material behavior. For example, as discussed elsewhere (*6*), annealed copper wire has behavior identical to that shown in Figure 2. The key difference is that for solids such as EPS and copper wire, yield stress is built in during manufacture, so soil mechanics concepts such as "maximum past stress" have no physical relevance. On the other hand, for a particulate material such as soil, yield stress is not unique to the particular soil but depends primarily on stress history and other factors such as aging.

In summary, I believe that the authors have provided some potentially useful information concerning the relative behavior of EPS in unconfined versus one-dimensional axial compression if additional information concerning the type and duration of test loading is given. On the other hand, the comparisons with soil behavior are misleading because of the lack of key soil mechanics information concerning stress history and so forth of the soil specimens. Conclusions as to the relative strength and stiffness of EPS and soil are probably

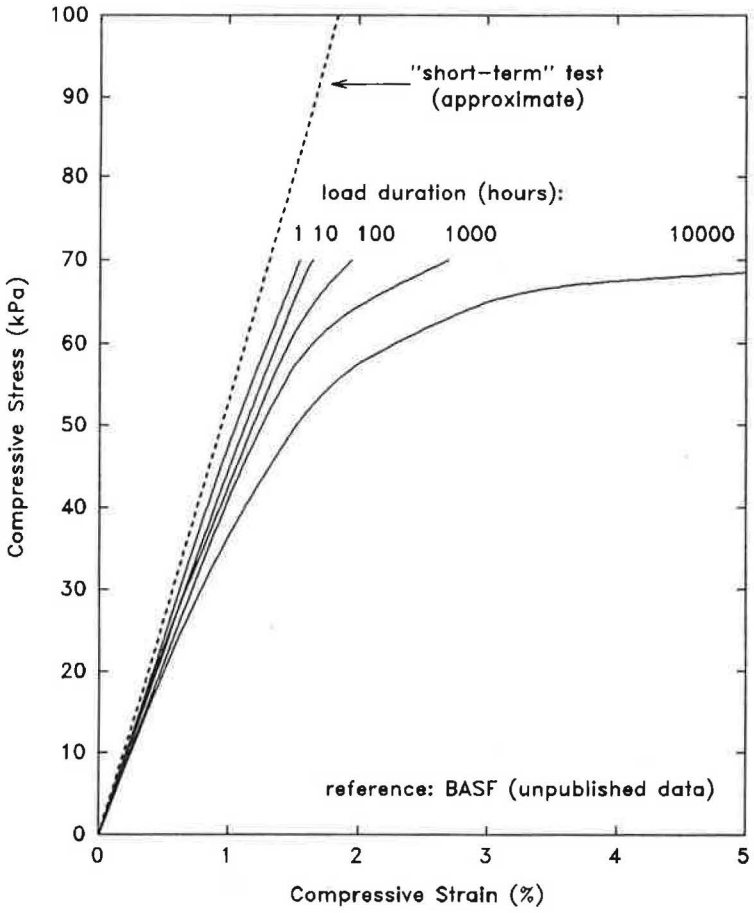

FIGURE 9 Creep behavior of 23.5-kg/m³ EPS in unconfined axial compression.

impossible to generalize because of the lack of unique behavior for a given type of soil.

REFERENCES

1. Horvath, J. S. Geofoam Geosynthetics: An Overview of the Past and Future. *Geosynthetics World* (in press).
2. Horvath, J. S. New Developments in Geosynthetics: "Lite" Products Come of Age. *Standardization News,* ASTM, Sept. 1992, pp. 50–53.
3. Horvath, J. S. Dark, No Sugar: A Well-Known Material Enters the Geosynthetic Mainstream. *Geotechnical Fabrics Report,* IFAI, Oct. 1992, pp. 18–23.
4. Horvath, J. S. Expanded Polystyrene (EPS) Geofoam: An Introduction to Material Behavior. *Geotextiles and Geomembranes* (submitted for publication).
5. *Styropor; Processing—Measurements/Tests.* TI 0-220 e. BASF AG, Ludwigshafen, Germany, 1990.
6. Wood, D. M. *Soil Behaviour and Critical State Soil Mechanics.* Cambridge University Press, Cambridge, United Kingdom, 1990.

AUTHORS' CLOSURE

We thank the discussant for his interest in the paper and contribution to a discussion.

At this stage and in this context, the comparison of EPS behavior with that of soils is general. The two broad but important classes of soils compared, clay and sand, are meant to be referenced generically. The range in compared behavior for a clean medium quartz sand, loose or dense, and a soft normally consolidated inactive clay would not overlap under conceivable sets of practical circumstances at corresponding stress levels. Physical, chemical, age, and stress attributes have individual and collective influence on the response and performance of a given soil. Drainage conditions, stress path, and loading rate would also be important. In a strict sense, quantitative results for a soil apply to the soil in question and prevailing test conditions. That is why specific soils for specific applications are tested in practice, and this approach will no doubt continue, when justified, in important applications that involve EPS and soils. However, useful qualitative and, in some cases, practically adequate quantitative observations are often drawn for a class of soils from results on specific soils through use of index properties. This is, of course, common in geotechnical engineering practice and is the sense we attempted to convey in the comparison of EPS with a clay and sand soils.

The arguments made by the discusser against recycling EPS are unfortunate and represent a special interest position. At present, the support for and awareness of the need for and benefits of recycling nonbiodegradable wastes are broad and do not require our further justification. For many subsurface applications of EPS, flame retardancy would not be critical. Potential compromise in flame retardancy due to mixing when recycling, as argued by the discussant, should not be a reason for discouraging EPS recycling.

The reference to air-resistance number made in the paper is in the context of a literature survey of published and acknowledged information. The discussant's information is presented as undocumented personal communication with sources that are not well defined. Mention of a traceable source reference would have been more useful than the name and rather flattering size description of a very large multinational manufacturer.

The behavior of EPS shows time dependence in preyield, at yield, and in postyield. This is shown by our results as well as by the unpublished secondhand data furnished by the discussant. We have noted that creep effects beyond 50 percent of yield and in postyield may be potentially excessive for most geotechnical applications. The specification of yield for EPS will no doubt benefit from further refinements in experimental observations.

In testing soils, special techniques are used to mitigate the influence of undesirable conditions that violate test assumptions. Side friction reduction in one-dimensional deformation tests by lubrication with vacuum grease is a well-known procedure. A very important finding shown in the paper is the observation that lateral stresses are low before yield, compared with vertical stresses, and actually diminish in postyield. One-dimensional and unconfined compression behavior are shown to be similar, and lateral stresses at large strains and large vertical stresses become insignificant. The interface friction between EPS and a smooth metal surface is low in addition to lateral stresses being small and becoming negligible. In view of the foregoing, the discussant's expressed concern regarding adverse effects of side friction and suggested need for lubrication is, in our view, not rational.

The strain rate for the constant rate of strain loading test on the clay soil was 0.006 percent/min. Load steps were maintained for 5 and 2 min during incremental loading and unloading of EPS, respectively. Creep observations were made within the load increment time base. Longer tests and other areas of EPS behavior are the focus of present and future investigations.

Uniqueness of engineering behavior is relative and contextual. The density, correspondence between constrained and unconfined compressions, lateral stress coefficients that develop during confined compression, and other properties of EPS would be considered unique compared with soils. To forge a favorable connection between these unique and important features of EPS and soils, the senior author proposed to representatives of the Society of the Plastics Industry and others, at a workshop held at Syracuse University in 1991, that EPS be referred to as geofoam.

We were careful to describe the observed breaks in one-dimensional response of EPS as apparent maximum past pressure. Because of the demonstrated correspondence between confined and unconfined behavior of EPS, yield and apparent maximum past pressure would be synonymous since they apply to EPS only.

The discussant views built-in stress in manufactured solids, and here he lumps copper and EPS, as not being analogous to maximum past pressure in soils. His reflections on this point are interestingly referenced to a textbook on soil behavior and critical state soil mechanics. The irony in the discussant's argument is that the development of critical state soil mechanics appealed to experimental studies of Cam-clay, a manufactured clay with built-in stress history. Needless to say, the critical state soil model is alternatively known as the Cam-clay model.

Publication of this paper sponsored by Committee on Soil and Rock Properties.

Resilient and Plastic Behavior of Classifier Tailings and Fly Ash Mixtures

SEUNG W. LEE AND K. L. FISHMAN

The resilient modulus and plastic deformation of two materials, currently considered waste products, were studied. The first material is fly ash, which is a waste product of coal combustion. The second is classifier tailings, a fine-grained material that is a by-product of aggregate processing. Results from cyclic triaxial testing used to study the resilient and plastic response of fly ash, classifier tailings, and a mixture of the two materials are presented. By itself neither material exhibits sufficient stiffness to realize any advantage in pavement construction. However, the resilient modulus of a mixture of the two materials is higher and plastic deformation lower than that of either material considered alone. Since no previously published experience with this material mixture exists, it is considered a new type of geomaterial. Historically, because of difficulties associated with cyclic triaxial testing, empirical formulas have been used to estimate resilient modulus. Therefore, the usefulness of applying existing empirical relations to the materials investigated to estimate resilient modulus is explored. Mechanistic-based pavement analyses were performed to predict pavement lives for flexible pavements having a subgrade of fly ash, classifier tailings, or a mixture of the two. The benefits of the material mixture in improving the pavement performance over that of either of its constituents are demonstrated.

In this study a mixture of two fine-grained materials, currently disposed of as waste products, is investigated for use as a roadbed material. The first is a Type F fly ash, a waste product from coal combustion. The second is the result of aggregate processing in the Buffalo, New York, area. Gravel is processed containing traces of native limestone and dolomite. Construction specifications limit the amount of material passing the No. 200 sieve in processed aggregate. Therefore, fine material is separated from the aggregate sluiced to detention basins, dredged, and stockpiled in landfill operations. This fine material is referred to throughout the aggregate processing industry as classifier tailings.

The use of fly ash as roadbed material has been the subject of previous research (*1–5*). These studies provided valuable data on engineering properties of fly ash or fly ash mixtures such as shear strength, permeability, moisture-density relationships, and so on. However, more information is required for predicting the performance of fly ash or fly ash mixtures as a component of a pavement structure.

Head (*6*) investigated mixtures of fly ash and coal refuse for potential highway base course material. On the basis of material characteristics including CBR, pavement performance was predicted using VESYS II, a pavement performance simulation program. Results indicated that thickness requirements for base courses constructed with the fly ash/coal refuse mixture are less than those for base courses constructed with conventional crushed stone. Head's study is prominent in the sense of introducing mechanistic-empirical pavement analysis to the evaluation of waste material as highway construction material. However, the evaluation of the fly ash/coal refuse mixture for potential base course material may be misleading. Estimations of resilient modulus for the material were based on empirical relationships that may not be appropriate for unusual materials such as waste product mixtures, which in many cases represent new types of geomaterials.

In this paper, resilient and plastic behavior of fly ash, classifier tailings, and mixtures of these two materials are studied from the standpoint of their potential for use as roadbed material within flexible pavement systems. The usefulness of applying existing empirical formulas for estimating resilient modulus of the investigated materials will be explored. Experience with roadbed soils in Korea demonstrating poor correlation between predictions of resilient modulus made with a popular empirical formula and actual measurements is also presented.

The benefits of using the material mixture to improve pavement performance are analyzed. Mechanistic pavement analyses are performed to predict pavement lives for flexible pavement having a subgrade of fly ash, classifier tailings, or a mixture of the two. For the purpose of comparison the pavement lives are predicted using both pseudoplastic analysis and multilayered elastic analysis with damage assessment of the pavement system. The latter involves the use of an empirical relationship to define pavement failure due to rutting, and its application to subgrade constructed with new geomaterials for which experience is limited is questioned.

RESILIENT AND PLASTIC BEHAVIOR

To investigate the potential use of fly ash, classifier tailings, or a mixture of the two materials in highway construction, a series of standard geotechnical tests was performed. Details of the tests and results are presented by Lee and Fishman (*7*), although salient details of the tests will be repeated here. The fly ash is nonplastic consisting of 24 percent sand, 48 percent silt, and 28 percent clay-size particles. The classifier tailings have a liquid limit of 31 percent and plastic limit of 17.5 percent consisting of 31 percent sand, 39 percent silt, and 30 percent clay-size particles. Mixtures of fly ash/classifier tailings exhibit increased permeability, increased unconfined

S. W. Lee, Institute of Daewoo Construction Technology, Chuiam Building, 8th Floor, Daichi-Dong 1001, Kángnam-Gu, Seoul, Korea. K. L. Fishman, Department of Civil Engineering, State University of New York at Buffalo, Buffalo, N.Y. 14260.

compressive strength, and decreased compressibility compared with either of its constituents and decreased maximum compacted density, increased optimum compacted water content, and decreased plasticity compared with classifier tailings.

Resilient and plastic behavior of the materials were studied via cyclic triaxial testing. Details of sample preparation, test procedures, determination of optimum mix ratio, and test data were reported by Lee and Fishman (*7*). A brief summary will be given here. The ratio of classifier tailings to fly ash used in the material mixture was 10:3 by weight. All testing was performed on materials compacted to maximum dry density as determined by the standard Proctor compaction test at a water content wet of optimum. A triaxial cell was used that can accommodate specimens 7.1 cm wide by 14.6 cm high, and water was used for confining fluid. Repeated axial loads were applied by pneumatic pump with loading time 0.25 sec and a load frequency of 0.5 Hz. Deformation and loads measured by an LVDT and load cell were collected by a computer-controlled data acquisition system every 0.05 sec. Samples were subjected to a range of maximum deviatoric stress from 6 to 110 kPa with confining pressure from 0 to 110 kPa. One thousand cycles of deviatoric stress was applied at a frequency of 0.5 Hz.

The resilient behavior of fly ash is similar to that of granular materials, which exhibit a dependency of resilient modulus, M_r, on the first invariant of the stress tensor, J_1. For fly ash M_r may be expressed (in kPa) as

$$M_r = 92.02 * J_1 + 8{,}943.2 \quad (1)$$

Figure 1 shows a plot of M_r for fly ash versus J_1. On the basis of the Asphalt Institute's recommendation (*8*), the typical range of confining pressure within a flexible pavement subgrade is 6.9 to 34.5 kPa (J_1 is 20.7 to 137.8 kPa). As shown in Figure 1, M_r of fly ash for this range is 11,000 to 21,000 kPa. On the basis of Asphalt Institute data (*8*), this condition indicates very poor roadbed soil.

The resilient modulus of classifier tailings was found to be dependent on the magnitude of deviatoric stress as shown in Figure 2. This behavior is typical for fine-grained materials. Resilient modulus for the classifier tailings may be expressed using a bilinear model (in kPa) as follows:

$$M_r = \begin{cases} -2{,}346 * (\sigma_d - \sigma_{db}) + 26{,}352 & \text{if } \sigma_d < \sigma_{db} \\ 51 * (\sigma_d - \sigma_{db}) + 26{,}352 & \text{if } \sigma_d > \sigma_{db} \end{cases} \quad (2)$$

where σ_d is deviatoric stress and σ_{db} is deviatoric stress at breakpoint. For comparison, Figure 2 shows the relation for M_r as a function of σ_d for typical fine-grained materials as discussed by Thompson and Elliot (*9*). The use of classifier tailings as subgrade material may not have an advantage over the use of medium stiff naturally occurring subgrade clay materials, which may be readily available near a given site.

The observed resilient behavior of the mixture of fly ash and classifier tailings also demonstrates dependence on J_1 as shown in Figure 3. For the mixture M_r may be expressed (in kPa) as

$$M_r = 196 * J_1 + 24{,}287 \quad (3)$$

Quantitatively, M_r values of the material mixtures are 31,000 to 48,000 kPa at states of stress of practical interest for subgrade material. On the basis of Asphalt Institute data (*8*) this range of M_r represents good subgrade soil. It is hoped that this preliminary data will inspire further study and encourage use of fly ash/classifier tailing mixtures as subgrade materials in flexible pavement structures.

Plastic behavior of investigated materials was studied through statistical analysis. Statistical models of accumulated axial plastic strain were established by correlating confining pressure (σ_c), deviatoric stress (σ_d), and number of load applications (N). The following expressions were obtained by multivariate regression analysis:

$$\log \varepsilon_{p\,fly} = -3.946 - 0.109\log \sigma_c + 0.314\log \sigma_d + 0.460\log N$$
$$(R^2 = 0.8661 \quad S = 0.1285) \quad (4)$$

$$\log \varepsilon_{p\,mix} = -4.469 - 0.105\log \sigma_c + 0.472\log \sigma_d + 0.341\log N$$
$$(R^2 = 0.7998 \quad S = 0.1747) \quad (5)$$

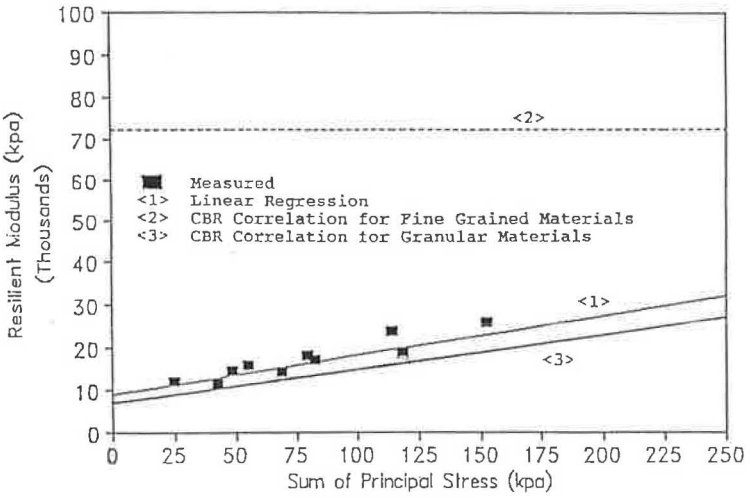

FIGURE 1 M_r **versus sum of principal stress for fly ash.**

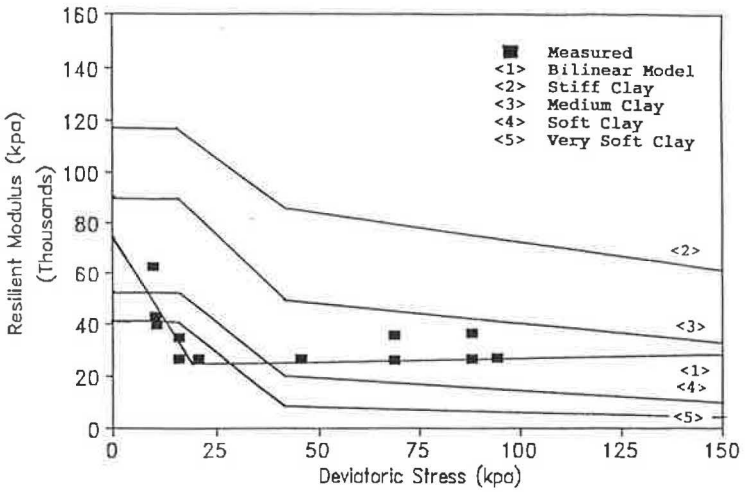

FIGURE 2 M_r versus deviatoric stress for classifier tailings.

$$\log \varepsilon_{p\ \text{classifier}} = -4.579 - 0.058\log \sigma_c + 0.782\log \sigma_d + 0.381\log N \quad (R^2 = 0.6821 \quad S = 0.2335) \tag{6}$$

A comparison of accumulated plastic strain versus number of load repetitions for the investigated materials at a typical subgrade stress condition is shown in Figure 4. The accumulation of plastic strain for the fly ash/classifier tailing mixture is distinctly less than that of either constituent. Pavement life predictions presented later in the paper will quantify the increased resistance to rutting that is a manifestation of improved plastic behavior.

ESTIMATION OF RESILIENT MODULUS (M_r) BY EMPIRICAL METHOD

Because of difficulties associated with cyclic triaxial testing, various approximate methods have been suggested to estimate M_r. In this paper, the ability of some approximate methods to predict M_r is investigated for fly ash, classifier tailings, and the fly ash/classifier tailings mixture. Results of grain size analysis indicate that materials are fine grained (*7*). For estimating M_r of fine-grained materials, the correlation proposed by Heukelom and Klomp (*10*) is the most popular method (the result is in kPa):

$$M_r = A * \text{CBR} \tag{7}$$

where A is a coefficient from linear regression. The range of A is from 5,167.5 to 20,670, and usually 10,335 is used. Use of Equation 7 has been recommended differently by AASHTO (*11*), the Asphalt Institute (*12*), and Klomp and Dormon (*13*). AASHTO (*11*) suggests that Equation 7 be used for soils with a soaked CBR of 10 or less, whereas the Asphalt Institute suggests the use of Equation 7 for soils up to CBR of 20 determined at a moisture content consistent with the field condition. Klomp and Dormon's suggestion is similar to the Asphalt Institute's and is also used for this study. CBRs de-

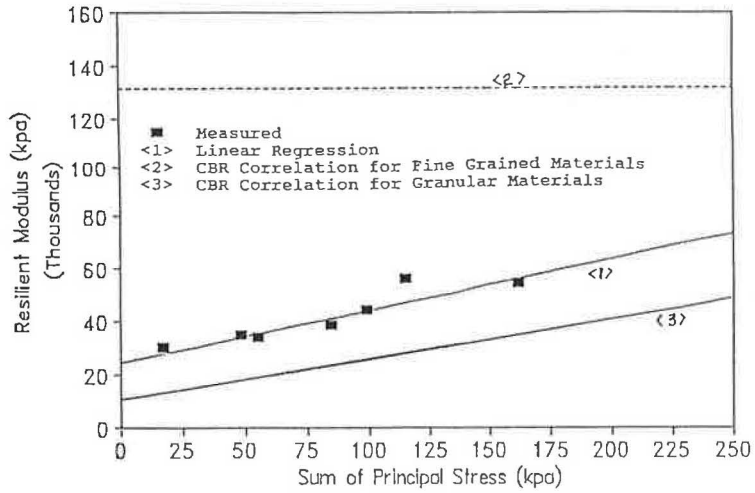

FIGURE 3 M_r versus sum of principal stress for material mixture.

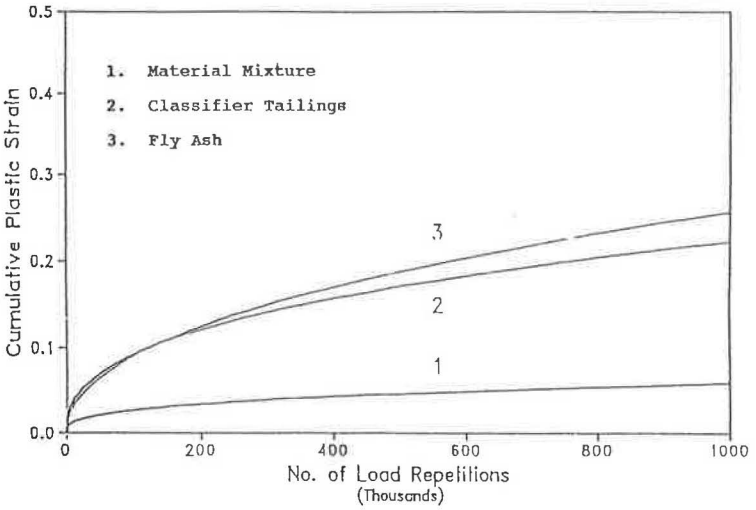

FIGURE 4 Accumulated plastic strain versus number of load repetitions (σ_c = 17.3 kPa; σ_d = 34.5 kPa).

termined for the materials investigated are summarized in Table 1.

By using the CBRs reported in Table 1 for each material, values of M_r are estimated with Equation 7 and compared with measurements. Figure 5 shows that Equation 7 provides a reasonable estimate of M_r for the classifier tailings. However, Figure 1 and Figure 3 show that Equation 7 overestimates M_r compared with direct measurements performed on samples of fly ash and fly ash/ classifier tailing mixture.

In Korea, research to establish simple estimation methods for M_r has been performed to facilitate the introduction of mechanics-based pavement design methods in the future. Since the CBR test is routinely performed as part of a site evaluation, the application of Equation 7 to commonly encountered Korean subgrade soils was studied. Woo et al. (*14*) concluded that Equation 7 is not appropriate for estimating M_r of Korean subgrade soils on the basis of a comparison, shown in Figure 6, with direct measurements of M_r from the results of cyclic triaxial testing. The usefulness of Equation 7 for Korean subgrade soils is questionable since the common type of Korean subgrade soil is silty sand or clayey sand, rather than clay type soil. Because of the difficulties associated with cyclic triaxial testing, several simple tests or approximate methods for determination of M_r have been proposed, but no reliable method is established yet. This is one reason why mechanics-based pavement design is avoided by many Korean engineers.

The poor estimation of M_r for fly ash and the fly ash/classifier tailings mixture is expected since Equation 7 was developed on the basis of a perceived M_r-CBR relationship for fine-grained materials. A relationship for granular materials discussed by AASHTO may be more suitable for fly ash and the material mixture, since the M_r of each is related to J_1. Correlations of M_r and CBR were provided by AASHTO (*11*) for granular materials including the effect of state of stress as follows:

J_1 (*kPa*)	M_r (*kPa*)
689.0	5,098.6*CBR
206.7	3,031.6*CBR
137.8	2,342.6*CBR
68.9	1,722.5*CBR

As shown in Figures 1 and 3, the preceding table gives a reasonable estimation of M_r for fly ash and the fly ash/classifier tailings mixtures.

Recent research has attempted to estimate the M_r of natural fine-grained subgrade material, accounting for dependence of M_r on deviatoric stress. On the basis of typical resilient behavior of fine-grained soils, Thompson and Robnett (*15*) investigated factors affecting the resilient behavior of fine-grained soils. The study indicated that the degree of saturation, distribution of particle size, plastic index, unconfined compressive strength, and modulus of elasticity are factors related to M_r. Similarly, Drumm et al. (*16*) proposed a hyperbolic model to describe the nonlinear relationship for the resilient modulus of fine-grained soils as function of deviatoric stress as follows:

$$M_r = (a + b * \sigma_d)/\sigma_d \quad (8)$$

TABLE 1 CBR Values Determined for the Materials Investigated

Materials	CBR (Unsoaked)
Fly Ash	7.0
Classifier Tailings	2.0
Material Mixture	12.6

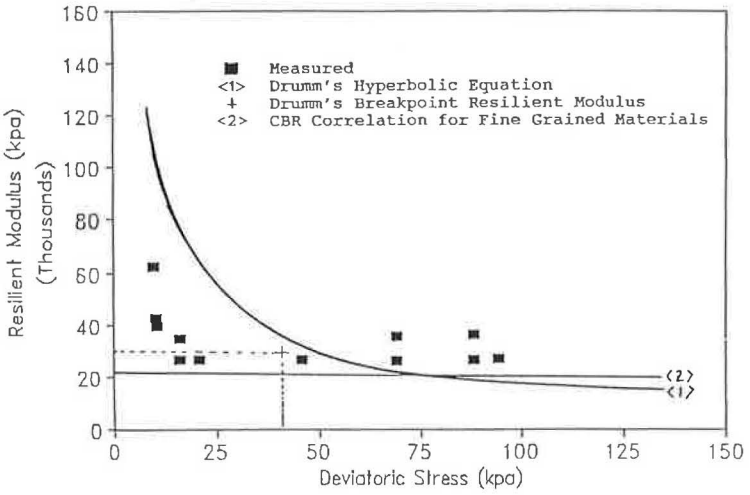

FIGURE 5 Measured and estimated resilient modulus for classifier tailings.

where a and b are material coefficients and are functions of previously mentioned factors. The expression of a and b is cited by Drumm et al. (*16*). Details of input data for the application of Drumm et al.'s study to the estimation of M_r for classifier tailings are presented by Lee and Fishman (*7*). For the classifier tailings M_r values estimated by Equation 8 are compared with direct measurements of M_r in Figure 5. As discussed by Drumm et al. (*16*), this empirical equation does not provide a good approximation in the range of low deviatoric stress. However, it renders a reasonable approximation when the deviatoric stress is 34.5 kPa or more.

Drumm et al. (*16*) also provide an empirical expression for M_r at a breakpoint, a significant parameter for bilinear representation of M_r versus σ_d. This expression is a function of the aforementioned factors included in Equation 8, and given data relative to the classifier tailings a breakpoint resilient modulus M_{rb} is estimated as 39.6 kPa. As shown in Figure 5, Drumm et al.'s empirical equation for estimating M_{rb} gives a good approximation of M_{rb} of classifier tailings determined by direct measurement. Though fly ash and fly ash/classifier tailing mixtures are fine-grained soils, Drumm et al.'s study is not applicable to these materials since M_r does not depend on the magnitude of deviatoric stress.

PAVEMENT LIFE PREDICTION

The benefits of using the material mixture to improve pavement performance is demonstrated through mechanistic pavement analyses performed to predict pavement lives for flexible pavement having a subgrade of fly ash, classifier tailings, or the fly ash/classifier tailings mixture.

For comparison, the pavement lives are predicted using both pseudoplastic analysis (Method 1) and multilayered elastic analysis (Method 2) with damage assessments of the pavement system. Pavement systems modeled by Methods 1 and 2 are shown in Figures 7 and 8. The algorithm describing Method 1 is shown in Figure 9. Method 2 is performed using

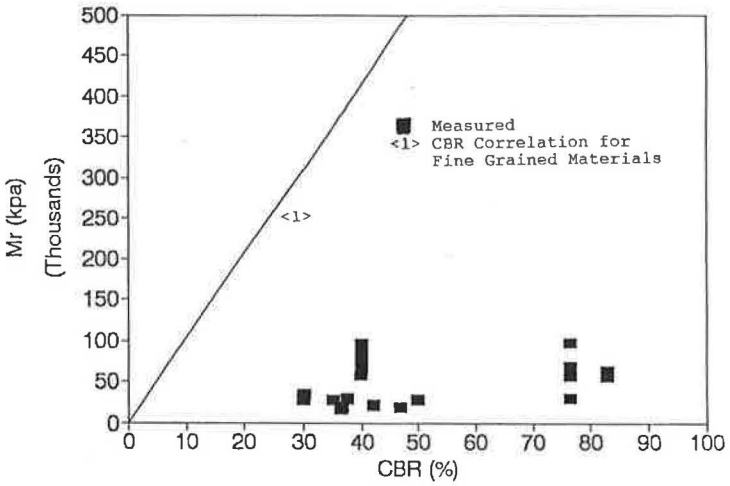

FIGURE 6 Measured and estimated resilient modulus for fine Korean subgrade (*14*).

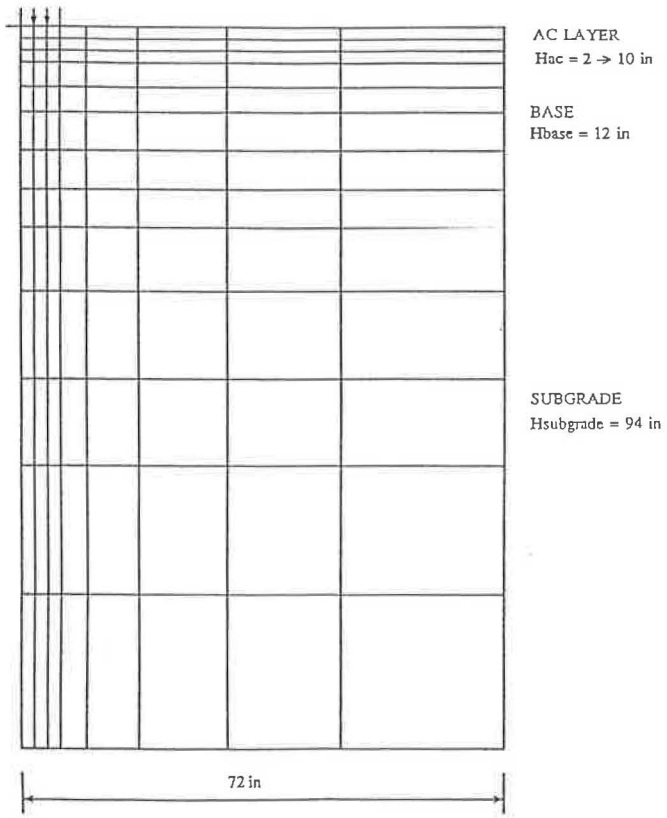

FIGURE 7 Representation of pavement system by FEM + pseudoplastic analysis (Method 1).

DAMA, which is a multilayered elastic analysis program distributed by the Asphalt Institute used to estimate repetitions to failure where pavement condition is described in terms of rutting and surface failure. In the analysis performed herein only rutting failure is considered.

Pavement life predictions made with Method 1 incorporate plastic behavior, which is unique to a given material, directly as input. For pavement damage assessment models such as Shell (*17*) or MS-1 (*8*), failure criteria incorporated in Method 2 are empirical relations that attempt to correlate observed damage in pavements with the computed elastic compressive strain at the top of the subgrade layer. Thus, the improved plastic properties of the fly ash/classifier tailings mixture are not accounted for directly in Method 2. Results from both methods indicate increased life for pavements having subgrades constructed with a fly ash/classifier tailings mixture compared with those constructed of either fly ash or classifier tailings.

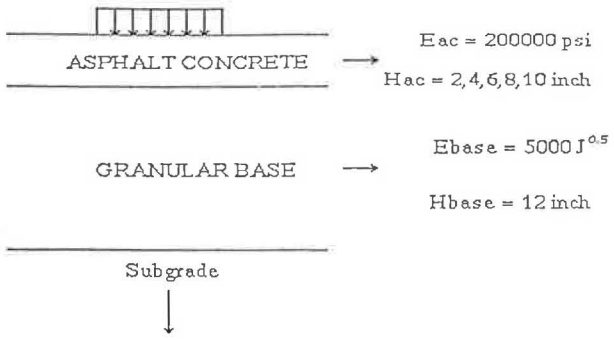

FIGURE 8 Representation of pavement system by layered elastic analysis (Method 2).

Pavement lives predicted by Method 1 are plotted in Figure 10 for pavements having subgrades constructed with fly ash, classifier tailings, or the fly ash/classifier tailings mixture. Pavement life realized by incorporating the fly ash/classifier tailing mixture in the subgrade is an order of magnitude higher than for pavements constructed with subgrades of fly ash or classifier tailings alone. The increased pavement life is due to the improved resilient and plastic behavior of the material mixture over that of its constituents.

Comparisons of pavement lives by Methods 1 and 2 for pavements having subgrade of fly ash, classifier tailings, and the fly/ash material mixture are plotted in Figures 11, 12, and 13, respectively. In all cases incorporating the Shell failure criterion with Method 2 renders a longer life prediction than if the MS-1 failure criterion is incorporated. Figure 11 indicates that for pavements having subgrades constructed with fly ash, the pavement life predicted with Method 1 lies between the predictions made with Method 2 incorporating the Shell or MS-1 failure criterion. Figure 12 indicates that for pavements having subgrade constructed with classifier tailings, the pavement life predicted with Method 1 is close to that predicted by Method 2 with the MS-1 failure criteria incorporated. Figure 13 indicates that for pavements having subgrades constructed with fly ash/classifier tailings mixture, the prediction pavement life with Method 1 is close to the

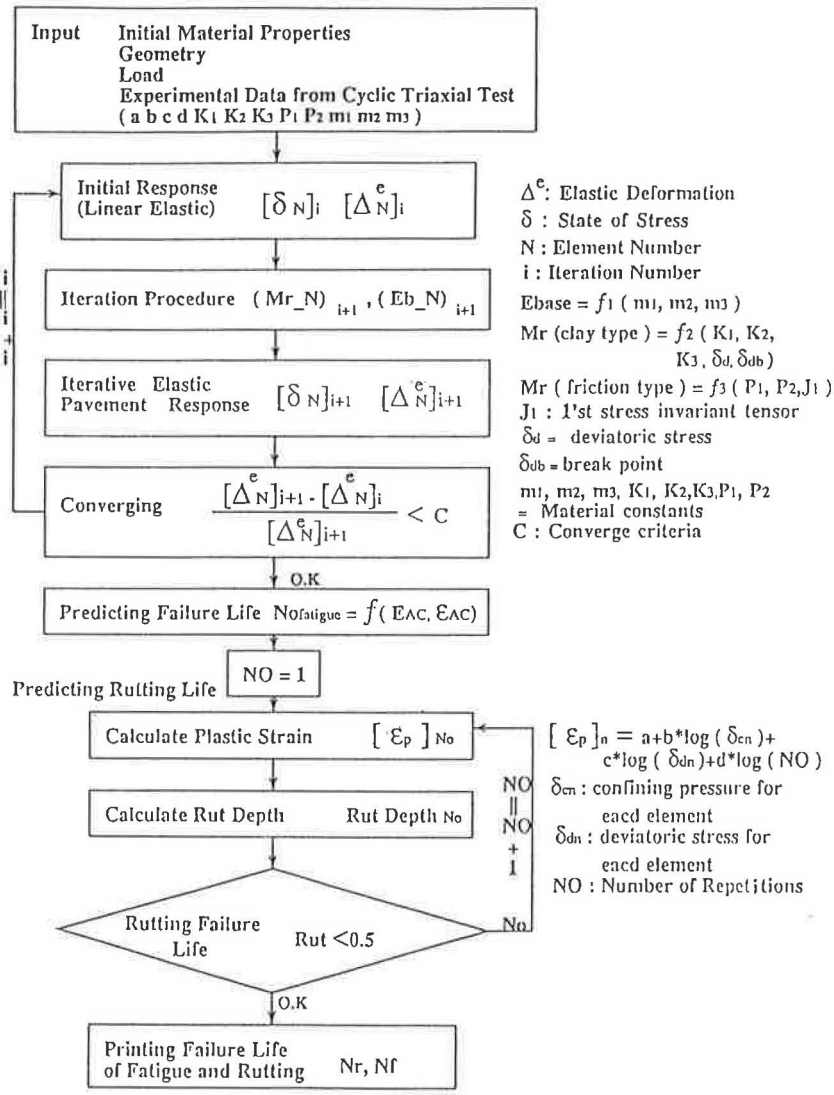

FIGURE 9 Algorithm for pavement analysis (Method 1).

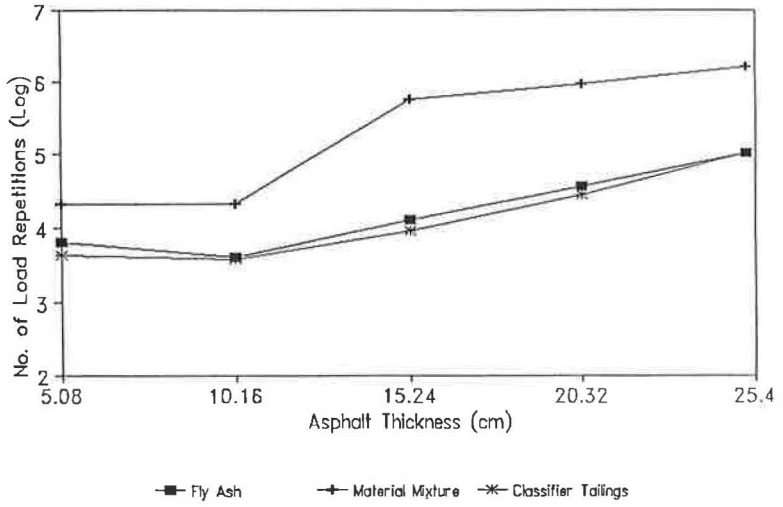

FIGURE 10 Predicted pavement life by Method 1.

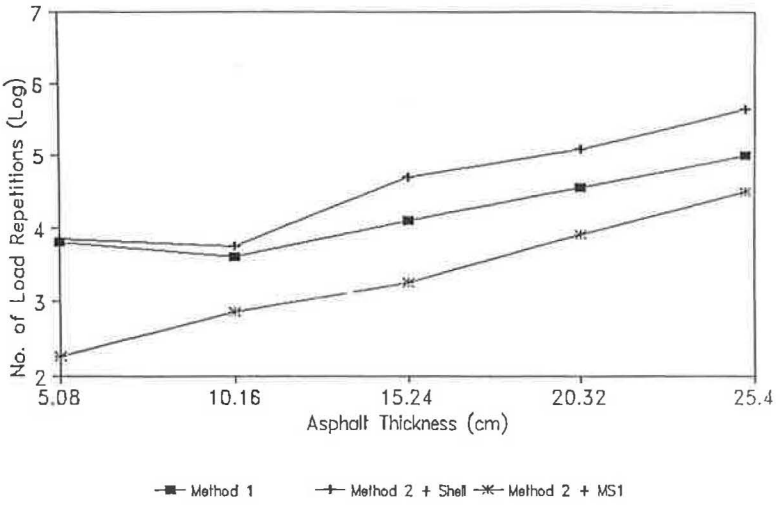

FIGURE 11 Predicted pavement life for fly ash subgrade, Methods 1 and 2.

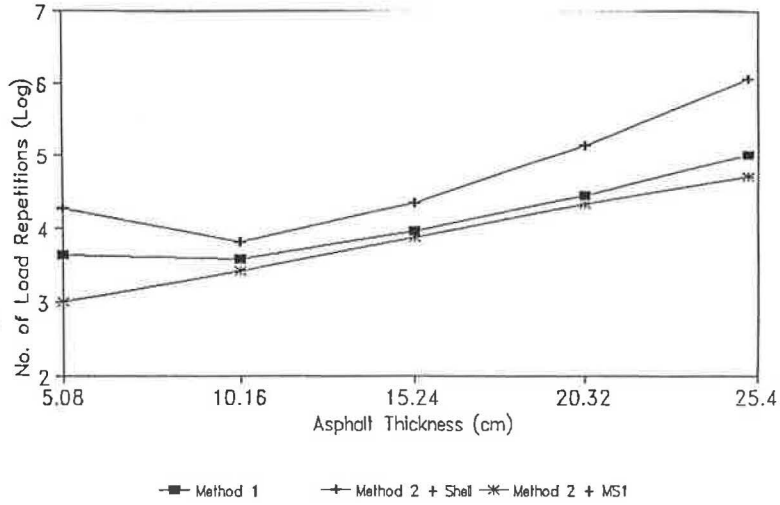

FIGURE 12 Predicted pavement life for classifier tailings subgrade, Methods 1 and 2.

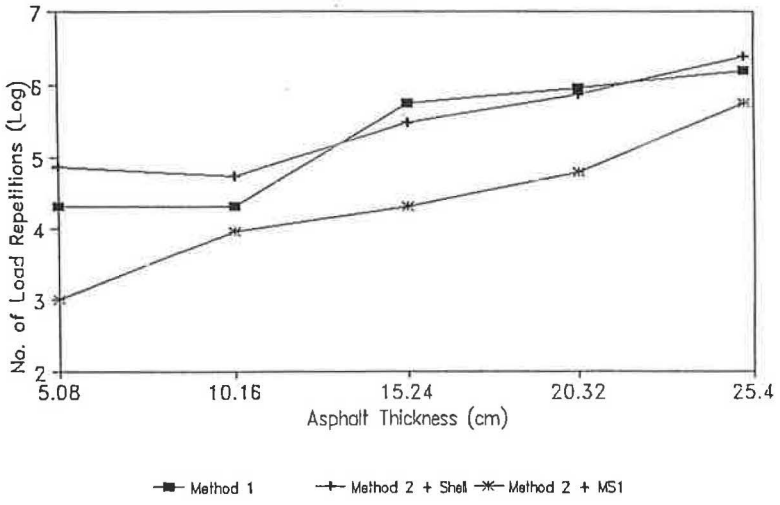

FIGURE 13 Predicted pavement life for a material mixture subgrade, Methods 1 and 2.

prediction of Method 2 with the Shell failure criterion incorporated. These data suggest that uncertainty exists in the use of limiting subgrade strain condition, such as the Shell or MS-1 criterion, for the prediction of pavement life. The use of Method 1 gives the analyst greater flexibility in the specification of individual material plastic behavior. Confidence in Method 1 is verified since results are within the range of field observations as described by the Shell and MS-1 failure criterion. For future pavement construction Method 1 is recommended for preliminary assessment of pavement performance.

CONCLUSIONS

1. The fly ash/classifier tailings material mixture demonstrates better resilient and plastic behavior than does either of its constituents.
2. Empirical expressions for estimation of M_r were examined for the investigated materials. For classifier tailings the M_r-CBR relationship for fine-grained soils described by Equation 7 provides a reasonable approximation. Drumm et al.'s empirical equation (Equation 8), also approximate for fine-grained materials, provides a better description of the dependence of M_r on material properties and σ_d than Equation 7; however, further research into functions of this type is required. On the basis of the experience in Korea, caution should be exercised in the sand or clayey sand, which may exhibit some behavior attributed to granular materials.
3. Neither Equation 7 nor Equation 8 is appropriate for estimating M_r of fly ash or fly ash/classifier tailings mixture. Since fly ash and fly ash/classifier tailings mixture exhibit behaviors similar to granular materials, M_r-CBR correlation, which includes a dependence on confining pressure (J_1), appears to be more appropriate.
4. Pavement rutting life predictions indicate that pavement life improved by an order of magnitude for flexible pavements having subgrades constructed with the fly ash/classifier tailings mixture over that of subgrades constructed with fly ash or classifier tailings alone. Results obtained with pseudoplastic analysis are considered more reliable than those obtained by limiting subgrade strain criteria since plastic behavior, which is unique to a material, is input directly in the pseudoplastic analysis.

REFERENCES

1. Barenberg, E. J., and M. R. Thompson. Design, Construction and Performance of Lime, Fly Ash, and Slag Pavement. In *Transportation Research Record 839,* TRB, National Research Council, Washington, D.C., 1982, pp. 1–6.
2. Matoes, M. Stabilization of Soils with Fly Ash Alone. In *Highway Research Record 52,* HRB, National Research Council, Washington, D.C., 1964, pp. 59–65.
3. Lambe, J. H. Type C Fly Ash and Clay Stabilization. *Proc., Developments in New and Existing Materials,* ASCE, 1985, pp. 20–25.
4. Lewis, T. S. Construction of Fly Ash Roadway Embankment in Illinois. In *Transportation Research Record 593,* TRB, National Research Council, Washington, D.C., 1976, pp. 20–23.
5. Faber, J. H. Use of Fly Ash in Embankment Construction. In *Transportation Research Record 593,* TRB, National Research Council, Washington, D.C., 1976, pp. 13–19.
6. Head, W. J. Coal Refuse and Fly Ash Composition: Potential Highway Base Course Materials. In *Transportation Research Record 839,* TRB, National Research Council, Washington, D.C., 1982, pp. 11–20.
7. Lee, S. W., and K. L. Fishman. Improved Resilient Modulus Realized with Waste Product Mixtures. *Proc., ASCE Conference on Grouting Soil Improvement and Geosynthetics,* New Orleans, La., 1992, pp. 1356–1368.
8. *Research and Development of the Asphalt Institute's Thickness Design Manual (MS-1) Ninth Edition.* Research Report 82-2. The Asphalt Institute, College Park, Md., 1982.
9. Thompson, M. R., and R. P. Elliot. Illi-Pave Based Response Algorithms for Design of Conventional Flexible Pavements. In *Transportation Research Record 1043,* TRB, National Research Council, Washington, D.C., 1986, pp. 50–62.
10. Heukelom, W., and A. J. Klomp. Considerations of Calculated Strains at Various Depths in Connection with the Stability of Asphalt Pavements. *Proc., 2nd International Conference on the Structural Design of Asphalt Pavement,* University of Michigan, Ann Arbor, 1967.
11. *AASHTO Guide for Design of Pavement Structures.* American Association of State Highway and Transportation Officials, Washington, D.C., 1985.
12. *Soils Manual for Design of Asphalt Pavement Structures.* MS-10. The Asphalt Institute, College Park, Md., 1967.
13. Klomp, A. G., and G. M. Dormon. Stress Distribution and Dynamic Testing in Relation to Road Design. *Proc., Australian Research Board,* Vol. 2, Part 1, 1964, pp. 701–728.
14. Woo, J. Y., et al. *Estimation of Load Bearing Capacity of Subgrade Soils for Pavement by Resilient Modulus.* Report 90-GE-114. Korean Institute of Construction Technology, 1990.
15. Thompson, M. R., and Q. L. Robnett. Resilient Properties of Subgrade Soils. *Journal of Transportation Engineering Division,* ASCE, Vol. 105, No. 1, 1979, pp. 71–89.
16. Drumm, E. C., et al. Estimation of Subgrade Resilient Modulus from Standard Tests. *Journal of Geotechnical Engineering Division,* ASCE, Vol. 116, No. 5, 1990, pp. 764–775.
17. Dormon, G. M., and C. T. Metcalf. Design Curves for Flexible Pavements Based on Layered System Theory. In *Highway Research Record 71,* HRB, National Research Council, Washington, D.C., 1965, pp. 69–84.

Publication of this paper sponsored by Committee on Soil and Rock Properties.

Strength and Life of Stabilized Pavement Layers Containing Fibrillated Polypropylene

W. W. CROCKFORD, W. P. GROGAN, AND D. S. CHILL

Laboratory and field results are presented indicating that discrete, fibrillated fibers mixed with chemically stabilized sand or clay soils improve the life of those materials in pavement layers. The improvement can be seen in axial compression stress-strain curves as an increase in both modulus and strength. In some cases, the fibers appear to alter the material response by moving from a strain softening response toward a response analogous to strain hardening.

Flexible pavement base courses, rigid pavement subbase courses, and gravity wall retaining structures that are used in the construction of transportation infrastructure must perform effectively while being subjected to a variety of stresses and a wide range of environmental conditions. Often, a process of improving locally available soils by the use of chemical or mechanical stabilization is used to meet the challenge posed by these conditions. When chemical stabilization is used to decrease the potential for a pavement to rut or pump, or if it is used to help a gravity wall structure resist the undesirable effects of differential movement of the subgrade, a conscious choice is being made to trade flexibility for strength and stiffness. The improvement in stiffness is desirable only to the extent that it can be maintained in service without cracking, eroding, or losing internal friction. This means that the material should not be subjected to any conditions that will cause its strain response to exceed the limit of elastic behavior. Once the elastic limit is exceeded, most chemically stabilized materials enter into the strain-softening portion of their characteristic stress-strain curve. The descending branch for the silty sand tested in this study containing 9 percent portland cement is quite steep, and this softening is often attributed to microcracking and crack coalescence. The same soil has been stabilized with 5 percent portland cement and 0.5 percent fibrillated polypropylene fibers. The fiber material retains approximately the same initial tangent modulus as the material having a higher stabilizer content and containing no fiber, but the descending branch is more gradual, indicating the potential importance of the fibers in controlling cracking.

W. W. Crockford, Texas Transportation Institute, Texas A&M University, College Station, Tex. 77845-3135. W. P. Grogan, Waterways Experiment Station, CEWES-GP-T, 3909 Halls Ferry Road, Vicksburg, Miss. 39180-6199. D. S. Chill, Synthetic Industries, Construction Products Division, 4019 Industry Drive, Chattanooga, Tenn. 37416.

FIBER CHARACTERISTICS

The fibers are constructed from parallel oriented long-chain polypropylene. In the manufacturing process, tapes of the material are caused to split lengthwise in such a way that crossover segments are left intact to connect the coarser stem fibrils. The resulting fiber, when stretched perpendicular to the direction of the long-chain polymer, looks like a miniature mesh with a diamond-shaped pattern. The fibers used in this study were approximately 2.54 cm (1 in.) long, 0.254 cm (0.1 in.) wide, and 1000 denier. Table 1 summarizes other properties of the fibers.

LABORATORY ASSESSMENT OF COMPOSITE MIXTURE CHARACTERISTICS

Several types of tests were conducted on the materials by different laboratories. Studies included different compaction efforts, confined and unconfined compressive strengths, and basic soil properties of the two soil materials chosen for the study. Basic properties of the clay found at the field site and a select sand material are given in Table 2.

In the laboratory, the mixing procedure was slightly different for the clay and sand materials. The sand was mixed with a wire wisp, whereas the clay required a stiffer mixing blade. The fibers "opened up" from the shape as manufactured to the deformed "grid" shape quickly in the sand mixtures. The clay required a slightly longer mixing time and a fairly gradual addition of water during mixing to minimize the amount of caking on the mixing tools.

Figure 1 shows the variation in maximum dry unit weight and optimum moisture content with fiber content in the unstabilized clay and sand. Apparently, there is an optimum fibers-density curve analogous to the familiar moisture-density curve that can be used in conjunction with other laboratory tests to select fiber content. The reason for this optimum is uncertain. Because the fibers have a lower specific gravity than the soils, one might expect that the introduction of fibers would always decrease the unit weight of soil mixtures. However, the interactions among the soil, the shearing action of the mixer, the compaction technique, volume fractions of the components, and the frictional characteristics of the components of the composite material produce an optimum response as shown in the figure so that unit weight has a peak value (assuming the absence of systematic errors). These curves are the result of testing materials compacted at a nominal com-

TABLE 1 Fiber Properties

PROPERTY	VALUE
Specific gravity	0.91
Tensile strength	552-758 MPa (80-110 ksi)
Modulus	3.5 GPa (508 ksi)
Melting point	162°C (324°F)
Ignition point	593°C (1100°F)
Absorption	Nil
Acid and salt resistance	High
Alkali resistance	High
Electrical conductivity	Low

TABLE 2 Soil Properties

PROPERTY	CLAY	SAND
Classification	CL-CH	SM
Specific gravity	2.694	2.500
Plasticity index	22	nonplastic

paction energy of 2,693 kJ/m³ (56,250 ft-lb/ft³, 100 percent of ASTM D1557).

Specimens of the materials were compacted for strength testing using approximately 44 percent of ASTM D1557 nominal compaction effort with a cylindrical mold 15.24 cm (6 in.) in diameter by 20.32 cm (8 in.) tall. This compaction effort is similar to the effort used in Texas and lies between modified (ASTM D1557) and standard Proctor efforts (ASTM D698, which is approximately 22 percent of modified effort). Various combinations of the components with and without stabilizers and fibers and with varying percentages of the stabilizers and fibers were tried. The stabilizer selected for the sand was portland cement, and that selected for the clay was hydrated lime. Cement-stabilized sand was cured for 7 days at 22.8°C (73°F), whereas the lime-stabilized clay was subjected to an accelerated curing process using a temperature of 48.9°C (120°F) for 48 hr followed by cooling at 22.8°C (73°F) for 24 hr before testing. The strength tests were conducted in a Texas triaxial cell using a 34.5-kPa (5-psi) confining pressure and a controlled displacement rate of 0.006 cm/sec (0.135 in./min). (The Texas cell uses a thick rubber membrane and applies pressure only to the curved surface of the specimen. Therefore, the applied axial stress is the major principal stress, not the deviatoric stress.) Figure 2 shows results for clay and sand. For both materials, the fibers increased the modulus of elasticity, the strength, and the strain energy density (which is basically the area under the stress-strain curve). (The analysis performed in this paper assumes that integration of the full tensor is not required and that the area under the stress-strain curve yields a value for strain energy density that is adequate for use in the study.) Implications are that simultaneously increasing the modulus and the strength may delay the onset of failure, whereas an increase in strain energy may help slow down the failure process once it has started.

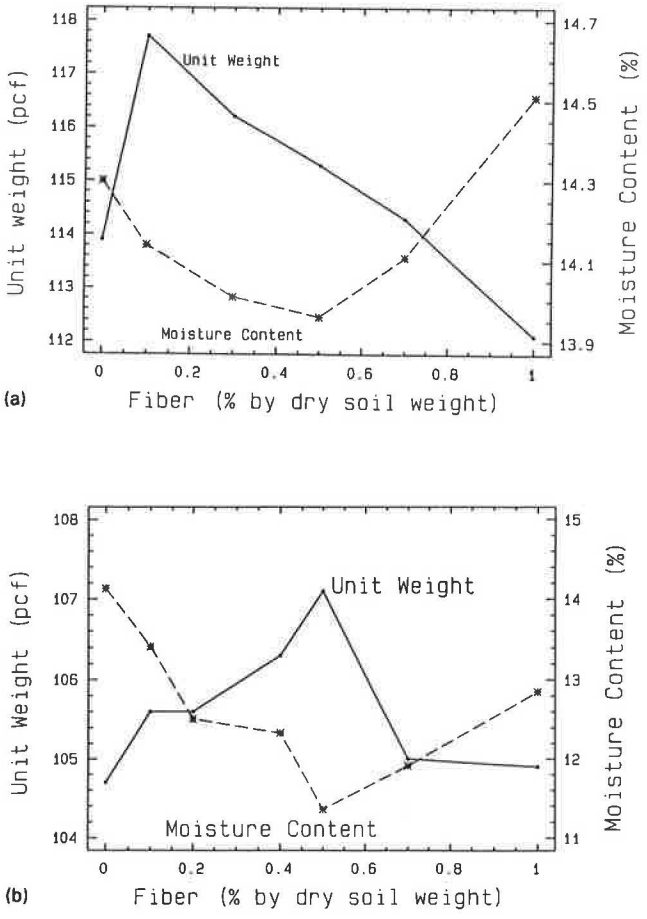

FIGURE 1 Optimum fibers-density (solid) and fibers-moisture (dashed) curve for (*a*) clay material [115 pcf (18.1 kN/m³)] and (*b*) sand [106 pcf (16.7 kN/m³)].

Interesting indications of the effects of the various mix components on the measured strain energy density (W, computed between strain levels of 0 and 0.05) from the strength tests are shown in Figure 3. In Figure 3a, it appears that the addition of fibers to the soils with no stabilizers results in a recognizable trend in the strain energy density with fiber content. However, the directions of the trends are opposite for the two types of soil. The increasing trend with increasing fiber content in the sand might be expected on the basis of speculation. The decreasing trend seen in the clay may be a manifestation of the characteristics of the mixing or compaction equipment and procedures. Alternatively, a phenomenon similar to bulking may be at work. In Figure 3b, it is seen that strain energy density can be related linearly to the port-

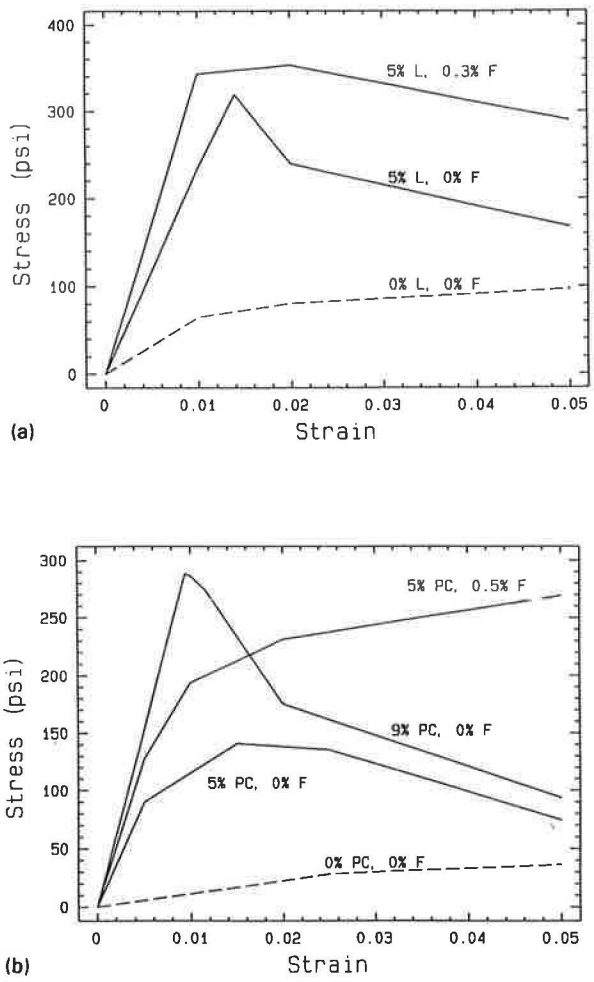

FIGURE 2 Stress-strain curves for (*a*) clay [300 psi (2.1 MPa)] and (*b*) sand [200 psi (1.4 MPa)].

land cement content of the stabilized sand mixtures used in this study. However, the clay appears to show a peak at approximately 5 percent lime content. Finally, Figure 3c shows that both sand and clay containing 5 percent chemical stabilizer have a peak in strain energy density (at 0.5 and 0.3 percent content, respectively).

On the basis of the location of the peaks in Figure 1 coupled with the strain energy density results of laboratory strength testing shown in Figure 3c, 0.3 percent fibers by dry weight of the clay and 0.5 percent by dry weight of the sand appeared to be appropriate choices for optimum fiber contents. The choice of the optimum fiber content for the clay was a compromise between unit weight and strain energy density, but the strain energy density results were considered to be the most important factor. In addition to the compromise value of 0.3 percent for the optimum fiber content with clay, a lower fiber content of 0.1 percent, which was closer to the maximum observed unit weight, was included in the field study treatments. Lime content for the clay material was selected using the procedure suggested by Eades and Grim (*1*). Strain energy density results for Figure 3b showed a maximum value at 5 percent lime, which supports the selection of lime content on the basis of pH. With regard to the sand materials, Figure 3b

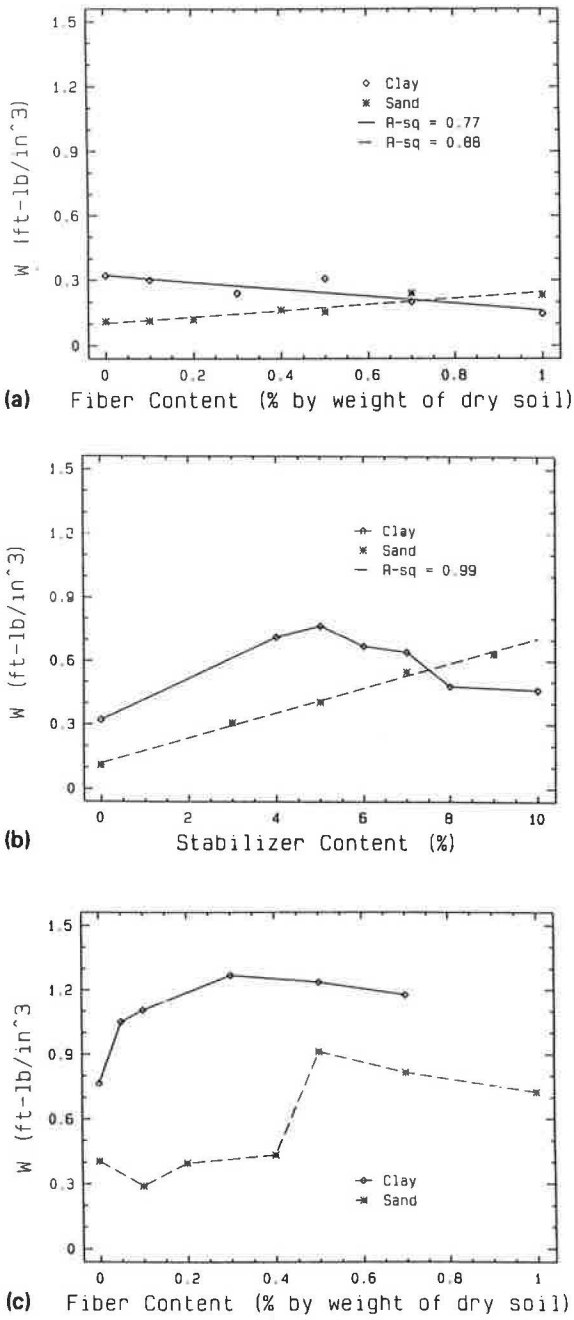

FIGURE 3 Effects on strain energy density: (*a*) fibers, no chemical stabilizer; (*b*) chemical stabilizer, no fibers (lime with clay, portland cement with sand); and (*c*) combined effect, 5 percent chemical stabilizer with fibers.

shows that the strain energy density continues to increase with cement contents up to 9 percent, which approaches a mix that is not economical to produce. Even at 9 percent cement, this material would not meet the Texas specification for cement-stabilized base. However, this study did not purport to meet such a specification. Therefore, the cement content for the sand was selected somewhat more qualitatively than the lime content for clay and was based substantially on soil classification (*2*).

FIELD TEST SECTION

Design

The design was a racetrack pattern with a lane width of 4.9 m (16 ft). The straightaway section on each side of the oval was 67 m (220 ft). Each of the 14 sections was 9.4 m (31 ft) long with the four sections at the ends of the straightaways being slightly longer to provide a transition to the turning operation in the curve. The geometric design, section numbering scheme, and the different mixtures planned for the experimental treatments are shown in Figure 4. The site was selected to ensure a relatively homogeneous subgrade with a very low California bearing ratio (CBR). The CBR at the top of the subgrade on the test track immediately before traffic averaged 4.5. The track had no surface course or seal coat and was designed so that it would fail within approximately 5,000 passes of the loading vehicle. Sections 4, 5, 9, and 10 had not failed at the time traffic was suspended.

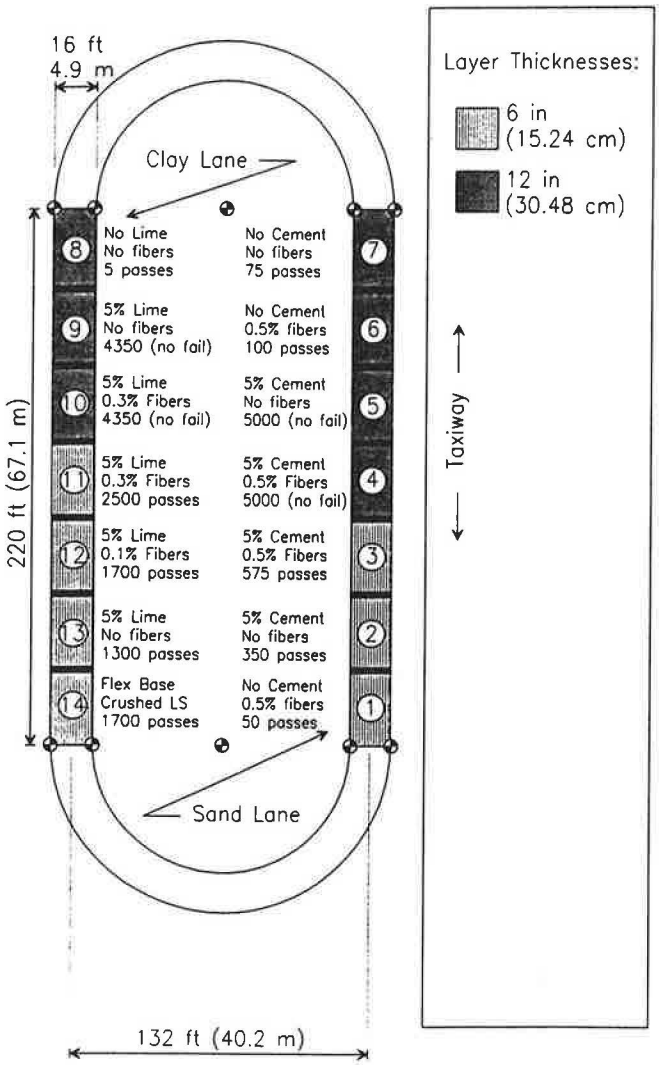

FIGURE 4 Test section design, numbering scheme, and number of passes to failure.

Construction

After initially surveying the track, the surface root zone was removed and an attempt was made to achieve a uniform density and moisture content at least 15.24 cm (6 in.) into the subgrade throughout the test track. A borrow pit was excavated in the infield of the track, and the material from this pit was used for the experimental stabilized materials on the clay lane. When sufficient material was in place, the construction of the different material treatments began.

On the basis of a knowledge of existing construction practice and the laboratory results, the following construction procedures were selected. All materials were mixed in place using a rotary mixer with the exception of sand-cement, which was mixed in a central pugmill plant. After mixing at the pugmill, the sand-cement was delivered to the site and fibers were mixed with the material in place.

The lime was mixed in place with the clay, followed by mixing the fibers in place. Visually, it appeared that the fibers opened up better in the clay than in the sand sections during field operations. This was opposite to the experience in the laboratory and is attributed to differences in the shearing mechanisms of the various agitators. In the clay lane, two passes of the mixer were used to mix in the lime. The mixing blades were raised at the transitions between each section. An additional five passes (three sets of five passes each were required to cover the width of the lane) were applied to the sections after the fiber was added. Two compaction passes without vibration and three passes with vibration were then applied using a padfoot roller. Four passes with a pneumatic roller were applied followed by finish rolling with a steel wheel roller. The desired density was not obtained in all of the sections. Therefore, additional scarification and compaction were performed (approximately eight passes with a vibrating padfood roller, four with a light pneumatic roller, three with a steel wheel roller, five with a loaded track loader, and final passes with a heavy pneumatic roller). The large number of passes with the various compactors was applied in an attempt to reach a specified density. However, the consensus was that it was almost impossible to obtain laboratory densities in the field because the subgrade was so soft and therefore provided little support to compact against.

In the sand lane, the fibers were mixed with the pugmill mixed sand and cement. Approximately seven passes with the mixer were applied to these sections. Compaction was accomplished with five passes of a vibrating steel wheel roller, one pass without vibration, and two passes with a heavy pneumatic roller. This sand material seemed to be easier to compact to the desired density than the clay material.

Approximately 3 weeks was planned for curing of the stabilized material. Drainage was lacking at the site, a relatively low-lying flat area. In a normal year in College Station, Texas, this lack of drainage probably would not have been a problem if the section had been constructed on schedule. However, shortly after construction, an abnormally high-rainfall rainy season ensued from December 1991 through April 1992. There was never a long-enough time between rainfall events for the clay to return to a reasonable moisture content during this period. Two of the implications of this rain delay were that the stabilized sections cured for a much longer time period than planned and the surface of the track was exposed to

more severe environmental conditioning than had been anticipated. The sections were covered with plastic during many of the rainfall events and uncovered during many of the drying periods, but this activity was only partially successful in reducing the effects of the environmental conditions.

Traffic

The traffic was applied only in one direction (counterclockwise when viewed from above) with a nonarticulated, single-axle, dual wheel, flatbed truck between mid-May and mid-June. The rear tires were Summit Duro-mile Lug Regroovable 9.00-20 E, and the steering axle tires were Firestone 9.00-20 Transport 1. Concrete median barriers were used to load the truck. Primarily because of time limitations, the load on the rear axle was increased at Pass 1,100 to 77.4 kN (17.4 kip) from 56.27 kN (12.65 kip). The heavier rear load actually decreased the steering axle load from 22.6 kN (5.09 kip) to 21.5 kN (4.84 kip).

FIELD RESULTS

The results given herein are based primarily on measurements taken perpendicular to the centerline. These cross section measurement locations were spaced at 1.2-m (4-ft) intervals along the centerline and included only the central 3.7 m (12 ft) of each test section longitudinally. The measurements extended the full width of the lane, 4.9 m (16 ft). "Failure" was determined by average rut depths of 7.62 cm (3 in.) and is recorded in Figure 4. In Table 3, the moisture contents just below the surface and at the top of the subgrade are presented for each experimental section as measured before the traffic was applied and at the time each section failed.

Figures 5 and 6 show a more continuous measure of the progression of the failure over the period of the test and include data on Sections 4, 5, 9, and 10. The ordinate on these plots is termed the strain index. This terminology is used to emphasize that the value is nondimensional (i.e., a strain) but does not meet the mathematical definition of strain (hence the use of the term "index"). It is computed as follows:

$$\text{Strain index} = \overline{\sum_{0}^{16} \left| \frac{\Delta h}{h} \right|} \quad (1)$$

where h is the elevation (relative to an arbitrary datum) before traffic and the relatively small Δh is the change as traffic is applied. The absolute value of the "strain" is taken at each of the measurement points along the cross section (0–16) and then summed and averaged over the four cross sections in each experimental section. Therefore, the strain index gives a measure of the total vertical movement (both up and down) of the surface about the original location of that surface. On these plots, the lower strain index values at large pass numbers indicate longer life. In each case shown in the figures, the fibers appear to improve the life over the comparable materials and thicknesses without fibers. For instance, Figures 5b and 6b show that the sections without fibers were approaching failure more rapidly than the sections with fibers at the time traffic was suspended.

CONCLUSIONS

Laboratory mix design was relatively straightforward for the materials tested in this study. It appears possible to design the mix on the basis of curves from laboratory testing: the stabilizer-strain energy density curve (e.g., Figure 3b), the fibers-strain energy density curve for the optimum stabilizer content (e.g., Figure 3c), and the optimum fibers-density curve (e.g., Figure 1).

Qualitative as well as quantitative observations suggest that fibers alone can not completely replace chemical stabilizers in certain relatively high-stress pavement applications. However, it is apparent that the fibers tested in this study enhance the performance of chemically stabilized materials. The fibers increased the modulus, strength, and strain energy of the sand and clay materials as tested in this study. In certain situations, the use of fibers may allow for a reduction in chemical sta-

TABLE 3 Field Moisture Contents (percent, by Oven Drying)

Section	Surface		Top of Subgrade†	
	Start	Final	Start	Final
1	19.0	14.8	21.4	14.0
2	18.7	5.2	20.5	20.6
3	20.2	10.0	23.0	21.2
4	15.7	4.7	21.2	17.7
5	13.4	11.8	22.7	24.8*
6	14.8	14.9	23.0	23.8
7	19.3	12.1	25.6	23.3
8	28.5	31.2	27.0	27.8
9	25.9	31.3	26.2	36.9
10	23.2	39.0	28.2	37.6
11	21.8	16.1	27.3	25.4
12	20.5	18.2	28.9	27.8
13	25.4*	20.2*	28.8	26.9
14	9.4	1.5	25.9	26.0

*by nuclear gage measurement.
†measurement taken in clay subgrade, depth depends on layer thickness (see Figure 6 for thicknesses).

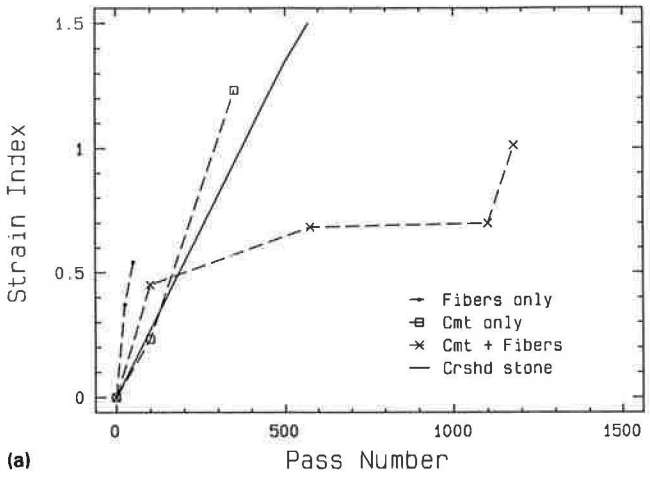

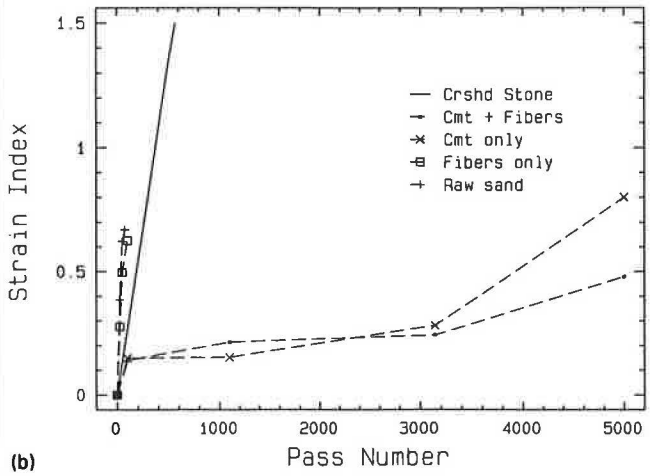

FIGURE 5 Strain index—sand (vehicle load increased at 1,100 passes): (*a*) 6-in.-thick sections and (*b*) 12-in.-thick sections (1 in. = 2.54 cm).

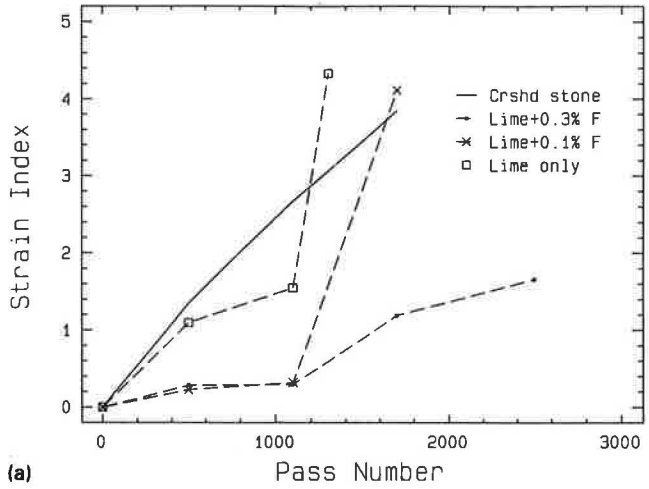

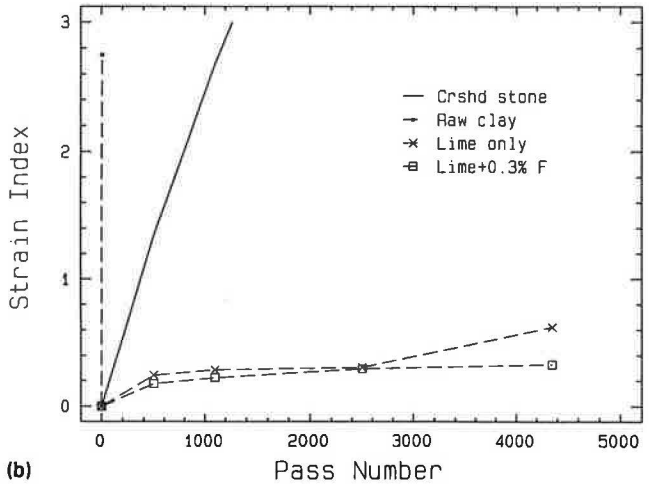

FIGURE 6 Strain index—clay: (*a*) 6-in.-thick sections and (*b*) 12-in.-thick sections (1 in. = 2.54 cm).

bilizer content. Alternatively, the use of fibers may allow reduction in the thickness of the layer in which they are used. Sangineni (*3*) computed thickness reductions on the order of 5 to 16 percent using data for chemically stabilized materials incorporating fibers in an AASHTO analysis (*4*) of a fictional pavement structure with a 5-cm (2-in.) hot mix asphalt surface course.

RECOMMENDATIONS

Our experience with the in-place mixing and grading operations was that the test sections shown in Figure 4 were almost too short. Future experiments should use longer individual test sections. Adjacent sections of dissimilar materials require that the rotary mixing operation be started and stopped frequently by lifting up the tines. This process adversely affects the material uniformity in the area of the lifting operation and becomes a more significant problem as the sections become shorter.

There has been some speculation and limited experience with the use of concrete ready mix trucks to mix the material and cause the fibers to open up. There is a need to explore this approach further, since it is very attractive in terms of cost, efficiency, and potential quality of the final product. The idea has the potential to deliver a homogeneous product at minimum cost. The primary use for this type of approach is in applications that use select, cement-stabilized, fiber-reinforced, cohesionless (or low-cohesion) soils.

It should be possible to develop a simple procedure for estimating life on the basis of the stress-strain curves from the mix design process. Standard techniques are available in the literature that use strength or modulus from the stress-strain curves (*4*). However, strain energy density might be useful as well. An example of the potential of this approach is shown in Figure 7, wherein there appears to be an identifiable relationship between strain energy and the number of passes to failure. The strain energy presented in this figure is the result of multiplying the strain energy density from the mix design strength tests by a volume of material. In this case, a cylindrical volume with a unit radius and a height equal to the thickness of the pavement layer in the field was used. The technique might be improved by taking the volume as that of a frustum of a right circular cone defined by the contact area

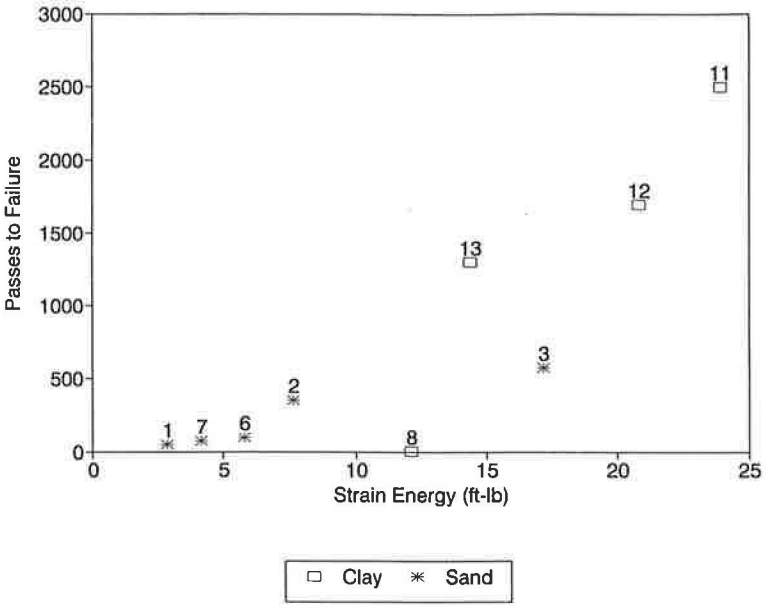

FIGURE 7 Potential relationship between strain energy and number of passes to failure (1 ft-lb ≈ 1.36 J). Numbers above symbols indicate experimental section numbers.

of the tire, the depth of the layer, and the stress distribution within the layer. The approach is a simplistic form of energy approaches that have been used in the past (*5*) and that are being used currently by at least two of the major contractors in the Strategic Highway Research Program.

The surface of pavement layer materials containing fibers should be sealed in some fashion (e.g., with an emulsion). Although no quantitative measurements were taken, visual indications were that the fibers can provide a path for capillary absorption of water into the shallow layer of soil near the surface, which can result in weak support in that area. This weakness could lead to other problems such as rutting and slippage of asphalt pavements and pumping under portland cement concrete pavements. It is anticipated that correct application of sealing or tacking material at the fiber-stabilized layer interfaces will eliminate these potential problems.

The mix design procedure should be validated by an independent laboratory. Studies of drainage characteristics such as permeability and critical shear stress should be conducted. Life cycle cost analyses should be accomplished. Accelerated tests simulating combined distresses from traffic and environmental conditions, coupled with full-scale test sections on public or private roads, would be useful. Laboratory fracture testing is being conducted.

REFERENCES

1. Eades, J. L., and R. E. Grim. A Quick Test To Determine Lime Requirements for Lime Stabilization. In *Highway Research Record 139*, HRB, National Research Council, Washington, D.C., 1966, pp. 61–72.
2. Terrel, R. L., J. A. Epps, E. J. Barenberg, J. K. Mitchell, and M. R. Thompson. *Soil Stabilization in Pavement Structures, A User's Manual, Vol. 2, Mixture Design Considerations*. FHWA-IP-80-2. FHWA, U.S. Department of Transportation, 1979.
3. Sangineni, S. M. *Evaluation of the Performance of Polypropylene Fibers on Soil Stabilization*. Master's thesis. Texas A&M University, College Station, 1992.
4. *Guide for Design of Pavement Structures*. AASHTO, Washington, D.C., 1986.
5. Southgate, H. F., R. C. Deen, and J. G. Mayes. Strain Energy Analysis of Pavement Designs for Heavy Trucks. In *Transportation Research Record 949*, TRB, National Research Council, Washington, D.C., 1983, pp. 14–20.

Publication of this paper sponsored by Committee on Soil and Rock Properties.